INVESTIGATION OF THE CRUST AND UPPER MANTLE STRUCTURES FROM TELESEISMIC P-WAVE TRAVEL TIME RESIDUALS BENEATH SOME SEISMIC STATIONS IN NIGERIA

BY

YAKUBU, TAHIR ABUBAKAR (B.Sc (Hons) ABU, M.Sc, Ibadan)
(PhD/SCIE/01043/2008-9)

A DISSERTATION SUBMITTED TO THE POSTGRADUATE SCHOOL, AHMADU BELLO UNIVERSITY, ZARIA IN PARTIAL FULFILLMENT OF THE REQUIREMENTS FOR AWARD OF THE DEGREE OF DOCTOR OF PHILOSOPHY IN APPLIED GEOPHYSICS

DEPARTMENT OF PHYSICS
FACULTY OF SCIENCE
AHMADU BELLO UNIVERSITY
ZARIA, NIGERIA

MAY, 2014

DECLARATION

I hereby declare that:

i. The report presented in this dissertation is the result of original research of the author.

ii. This dissertation has not been submitted to any other institution, organization or body for

any award.

iii. All inclusions from the author's earlier works and of others have been duly acknowledged.

_____ _____

Yakubu, Tahir Abubakar Date

DEDICATION

This work is dedicated to Almighty Allah, my sweet mother Hajiya Hauwa Abubakar and to my Late father Alhaji Abubakar Sani Bima.

CERTIFICATION

This dissertation entitled: INVESTIGATION OF THE CRUST AND UPPER MANTLE STRUCTURES FROM TELESEISMIC P-WAVE TRAVEL TIME RESIDUALS BENEATH SOME SEISMIC STATIONS IN NIGERIA, by YAKUBU, TAHIR ABUBAKAR, meets the regulation governing the award of the Degree of Doctor of Philosophy of Ahmadu Bello University, and is approved for its contribution to knowledge and literacy presentation.

Prof. B. B. M. Dewu Chairman, Supervisory Committee	Date
Dr. K. M. Lawal Member, Supervisory Committee	Date
Dr. P. Sule Member, Supervisory Committee	Date
Dr. Sadiq Umar HOD, Department of Physics	Date
Prof. A. A. Joshua Dean, Postgraduate School	Date

Acknowledgement

All praise is to Allah whose grace and tidings bring all good things to fruition. My sincere greetings and appreciation goes to my supervisors, Prof. B. B. M. Dewu, Dr. K. M. Lawal and Dr. P. Sule for their immense contributions, tolerance, patience and understanding toward the success of this research work.

My gratitude and appreciation also goes to the management of the National Space Research and Development Agency (NASRDA) for approving and funding the programme. To the Director -General of the Agency, Prof. Seidu Onailo Mohammed, I say a big thank you for your special interest and encouragement while the program lasted. To all the staff of NASDRA and Center for Geodesy and Geodynamics, Toro (CGG), you're all wonderful people to work with. Special appreciation goes to the staff of the Department of Earthquake Seismology, CGG, Toro, for their contribution during data collection and processing.

My appreciation also goes to the Head of Department, and staff of the Department of Physics, Ahmadu Bello University, Zaria for their commitment and dedication to duty. I'm also indebted to Dr. Oniku S. Adetola of the Department of Physics, Modibbo Adama University of Technology, Yola for useful discussions with him, which has contributed to the success of this work. Thank you, may Allah reward you.

Finally, I owe my unreserved gratitude to my wife Zainab Tahir and my children for their patience and encouragement which has been my major source of inspiration throughout the period of this research work.

ABSTRACT

The crust and upper mantle structure beneath some seismic stations in Nigeria from the study of teleseismic P-wave travel time residuals has been investigated with the aim of determining the velocity structure within the crust and the upper mantle. This was achieved by using Seismic data from three stations at Ile-Ife, Nsukka and Kaduna which were consistent with data from July 2009 to July 2011. Five hundred and sixty-six (566) events were recorded: Ile-Ife, 109 events, Nsukka, 240 events and Kaduna, 217 events. The travel time plot for each of the three stations shows correlation with the standard travel time plot. The travel time residuals calculated with respect to the International Association for Seismological Practices 91(IASP91) model for each of the stations ranges from -0.52 s to 4.93 s with an average value of 1.8 ± 1.3 s for Ile-Ife station, -1.15 s to 4.4 s, with an average of 1.9 ± 1.4 s for Nsukka station and from -0.35 s to 4.86 s with an average 2.2 ± 1.3 s for Kaduna station. The large standard deviation in the average residuals is accounted for by considering the heterogeneity in the travel paths of the seismic waves to the recording stations. Therefore, to ensure that the data belong to a fairly homogeneous path, the events were divided into three azimuthal regions where the events are more concentrated and new residuals for each region were calculated for each station: For Ile-Ife station Region I (30^o-90^o) has average new residuals of 1.8 ± 0.3 s, Region II (210^o-270^o), 1.8 ± 0.3 s and Region III (270^o-330^o) 1.5 ± 0.4 s; For Nsukka station, Region I has new average residuals of 1.83 ± 0.9 s; Region II, 1.90 ± 0.5 s and Region III 1.5 ± 0.7 s while for Kaduna station, we have Region I, 2.2 ± 0.6 s; Region II, 2.2 ± 0.5 s and Region III, 1.7 ± 0.6 s. The new station residuals show less scatter hence the standard deviations are lower because the data sets now belong to fairly homogeneous travel paths. The positive residual

observed for all the stations is an indication of the presence of a low velocity structure within the crust and the upper mantle along the propagation path. Azimuthal variations of the residuals also show that the velocity structure along the regions I and II are thicker than in region III. This is accounted for by low value of the residuals compared with the total event residuals.

In other to remove the earthquake source and travel path effects from the travel time residuals, relative travel time residuals were computed for each of the three stations under considerations. The results shows that IFE and NSUKKA stations have negative (-0.03 s and -0.13 s respectively) relative travel time residuals, while KADUNA station has positive (0.15 s) relative travel time residual. Inversion of the travel time data reveals a velocity variation between 8.5 and 12.8 km/s indicating that the waves travel mainly in the mantle. The plot of the velocity-depth model for the three stations revealed a three layer mantle model, with transition at an average depth of 720 km.

TABLE OF CONTENTS

LIST OF TABLES

Table
Page

LIST OF FIGURES

FIGURE **PAGE**

CHAPTER ONE

INTRODUCTION

1.1 General Background

An earthquake is the result of sudden release of energy in the earth's crust that creates seismic wave. Everyday about fifty or more of such events occur worldwide, with the magnitudes which are strong enough to be recorded in Nigeria. Each earthquake event radiates seismic waves which travel throughout the earth, some of these waves are readily detected with modern instrument (seismometer) stationed anywhere on the globe. Depending on the distance of the earthquake focus from the recording station, the recorded seismic events are classified as local, regional or teleseismic event (Lay and Wallace, 1995).

The branch of science which deals with the study of generation, propagation and recording of elastic waves through the earth and of the sources that produce them is known as seismology. Seismological procedures provide the highest resolution of internal earth structure of any geophysical method. This is because elastic waves have the shortest wavelength of any geophysical wave and the physics that governs them localizes their sensitivity spatially and temporarily to the precise path travelled by the energy (Lay and Wallace, 1995). Recordings of ground motion as a function of time, known as seismograms provide the basic data that seismologists use to study elastic wave as they spread throughout the earth.

The first time-recording seismograph was built in Italy by Filippo Cecchi in 1875. Soon after this, suitable instruments with better precision and accuracy were developed

by the British in Japan. The first observation of a distant earthquake, also known as teleseism, was made in Potsdam in 1889 for an event that occurred in Japan (Shearer, 1999). In 1897, the first North American seismograph was installed at Lick observatory near San Jose in California; this device was later to record the 1906 San Francisco earthquake (Shearer, 1999). The early seismic instrumentation was based on undamped pendulums, but all modern seismographs work on the principles of electromagnetism.

The availability of seismograms recorded at a various distance from earthquakes led to rapid progress in determining Earth's seismic velocity structure. By 1900, Richard Oldham reported the identification of P-, S- and surface waves on seismograms, and latter in 1906 proposed that the best explanation for the travel times of teleseismic waves through the body of the earth requires a large, dense and probably fluid core (Lay and Wallace, 1995). From the analysis of the travel – times of seismic body waves from near earthquake in Yugoslavia, Andrija Mohorovicic in 1909 inferred the existence of the crust-mantle boundary (CMB) and the interface is now generally referred to as the Moho (Lowrie, 1997). The tabulations of arrival times led to the construction of Travel Time Tables (arrival time as a function of distances from the earthquake). The first widely use Tables were produced by Zoppritz in 1907 while in 1940, Harold Jefferys and K. E. Bullen published the final version of their travel time Tables (referred to as the JB Tables), for a large number of seismic phases (Lowrie, 1999). Other versions of travel time Tables have since been published; these are AK135 compiled by Kennett (2005) and IASP91 by Kennett and Engdahl (1991). All these Tables and the JB Tables are still in use today and only differ by a few seconds.

The knowledge of the travel times of seismic arrivals based on the published Tables has been used by various authors in various regions of the world to determine average velocity versus depth structure for these regions.

1.2 Earthquake

An **earthquake,** also known as a **quake**, **tremor** is the result of a sudden release of energy in the Earth's crust that creates seismic waves. At the Earth's surface, earthquakes manifest themselves by shaking and sometimes displacement of the ground.

Occasionally, the word earthquake is used to describe any seismic event — whether natural or caused by humans — that generates seismic waves. The main causes of earthquakes are mostly; rupture of geological faults, but also by other events such as volcanic activity, landslides, mine blasts, and nuclear tests (Thorne and Terry, 1995). An earthquake's point of initial rupture is called its focus or hypocenter. The epicenter is the point at ground level directly above the hypocenter. When the epicenter of a large earthquake is located offshore, the seabed may be displaced sufficiently to cause a tsunami.

The moment magnitude is the most common scale on which earthquakes larger than approximately 5 are reported for the entire globe. The more numerous earthquakes smaller than magnitude 5 reported by national seismological observatories are measured mostly on the local magnitude scale, also referred to as the Richter scale. These two scales are numerically similar over their range of validity. Magnitude 3 or lower earthquakes are mostly almost imperceptible and magnitude 7 and over potentially causes serious damage over large areas, depending on their depth (Lawrence, 2007). The largest earthquakes in

historic times have been that of March 2011 in Japan with moment magnitude slightly over 9, and it was the largest Japanese earthquake since records began (Shearer, 1999)

1.3 Seismic wave propagation in the Earth's Interior

Seismic waves are seismic energy propagated as waves caused by the sudden breaking of rock within the earth or an explosion (Lawrence, 2007). They are the energy that travel through the earth and is recorded on seismographs. The two main types of waves are *body waves* and *surface waves*. Body waves can travel through the earth's inner layers, while surface waves can only move along the surface of the earth like ripples on water. Earthquakes radiate seismic energy as both body and surface waves (Gubbins, 1990).

Travelling through the interior of the earth, body waves arrive before the surface waves emitted by an earthquake. Both waves are of higher frequency than surface waves. The first kind of body wave is the *P wave* or *primary wave*. This is the fastest kind of seismic wave, and, consequently, the first to arrive at a seismic station. The P wave can move through solid rock and fluids, like water or the liquid layers of the earth. P waves are also known as *compressional waves*, because of the pushing and pulling they do. Particles in P wave move in the same direction that the wave is moving in, which the direction that the energy is travelling is or the direction of wave propagation.

The second type of body wave is the *S wave* or *secondary wave*, which is the second wave felt in an earthquake. An S wave is slower than a P wave and can only move through solid rock, not through any liquid medium. It is this property of S waves that led seismologists to conclude that the Earth's outer core is a liquid. S waves move rock particles up and

down, or side-to-side--perpendicular to the direction that the wave is travelling in (the direction of wave propagation).

Travelling only through the crust, *surface waves* are of a lower frequency than body waves, and are easily distinguished on a seismogram as a result. Though they arrive after body waves, it is surface waves that are almost entirely responsible for the damage and destruction associated with earthquakes.

The first kind of surface wave is called a *Love wave*. It's the fastest surface wave and moves the ground from side-to-side. Confined to the surface of the crust, Love waves produce entirely horizontal motion. The other kind of surface wave is the *Rayleigh wave*. A Rayleigh wave rolls along the ground just like a wave rolls across a lake or an ocean. Because it rolls, it moves the ground up and down and side-to-side in the same direction that the wave is moving. Most of the shaking felt from an earthquake is due to the Rayleigh wave, which can be much larger than the other waves.

Propagation velocity of the seismic waves ranges from approximately 3 km/s up to above 13 km/s, depending on the density and elasticity of the medium. In the Earth's interior the shock- or P waves travel much faster than the S waves. The differences in travel time from the epicenter to the observatory are a measure of the distance and can be used to image both sources of quakes and structures within the Earth. Also the depth of the hypocenter can be computed.

In solid rock, P-waves travel at about 6 to 7 km/s; the velocity increases down to the mantle to ~13 km/s. The velocity of S-waves ranges from 2–3 km/s in light sediments and

4–5 km/s in the Earth's crust up to 7 km/s in the deep mantle. As a consequence, the first waves of a distant earthquake arrive at an observatory via the Earth's mantle.

Because seismic waves propagate efficiently and interact with internal structure, they provide high-resolution noninvasive methods for studying Earth's interior. One of the earliest important discoveries (Oldham, 1906) was that the outer core of the Earth is liquid. Since S-waves do not pass through liquids, the liquid core causes a shadow on the side of the planet opposite of the earthquake where no direct S-waves are observed. In addition, P-waves travel much slower through the outer core than the mantle.

1.3.1 Body waves

There are two types of body wave, P-waves and S-waves. P-waves (Fig.1.1) are longitudinal waves that involve compression and rarefaction (expansion) in the direction that the wave is traveling. P-waves are the fastest waves in solid medium and are therefore the first waves to appear on a seismogram. S-waves, also called shear or secondary waves, are transverse waves (Fig.1.2), which involve motion perpendicular to the direction of propagation. S-waves appear later than P-waves on a seismogram. Fluids cannot support this perpendicular motion, or shear, so S-waves only travel in solids. P-waves travel in both solid and fluid media.

The velocity of P-waves in a homogeneous isotropic medium is given by

$$v_p = \sqrt{\frac{K + \frac{4}{3}\mu}{\rho}} = \sqrt{\frac{\lambda + 2\mu}{\rho}} \qquad \ldots\ldots\ldots\ldots\ldots\ldots\ldots\ldots\ldots\ldots \quad 1.1$$

Where K is the bulk modulus (the modulus of incompressibility), μ is the shear modulus (modulus of rigidity, sometimes denoted as G and also called the second Lamé parameter), ρ is the density of the material through which the wave propagates, and λ is the first Lamé parameter.

Of these, density shows the least variation, so velocity is mostly controlled by K and μ.

The elastic moduli M, is defined so that $M = K + 4\mu / 3$ and the P-wave velocity given as

$$v_p = \sqrt{M/\rho}. \quad \ldots\ldots\ldots\ldots\ldots\ldots\ldots\ldots\ldots\ldots\ldots\ldots\ldots\ldots\ldots\ldots \quad 1.2$$

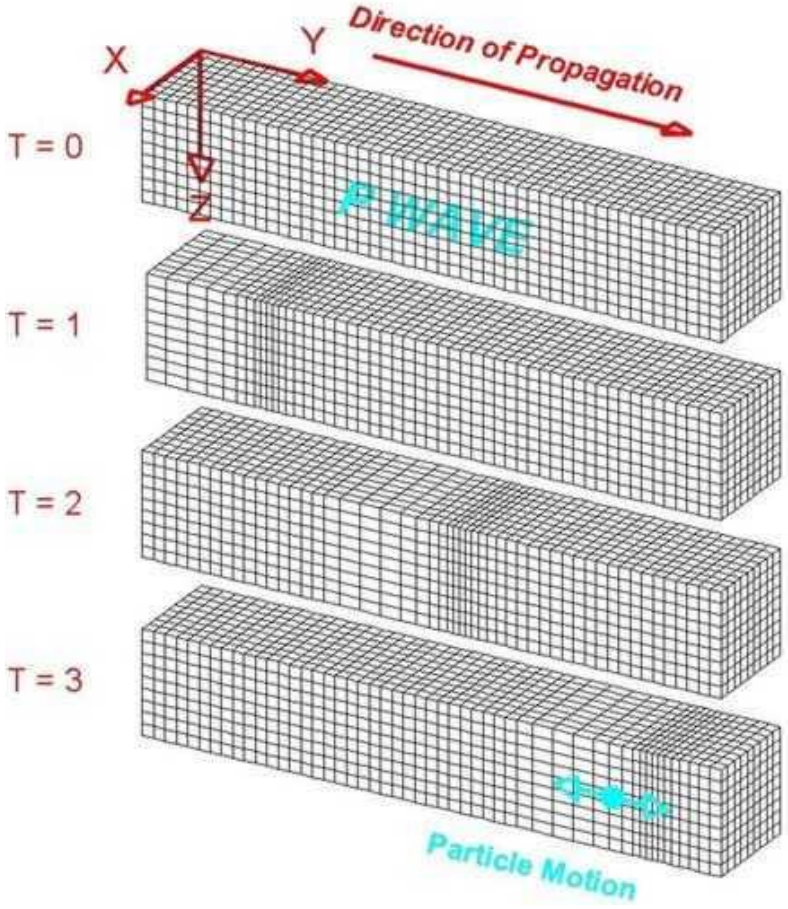

Fig. 1-1: P-wave propagation through a medium, motion represented by cubes for this Model (After Lawrence, 2007)

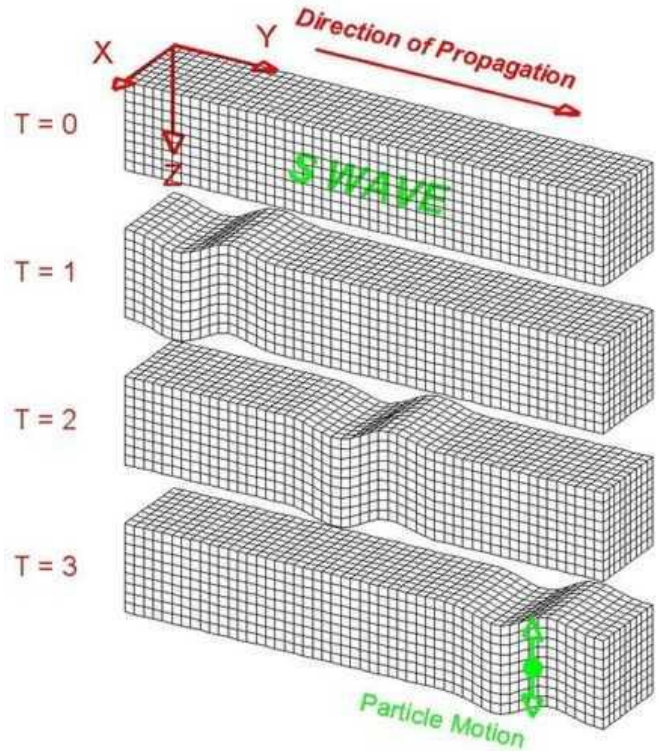

Fig. 1.2: S-wave propagation through a medium (After Lawrence, 2007)

1.3.2 Surface waves

The two main kinds of surface wave are the Rayleigh wave and love wave. The Rayleigh wave (Fig. 1.3), has some compressional motion. It rolls along the ground just like a wave rolls across a lake or an ocean and because it rolls, it moves the ground up and down and side-to side in the same direction that the wave is moving. The Love wave (Fig. 1.4) is the fastest surface wave and it moves the ground only from side-to side. The surface waves can be theoretically explained in terms of interacting P- and/or S-waves. Surface waves travel more slowly than P-waves and S-waves, but because they are guided by the surface of the Earth and their energy is thus trapped near the Earth's surface, they can be much larger in amplitude than body waves, and can be the largest signals seen in earthquake seismograms.

They are particularly strongly excited when their source is close to the surface of the Earth, as in a shallow earthquake or explosion (Gubbins, 1990).

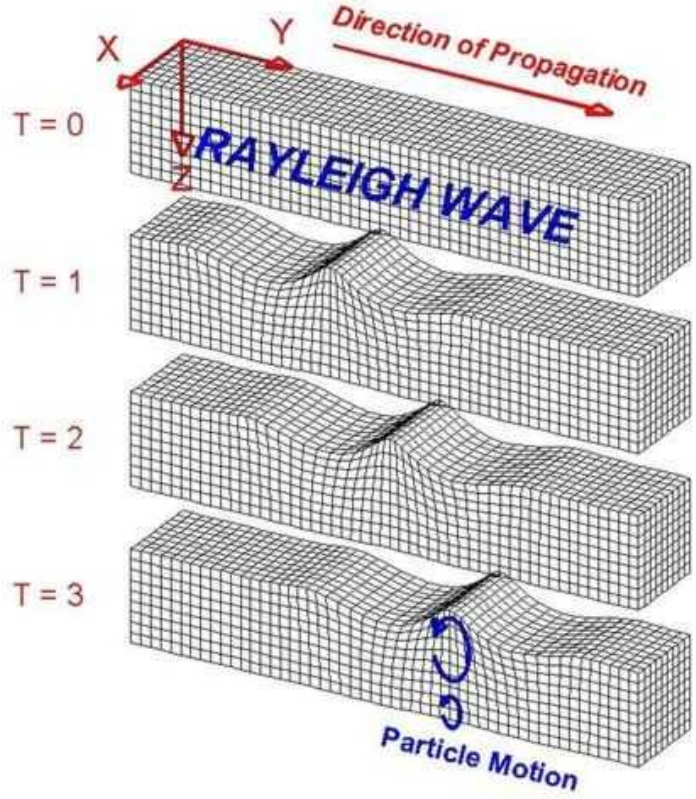

Fig. 1.3: Rayleigh wave propagation through a medium (After, Lawrence, 2007)

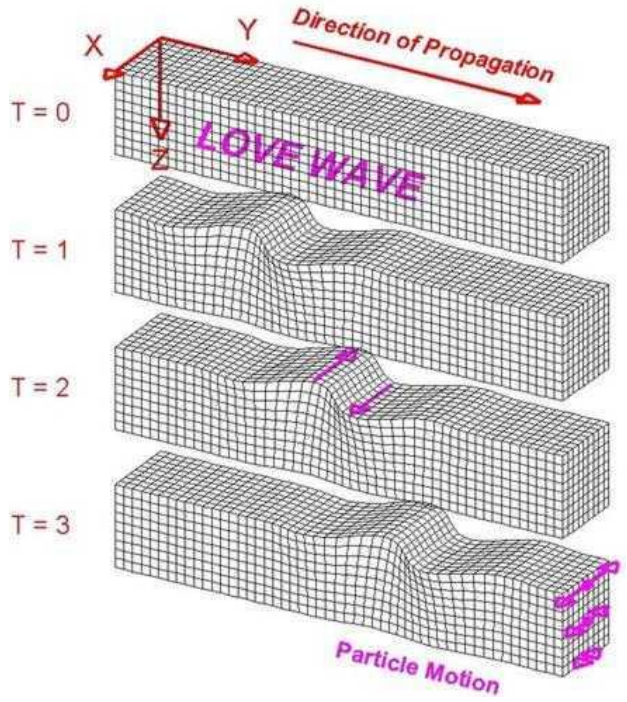

Fig.1.4: Love wave propagation in a medium (After Lawrence, 2007)

1.4 Seismological observatory and Seismograph networks

Seismological observatories are houses specifically built to house seismic hardware, e.g. seismic recorder, sensors and other necessary accessories and software. The science of seismology depends critically on data collected at hundreds of observatories world-wide. These observatories are operated by a variety of agencies, staffed by seismologists and technicians whose training and interests vary widely. While in industrialized countries the observatory personnel normally have easy access to up-to-date technologies, spare parts, infrastructure, know-how, consultancy and maintenance services, those in developing countries are often required to do a reliable job with very modest means.

To ensure that the data from these observatories are properly processed and interpreted once it has been acquired and compiled, it is necessary to establish protocols for all aspects of observatory operation which may affect the seismological data itself. In addition, competent guidance is often required in the stages of planning, bidding, procurement, site-selection, and installation of new seismic observatories and networks so that they will later meet basic international standards for data exchange and processing in a cost-effective and efficient manner.

Presently in Nigeria, Centre for Geodesy and Geodynamics, Toro, National Space Research and Development Agency, under the Federal Ministry of Science and Technology has been saddled with the responsibility of establishing and networking of the Nigeria network of seismographic stations. Ten of such stations were proposed, with only six at Oyo, Ile-Ife, Awka, Nsukka, Toro and Kaduna established and Minna, Ibadan, Abakiliki and Abuja are still in the pipe-line (Fig.1.5). Scientists and technicians at the centre have been working round the clock to ensure that the quality of data obtained from these stations is of international standard. The data used in this study was obtained from Ile-Ife, Kaduna and Nsukka Stations.

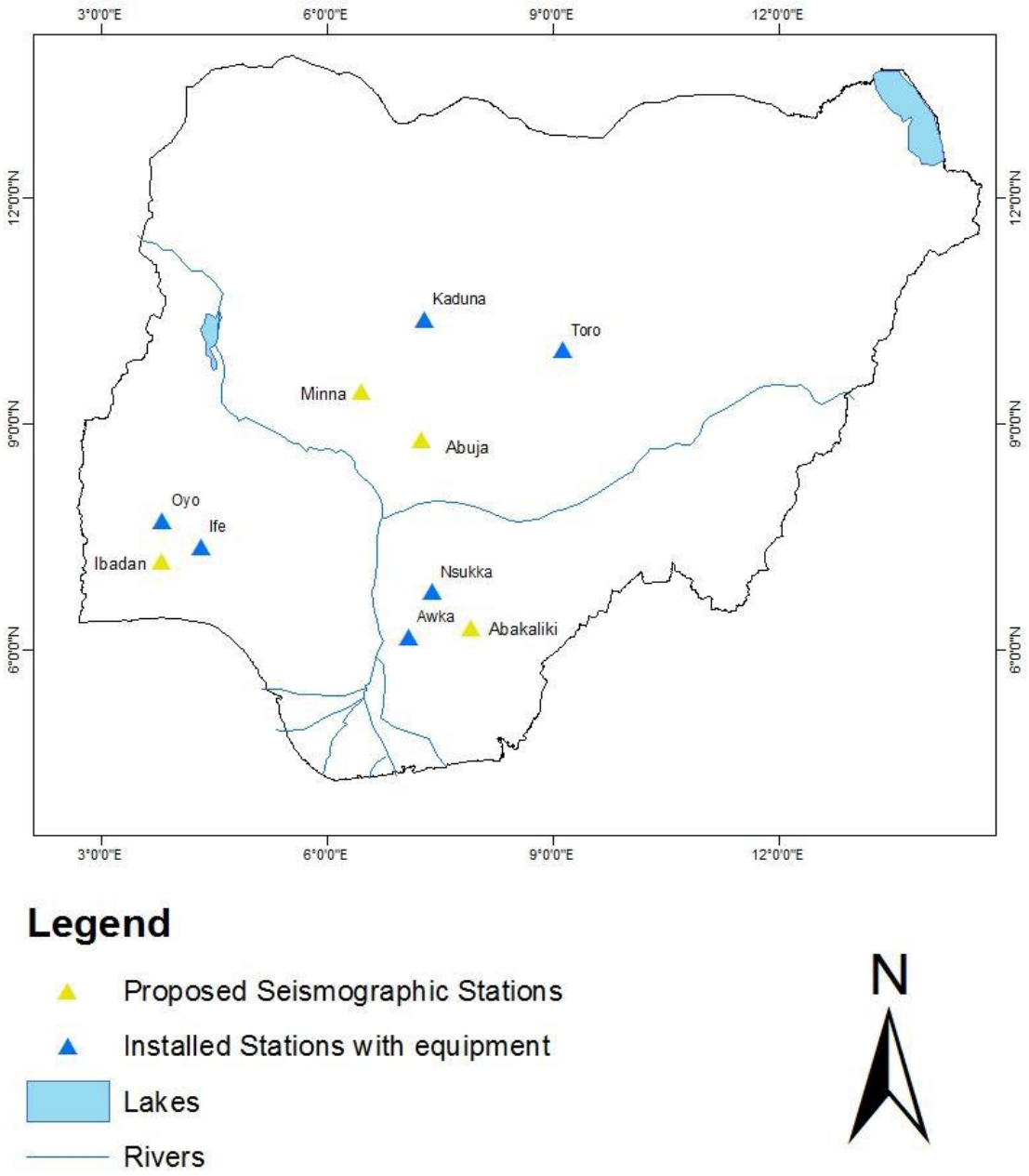

Fig. 1.5: Distribution of Seismographic stations in Nigeria

1.5 Aim and Objectives

Knowledge of upper mantle seismic velocity structure is crucial to understanding the earth's evolution and regional or global tectonics. The aim of this study is to investigate the Crust and upper mantle velocity structure using P waves from Teleseismic events monitored in Nigerian Network of Seismographic Stations. As will be discussed in the following sections, there are many different techniques used for the determination of Crust and upper mantle structure, however, there is paucity of relevant research work in the Nigerian context. Thus, this study aims to fill this gap by using P waves for Teleseismic event monitoring. The focus of this study is on the fundamental theory and Physics of seismic waves and the application of this theory to extract the vital and useful information about internal structure and dynamical processes in the Earth that is contained in seismograms.

The objectives of this study therefore are:

(i) To pick the travel time of event from the seismograms recorded at each station (*i.e.* the time of day that a wave from the earthquake arrives at a seismograph station)

(ii) To determine the arrival time of every event received at the station (*i.e.* travel time minus origin time of event)

(iii) To prepare the graph of travel time versus the epicentral distance for each of the station

(iv) To prepare the location map of all the events against the azimuth centered on the stations.

(v) To investigate the gross properties of the source, travel path and the receiver by considering the absolute travel time residuals

(vi) To estimate the Relative travel time residual between the stations.

(vii) To develop a velocity model using travel-time data from teleseismic events recorded at the Nigeria National Network of Seismographic Stations (NNNSS).

1.6 Statement of Problem

Nigeria lies on the eastern flank of the Atlantic Ocean and unlike the Pacific Ocean margins which are characterized by subduction tectonics and occurrence of devastating earthquakes, the Atlantic margins are generally quiet and free of diastrophic activities. Therefore, the occurrence of natural earthquakes in Nigeria is uncommon because of its location on a passive continental margin with the nearest active plate boundaries lying very far away at the Mid-Atlantic Ridge; hence the country is referred to as being aseismic. However recent seismic activities in Nigeria and some parts of the west - African sub-region have shown that the region is most probably seismically unstable. Also, the existence of a rift zone as well as major faults within the Nigerian land mass, and the occurrence of possible active transcurrent faults offshore may be a pointer to the fact that Nigeria may not be seismically stable as thought. Therefore, the need to continuously monitor the crust and the upper mantle for possible prediction of earthquake phenomena informed the establishment of the Centre for Geodesy and Geodynamics. The centre has about ten seismograph stations spread across the Nigeria land mass; four of these stations have since 2009 monitored earthquakes at local, regional and teleseismic distances. This

research work is therefore tailored towards the analysis of these data with a view to developing a velocity model for beneath some of the stations and also to study the geodynamic processes taking place along the propagation path of the seismic wave as well as establishing the crustal and upper mantle boundary topography.

CHAPTER TWO

LITERATURE REVIEW

2.1 Previous Studies

Prior to the 1984 earth tremors which occurred in Ijebu-Ode, South-western Nigeria earthquake studies in Nigeria has been on the low level. However, since then the need to study earth structures in Nigeria to better predict possible occurrence of earthquakes and other natural disaster became a major concern. Immediately following the event, was national seminar with the theme "The implications of earthquakes in Nigeria" was held at Ahmadu Bello University, Zaria. The seminar focused on with the following sub-themes:

(i) Detection and prediction of earthquakes

(ii) Historical perspective of earthquakes in West- Africa

(iii)Faults/fractures in the Nigeria landmass

(iv)Engineering design considerations for earthquake prone areas.

A communiqué issued at the end of the seminar informed the establishment of some seismic stations in different parts of the country (Kujama NITEL Substation, Kaduna; Karshi, Abuja; Federal University of Science and Technology, Minna; Obafemi Awolowo University, Ile-Ife; Federal Government Girls College, Oyo; University of Nigeria, Nsukka; Nmamdi Azikiwe University, Awka and Ebonyi State University, Abakalaki) by the Federal Ministry of Science and Technology through its National Technical Committee on Earthquake phenomena. Suitable sites were selected, vaults constructed for nine of the Stations and equipment installed in Five of the Stations. These stations have since been

handed over to the Centre for Geodesy and Geodynamics, Toro, by the Federal Ministry of Science and Technology. The Centre is one of the Centres of the National Space Research and Development Agency saddled with the responsibility of carrying out the earthquake studies in Nigeria among other things.

Historically, some earth tremors have been documented in the country especially in the south-western part (Osagie, 2008; Akpan and Yakubu, 2010). The areas which have experienced ground motion include Lagos, Ibadan and Ile-Ife on 22nd June 1939. On the same day, the event was recorded in Accra (Ananaba, 1991); Ijebu-Ode on 21st December, 1963 (Ajakaiye *et al*., 1987); Ibadan, Ijebu-Ode, Shagamu and Abeokuta on 28th July and 2nd August, 1984 (Ajakaiye *et al*., 1987); Ibadan and Ijebu-Ode on 27th June, 1990 (Ananaba, 1991; Ojo, 1995 and Osagie, 2008); Okitipupa in 1997 (Odeyemi, 2006), Okitipupa, Ibadan, Ijebu-Ode, Akure, Shagamu, Abeokuta and Oyo on 7th March, 2000 (Elueze, 2003; Odeyemi, 2006; Akpan and Yakubu, 2010). Tremors were also felt in other parts of the country, Gembu and Jalingo on 16th October 1982, Yola on 8th December 1984 and March 2005 (Akpan and Yakubu, 2010), Kombani Yaya in present day Gombe State between 18th to 19th June 1985 (Ugodulunwa et al., 1986; Ajakaiye et al., 1988). Dan Gulbi near Gusau in Zamfara State on November 7 1994 witness someground motion caused by an earthquake of local magnitude 4.2 (Akpan and Yakubu, 2010). Lupma near Minna in Niger State also experienced ground motion on 25th March, 2006 (Akpan and Yakubu, 2010). However, the veracity of some of these events cannot be ascertained as there were no seismic stations at the time the events occurred. A check on some of the international data centres did not reveal any information on the events. Later findings

suggested that some of them were major slope movements after torrential rainfall while some were vibrations that were felt as a result of earthquakes located hundreds of kilometres away or even outside the country (Onuoha, 1989).

The 28th July, 1984, 27th June, 1990 and 7th March, 2000 events were the only ones that were instrumentally recorded, but epicentres were only determined for the 1984 and 2000 events. The 2000 event was recorded teleseismically by twenty-seven seismological observatories around the world (Akpan and Yakubu, 2010). The National Earthquake Information Centre (NEIC) in the USA located the event at 6.224°N, 5.147°E (somewhere near Okitipupa), calculated a body wave magnitude (M_B) of 4.5 and a focal depth of 10 km. The International Seismological Centre (ISC) located the same event at 6.290°N, 5.070°E, with body wave (M_B) and surface wave (M_S) magnitudes of 4.4 and 3.9 respectively as well as focal depth of 10 km. The 1984 event was recorded by five stations (one in Nigeria and four in Cote d'Ivoire) and the epicentre was located somewhere near Ijebu-Ode (Ajakaiye *et al*., 1987) whereas the 1990 event which was recorded by only one station in Nigeria had its epicentre assumed to be near Ijebu-Ode based on previous occurrences and vibrations that were felt (Osagie, 2008; Akpan and Yakubu, 2010). The most recently felt earthquake in Nigeria occurred on Friday, 11th September, 2009. It was felt in parts of Abeokuta, Ago-Iwoye, Ajambata, Ajegunle, Imeko, Ijebu-Ode, Ilaro and Ibadan all in South-western Nigeria. The event was recorded by the three seismological stations operated by the Centre for Geodesy and Geodynamics, Toro and fifty-seven other seismological stations in the world. Analysis of the records showed the epicentral location at latitude 6.611°N and longitude 2.433°E about 129 km west of Lagos (close to Tori

Basito in the Republic of Benin) with a focal depth of 10.0 km. The local magnitude was determined as 4.5 and moment magnitude 4.2 (Akpan and Yakubu, 2010).

However, the travel time data obtained from earthquake studies have been used by several authors to get information on crustal and upper mantle structures and also the geodynamic process at work. Ojo, (1994) studied the teleseismic P-wave travel time residuals at the Ahmadu Bello University, Zaria seismic station, while Oniku, (1999, 2005) carried out detailed study of the P-wave travel time data at same station taking into considerations the absolute travel time and relative travel time residuals. Estimates of crustal and lithospheric thickness (Hansen, *et al.*, 2009; Dugda, *et al.*, 2009; Kumar *et al.*, 2007) in several terrains in southern, central, and eastern Africa have been obtained from modeling S-wave receiver functions.

2.2 Regional Geology and Tectonics of Nigeria

The geology of Africa is dominated by the Kalahari, Congo/Zaire and West African Cratons. These are composed of late Archean and early-middle Proterozoic crystalline basement rocks which are non-conformably overlain by middle to late Proterozoic – earliest Paleozoic shelf sedimentary sequence and succession within younger Paleozoic basins (Clifford, 1970) as quoted in Oniku (1999). Kennedy (1964), noted the dominance of 650-450 Ma K-Ar ages in the upper Precambrian terrains but did not recognize indications of the classic orogenesis in the non-Archean terrains, except in the Danara-Katanga belt, and hence used the term Pan-African thermo-tectonic event to identify major episode in the African geologic evolution. This tectonothermal episode identified by

Kennedy (1964) affected the borders of the previously cratonized West African Craton at 600 ± 150 Ma ago (Fig.2.1). Evidence from the eastern and northern margins of the West African craton indicates that the Pan-African belt evolved by plate tectonic processes which involved the collision between the passive continental margin of the West-African craton and the active continental margin (Pharusian belt) of the Tuareg shield about 600 Ma ago (Burke and Dewey, 1972; Leblanc, 1976; Black and Caby, 1979). The collision at the plate margin is believed to have led to the reactivation of the internal region of the Pan-African belt.

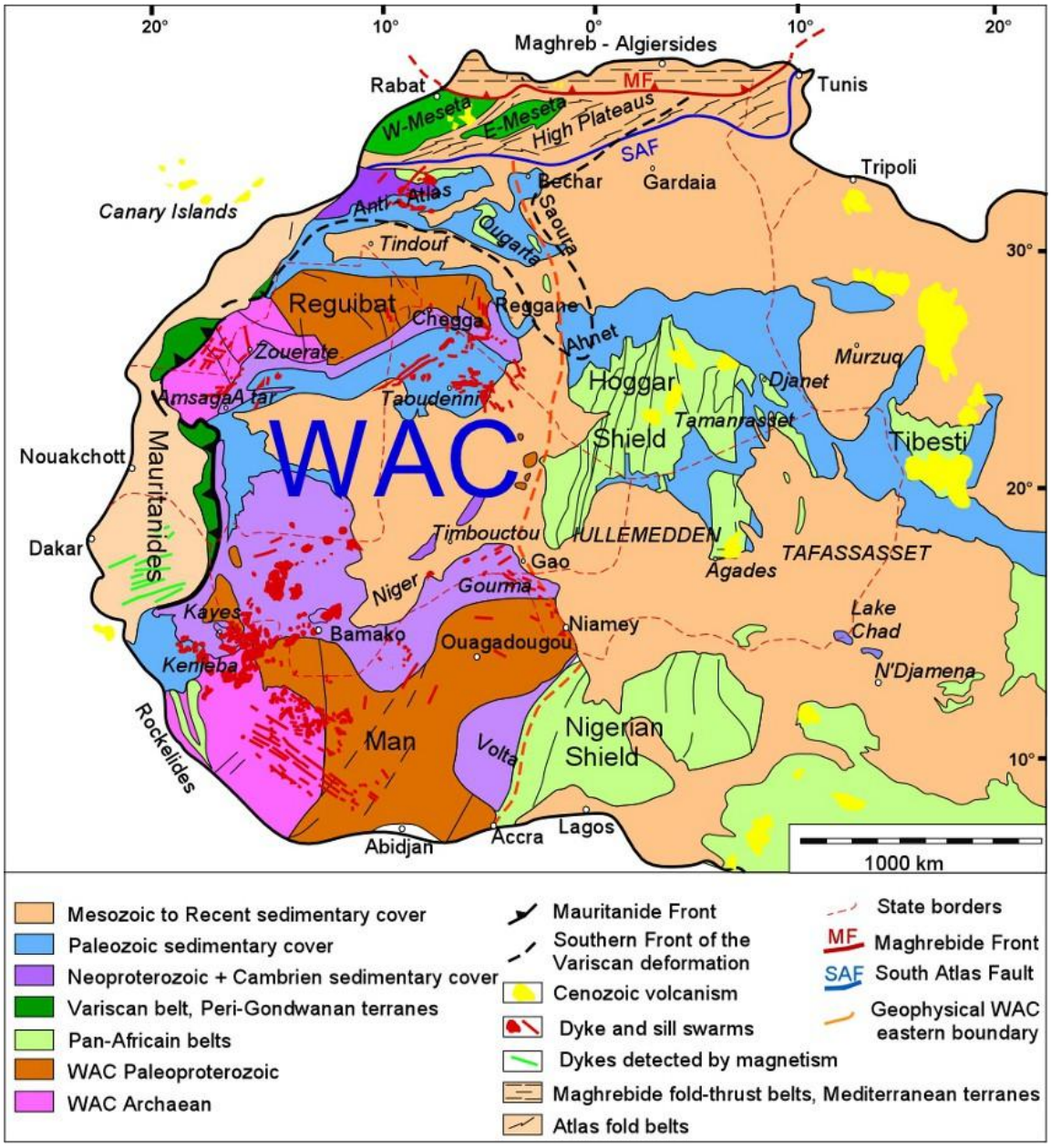

Fig. 2.1: West African Craton's (WAC) major outcrops and the Pan African zone (Fabre, 2005)

The Geology of Nigeria is shown in (Fig.2.2). About 50% of the area is underlain by Precambrian Basement Complex consisting of polymetamophic migmatite-gneiss complex, metasedimentary and metavolcanic rocks which are mainly N-S to NNE-SSW trending belts of low grade (greenschist facies) supracrustal assemblages. These are in places intruded and interspersed by the Older Granites which originated in the Pan-African Orogeny (600 Ma). The remaining half of the country is covered by various sedimentary basins (the Chad, Benue, Niger and Sokoto basins), with ages ranging from the Cretaceous to the Quarternary (Ajakaiye, *et al*.,1987).

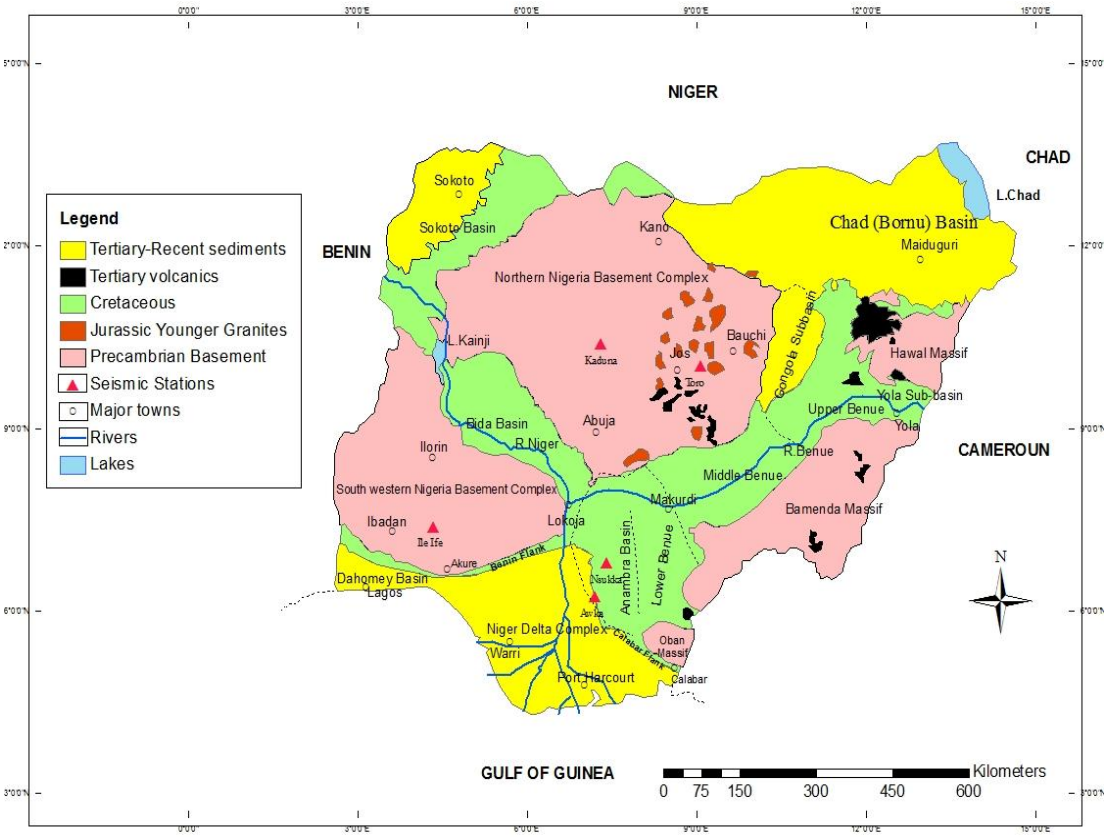

Fig.2.2: Geological Map of Nigeria showing some of the stations (red triangle) (Akpan and Yakubu, 2010)

Nigerian Basement Complex rocks occur between the West African Craton, and Congo Craton (Fig.2.3). Murat (1988) inferred a principal stress acting WNW-ESE direction in the basement rocks. This is in concordance with the geographical location of the cratons as the sources of compression which are also in a WNW- ESE direction with respect to the Nigerian Basement Complex.

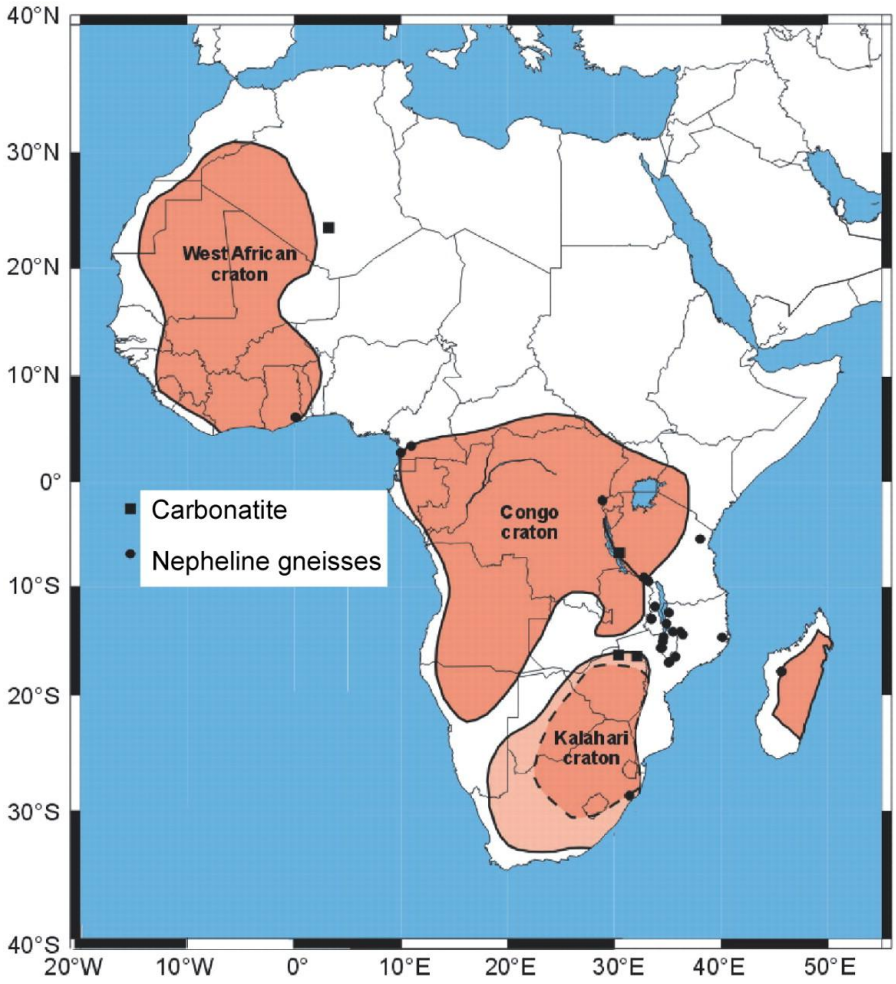

Fig.2.3: Map showing the three well formed African cratons (www.geosphere.gsapubs.org)

Basement Complex rocks outcrop in four main areas of the country: North of Rivers Niger and Benue, covering parts of Kaduna, Plateau, Bauchi, Kano and Sokoto States; southern Nigeria, covering the greater parts of Kwara, Oyo, Ogun; and Ondo States; southeast Nigeria, spanning the northern parts of Cross Rivers State and as far north as Yola; and north of Benue River in (old) Gongola State. These crystalline basement rocks have been subjected to deformation of different intensities throughout the geological period.

Consequently, North-South (N-S), Northeast-Southwest (NE-SW), Northwest-Southeast (NW-SE), North northeast-South southwest (NNE-SSW), North northwest-South southeast (NNW-SSE) and to a lesser extent, East-West (E-W) fractures have developed (Oluyide and Udoh, 1989).

In the Jos Plateau area, uplift occurred as a possible consequence of Jurassic intrusions that took place along fracture zones as suggested by Ajakaiye, *et al.*, (1982). These intrusions which contain alkaline feldspars are referred to as Younger Granites and they occur as ring dykes which represent old calderas or roots of volcanoes. The ring dykes aligned in the N-S direction become progressively older (500 Ma) towards the Algerian border and this has been interpreted as evidence for the existence of a possible episodic plume trace in West Africa (Ajakaiye and Verheijen, 1983).

The Basement rocks are overlain by Cretaceous and Tertiary sediments of the seven major sedimentary basins, viz, the Calabar Flank, the Benue Trough, the Chad Basin, lullemmenden (Sokoto) Basin, the Dahomey Basin, and the Niger Delta Basin. Sedimentary successions in these basins are of middle Mesozoic to Recent age (Kogbe, 1989). The Niger valley is possibly a graben and the Benue a sinistral shear zone that may be part of a fracture zone within the Pelsium Megashear system (Sheidegger and Ajakaiye, 1985). The Benue trough has also been considered as a "failed" rift since it contains no ophiolites (Nwachukwu, 1972).

In some cases, the Cretaceous sediments are cut by some major faults which may have been the result of the reactivation of post Pan-African fractures (Merki, 1970). It has been

suggested that the Dahomeyan Basin is bounded by the Romanche Fracture zones to the west and the Chain fracture zone to the East (Wright, 1976; Hastings and Bacon, 1979; Ige *et al*., 1985). Both fracture zones trend approximately in the NE-SW direction.

Some of the important fault systems in Nigeria are the Ifewara, Zungeru, Anka and Kalangai fault systems. They are interpreted to have resulted from transcurrent movements (Garba, 2003). Multispectral Scanner (MSS) and Side-looking airborne radar (SLAR) images confirmed the existence of the supposed Ifewara shear zone in the Precambrian basement complex of southwestern Nigeria formed by shearing activities during Late Precambrian times (Adepelumi *et al*., 2008). The 250 km-long, NE-SW trending Ifewara fault zone has been shown to be linked with the Atlantic fracture system (Adepelumi *et al*., 2008). Burke *et al*., (1977) and Hubbard (1975) believe that the pronounced age differences on both sides of the fault zone suggest that the zone may indeed be a suture of Kibaran age.

There are also many mid-Atlantic ridge transform fracture zones (St. Paul, Romanche, Charcot and Chain fracture zones) in the Gulf of Guinea which many believe form part of the Pelusium Megashear system that cuts across the continent of Africa from the West Africa Coast to the Nile basin in NE Africa (Neev *et al*., 1982; Ajakaiye *et al*., 1987). The compressional trough which follows the line has been ascribed to an oblique collision between a NW African plate and a central plate consisting of southern and eastern Africa, the Arabia Peninsula and the Levant (Neev *et al*., 1982).

2.3 Station location and Geology

The red triangles shown in Fig.2.2 represent the actual location of the four (Ile-Ife, Nsukka, Kaduna and Awka) of the ten network seismographic stations forming the Nigerian Network of Seismographic Stations. Three stations located in Ile-Ife, Kaduna and Nsukka were considered for this study therefore, I shall describe the geology settings at each of the station location.

2.3.1. Geology and Rock types at Ile-Ife

Ile-Ife is located within the southwestern Nigeria basement complex in the equatorial rain forest of Africa (Fig.2.2). The main lithologies include amphibolites, migmatite gneisses, granites and pegmatites. Other important rock units are schists, made up of biotite schist, quartzite schist, talc-tremolite schist, and the muscovite schist. The crystalline rocks intruded into these schistose rocks (Rahaman, 1988). The amphibolite and the hornblende gneiss are the mafic and intermediate rocks in southwestern Nigeria. In Ilesha and Ile-Ife areas these amphibolites occur as low lying outcrops and most are seen in riverbeds while, the hornblende gneiss crops out at Igangan, Aiyetoro and Ifewara, along Ile-Ife road as low lying hills in southwestern Nigeria (Rahaman, 1988). The hornblende gneiss is highly foliated, folded and faulted in places.

The magmatite-gnessic complex which constitutes over 75% of the surface area of the southwestern Nigerian basement complex is said to have evolved through 3 major geotectonic events:

(i) Initiation of crust forming process during the Early Proterozoic (2000 Ma) typified by the Ibadan (Southwestern Nigeria) grey gneisses considered by Woakes *et al*; (1987) to have been derived directly from the mantle.

(ii) Emplacement of granites in Early Proterozoic (2000 Ma) and

(iii) The Pan African events (450-750 Ma). Rahaman and Ocan (1978) on the basis of geological field mapping reported over ten evolutionary events within the basement complex with the emplacement of dolerite dykes as the youngest. On the basis of wide geochemical analyses and interpretation, tectonics studies, field mapping and plumb tectonics, Oyinloye (2011) had suggested a modified Burke *et al*; (1976) sequence of evolutionary events in the Southwestern Nigeria basement complex as detailed in Table 2.1.

Table 2.1: A modified sequence of events in the basement rocks in Ibadan-Ile-Ife-Ilesha area (modified from Burk *et al*; 1976)

S/No	**Sequence of Evolutionary Events in the South Western Nigeria basement complex**
11	Shearing, Chloritic and Zeolite mineralization of uncertain age.
10	Emplacement of dolerite dykes and gold mineralization at about 550 Ma **(Oyinloye, 2006)**
9	Formation of unsheared pegmatite, unfolded granitic veins of mid-Pan African age
8	Major remobilization and deformation in Early Pan-African
7	Minor metamorphic deformation in Kibaran
6	Emplacement of microdiorite
5	Emplacement of Ibadan-Ile-Ife-Ilesha Granite gneiss: F2 folding fabrics in Granite, Gneiss.
4	Emplacement of microdiorite dykes of uncertain age
3	Emplacement of semiconcordant aplite sheets in the banded gneiss, collision of plates subduction of ocean slab in to the mantle **(Oyinloye, 2002b)**
2	Deposition of ocean sediments covering the whole basement complex **(Oyinloye 2002a)**
1	Generation and differentiation of wet basaltic magma and formation of proto continent, **(Oyinloye, 2004)**.

2.3.2. Geology and tectonic setting of Nsukka

The Nsukka station at Nsukka southeastern, Nigeria is located in an area overlain by the Cretaceous sediments (Fig.2.2) and within the Nsukka formation. The origin and tectonic history of the southeastern Nigeria is associated with the break up of the continents of Africa and South America (Murat, 1972). The drifting apart of these continents, the opening of the South Atlantic and the growth of the mid-Atlantic ridge followed the break up. The major rocks in the southeastern Nigeria are igneous, sedimentary and

metamorphic. The igneous rocks include the older granite, pegmatite, rhyolite and dolerite while the sedimentary rocks include the Asu River Group (oldest), Eze-Aku Shale, Awgu Shale, Nkporo Shale, Coal measures, Imo Shale, Bende Ameki (youngest) and Coastal plains and Alluvium (Eze *et al.*, 2011). The metamorphic rocks include the undifferentiated basement complex.

2.3.3. Geology and tectonic setting of Kaduna

The Kaduna station is located within the northern Nigeria basement complex, and similar to Ile-Ife. It has been established that the Precambrian basement complex of Nigeria is a polycyclic ensemble of heterogeneous migmatites and gneisses, metasediments and granites that have undergone a complex evolutionary history spanning through 4 major orogenesis (Rahaman,1988; and Ajibade *et al*., 1981) :-

i. Liberian (Archaean) 2500 – 2750 ± 25Ma

ii. The Eburnean orogeny (Early Proterozoic), 2000 – 2500 Ma

iii. The Kibaran orogeny (Mid Proterozoic), 1100 – 2000 Ma

iv. The Pan African Orogeny, 450 -750 Ma.

Of all the above, the Eburnean and the Pan-African are major events which modified the Precambrian Geology of Nigeria basement complex. The basement is predominantly amphibolite - grade quartzofeldspar-biotite + hornblende gneisses and migmatites (Wright *et al*., 1987). Dada (1989) and Dada *et al.*, (1998) studied the petrogenesis and evolution of the basement around Kaduna. He assigned the amphibolite facies to subduction-related magma generation of volcanic arc settings for the gneisses of the basement based on the high Rb, Sr, K/Rb, K/Sr, low Ca and chondrite normalized negative anomalies of Nb, P, Ti

coupled with a high Al_2O_3/TiO_2 while the amphibolites are of the low Mg tholleites and poorer in LILE but enriched in P. This pattern tends to support a multistage evolution that involved an early basaltic crust transformed to amphibolite.

CHAPTER THREE

SEISMIC THEORY AND INSTRUMENTATION

3.1 Introduction

The seismic energy is propagated as seismic wave in all directions within the earth and its propagation is analogous to optical ray propagation in media; hence it is referred to as seismic ray.

The propagation of a seismic energy through the earth is governed by physical properties such as density, and by the way in which the material of the earth's interior reacts. Material within the seismic source suffers permanent deformation, but away from the source the passage of seismic energy takes place predominantly by elastic displacement of the medium, that is, it suffers no permanent deformation.

3.2 Seismic Rays

Seismic ray theory is a very convenient and intuitive way to model the propagation of seismic energy and in particular the propagation of body waves. The seismic ray theory is generally used to locate earthquakes and to determine focal mechanisms and velocity structure from body wave arrivals. Seismic ray theory, is easy to understand, simple to program, and very efficient. It is relatively straight forward to generalize to three dimensional velocity models. Using ray theory, it is important to keep in mind that it is an approximation that does not include all aspects of wave propagation. Ray theory is based on the so-called high-frequency approximation which states that fractional changes in velocity gradient over one seismic wavelength are small compared to the velocity. In other

words, we may use ray theory only if the dimension of structure to be considered is larger than the seismic wavelength used. These conditions are valid for most parts of the Earth (Kennett *et al*., 1995; and Dziewonski and Anderson, 1981) and for the wavelengths that are usually recorded and analyzed in seismological observatory practice. The problem of relatively sharp boundaries, as for example the crust-mantle interface (Moho-discontinuity), discontinuities in the upper mantle, and the core-mantle boundary (CMB) or the inner-core boundary (ICB) can be tackled by matching the boundary conditions between neighboring regions in which the ray solutions are valid.

3.2.1 Snell's law for a flat Earth

Consider a plane wave, propagating in material of uniform velocity v, which intersects a horizontal interface (Fig. 3.1). The wave fronts at time t and time t + Δt are separated by a distance Δs along the ray path. The ray angle from the vertical, θ is termed the incidence angle. This angle relates Δs to the wave front separation on the interface, Δx, by

$$\Delta s = \Delta x \sin\theta \quad \text{.....3.1}$$

Since Δs = vΔt, we have

$$v\Delta t = \Delta x \sin\theta \quad \text{.....3.2}$$

or

$$\frac{\Delta t}{\Delta x} = \frac{\sin\theta}{v} = u \sin\theta = p \quad \text{.....3.3}$$

where u is the inverse of velocity referred to as slowness (u = 1/v, where v is the velocity) and p is termed the ray parameter. If the interface represents the free surface, by timing the arrival of the wave front at two different stations, we could directly measure p. The ray parameter p represents the apparent slowness of the wave front in a horizontal direction, which is why p is sometimes called horizontal slowness of the ray.

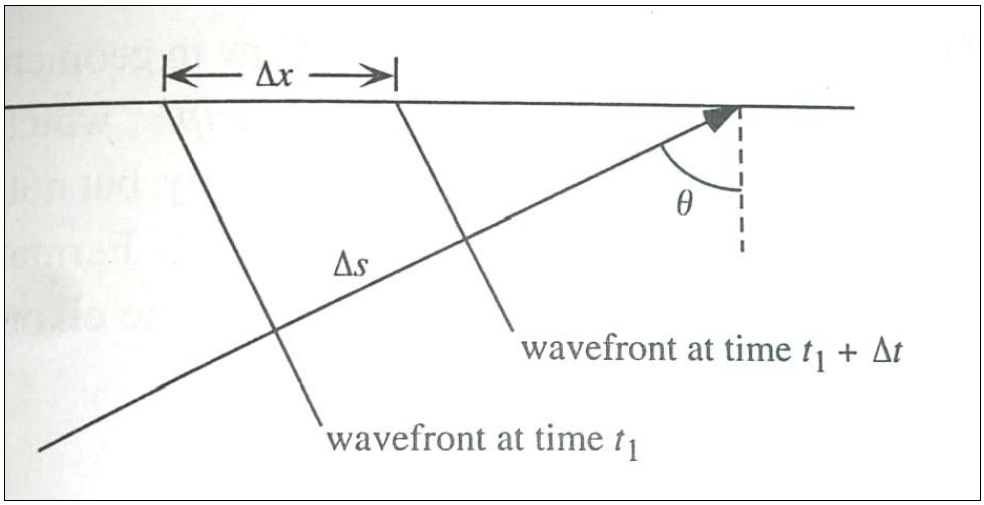

Fig.3.1: Plane wave incident on a horizontal surface.

We now consider a downgoing plane wave that strikes a horizontal interface between two homogeneous layers of different velocity and the resulting transmitted plane wave in the lower layer (Fig.3.2). If we draw wavefronts at evenly spaced times along the ray, they will be separated by different distances in the different layers, and we see that the ray angle at the interface also change to preserve the timing of the wavefronts across the interface. Considering Fig. 3.2, the top layer has a slower velocity ($v_1 < v_2$) and a correspondingly

larger slowness ($u_1 > u_2$). The ray parameter can be expressed in terms of slowness and ray angle from the vertical within each layer. That is

$$p = u_1 \sin \theta_1 = u_2 \sin \theta_2 \quad \text{.....3.4}$$

note that this is simply the seismic version of Snell's law in geometrical optics. Equation 3.4 can also be obtained from Fermat's principle, which states that the travel time between two points must be stationary with respect to small variations in the ray path.

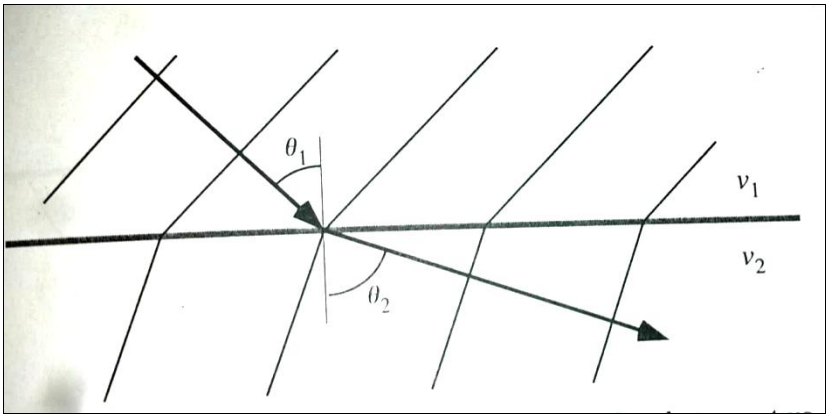

Fig.3.2: A plane wave crossing a horizontal interface between two homogeneous half-spaces

3.2.2 Snell's law for the spherical Earth

In the discussion above, a flat-layered case was considered; which is adequate for modeling crustal arrivals in the upper 30 km of the crust or epicentral distance of up to about 11^0. But the Earth is a sphere and its curvature has to be taken into account at distances greater than about 12°. In this case the ray parameter has to be modified to account for the fact that the ray angle from the radius (the local vertical) changes along the

ray path, even within homogeneous shells. Fig. 3.3 is a sketch of two such spherical shells in a spherically symmetric Earth. At the interface between shell 1 and shell 2, we have from Snell's law

$$u_1 \sin\theta_1(r_1) = u_2 \sin\theta_2(r_1) \quad \text{.....3.5}$$

As the ray travel through shell 2, the incidence angle changes

$$\theta_2(r_1) \neq \theta_2(r_2)$$

therefore, if the ray is projected to its turning point, as if layer 2 continued down, the incidence angle within layer 2 can then be expressed as a function of radius (Shearer, 1999):

$$\sin\theta_2(r) = \frac{r_{min}}{r} \quad \text{.....3.6}$$

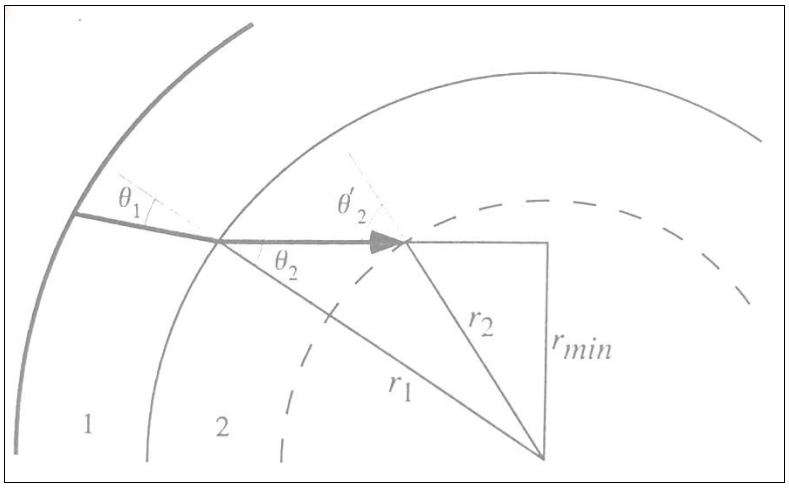

Fig.3.3: The ray geometry for spherical shells of constant velocity

Thus $\theta_2(r_1)$ in equation 3.5 is related to $\theta_2(r_2)$ by the expression

$$r_1 \sin\theta_2(r_1) = r_2 \sin\theta_2(r_2) \quad \text{.....3.7a}$$

or

$$\sin\theta_2(r_1) = \left({}^{r_2}/_{r_1}\right)\sin\theta_2(r_2) \qquad \text{.....3.7b}$$

Substituting this in equation 3.5, we obtain the generalization of Snell's law for spherically symmetric earth given as:

$$r_1 u_1 \sin\theta_1 = r_2 u_2 \sin\theta_2 \qquad \text{.....3.8}$$

In this case, the ray parameter p becomes

$$p_{sph} = r\, u \sin\theta \qquad \text{.....3.9}$$

Recall, in the case of the flat-earth ray parameter, that p is a measure of the horizontal slowness given by:

$$p_f = u \sin\theta = \frac{dT}{dX} \qquad \text{.....3.10}$$

In the spherical Earth, $dX = d\Delta\, r$, where Δ is the angle in radians. Thus

$$p_{sph} = \frac{r dT}{dX} = \frac{dT}{d\Delta} \qquad \text{.....3.11}$$

Note that the spherical-earth ray parameter p_{sph} has units of time (s/radian), whereas the flat-earth ray parameter p_f has units of slowness (time/distance).

3.2.3 Travel times in laterally homogeneous (1-D) media

In most cases the compressional and shear velocities increase as a function of depth in the earth. Consider Fig. 3.4 in which a ray travels down through a series of layers, in each of which the seismic wave is faster than the layer above. The ray parameter remains constant and we have

$$p = u_1 \sin\theta_1 = u_2 \sin\theta_2 = u_3 \sin\theta_3 \qquad \text{.....3.12}$$

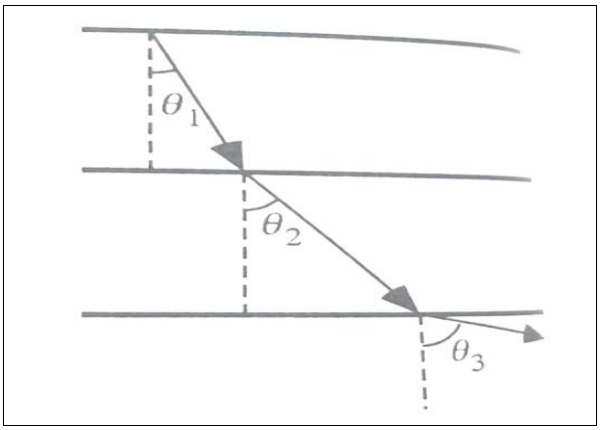

Fig.3.4: Ray travelling downward through a series of layers with velocity increasing with depth

if the velocity continues to increase, θ will eventually equal 90^o and the ray will be travelling horizontally.

For a generalized earth model with series of thin layers of continuous velocity increase with depth, the ray will curve back towards the surface (Fig. 3.5). The ray turning point is defined as the lowermost point on the ray. If the slowness at the surface is u_o and the takeoff angle is θ_o, we have

$$u_o \sin \theta_o = p = u \sin \theta \quad \text{.....3.13}$$

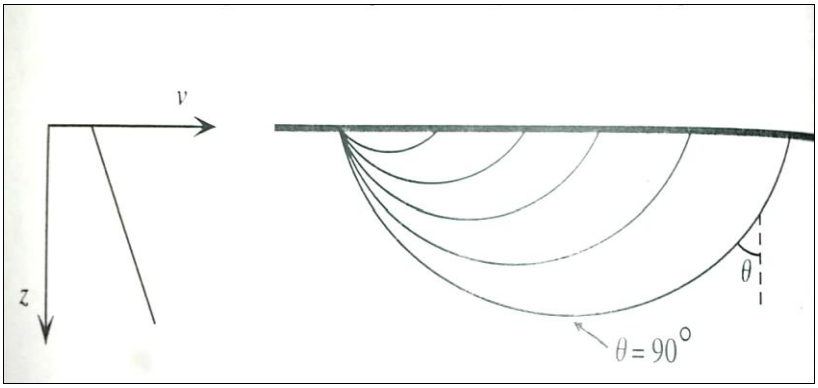

Fig.3.5: Ray paths for a model with a continuous velocity increase with depth

When $\theta = 90^o$, the ray is at its turning point (tp) and the ray parameter, $p = u_{tp}$, where u_{tp} is the slowness at the turning point. Since velocity generally increases with depth in the earth, the slowness decreases with depth.

The Travel time plot, a plot of the first arrival time versus distance, for a model in which the velocity increases with depth is shown in Fig. 3.6. The tangent dT/dX on the curve at any distance X, corresponds to the horizontal slowness u, and thus to the ray parameter p, of that ray which comes back to the surface at X. Each point on the curve results from a different ray path.

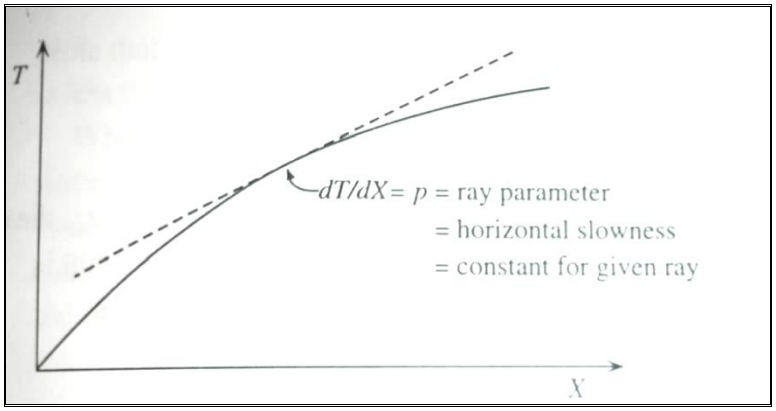

Fig.3.6: Travel time curve for a model with a continuous velocity increase with depth

The travel time and the distance along a particular ray for a flat earth model can easily be computed. To do this, consider the geometry shown in Fig. 3.7 where it can be seen that at each point along the ray, we have

$$\sin\theta = \frac{dx}{ds} = vp \qquad \text{.....3.14}$$

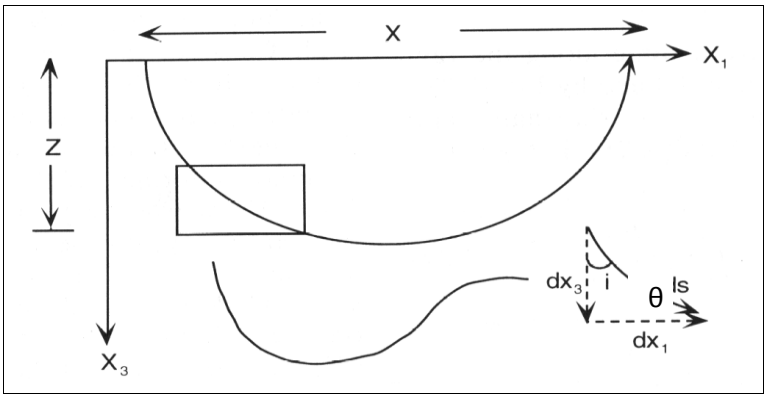

Fig.3.7: Geometry used in computing the travel time and distance for a flat earth model

Remembering that the ray parameter p is constant, and in this case v is the local velocity at a particular depth. From the geometry in Fig. 3.7

$$\cos\theta = \frac{dz}{ds} = \sqrt{1 - \sin^2\theta} = \sqrt{1 - v^2p^2} \quad \text{.....3.15}$$

From equation 3.14

$$dx = ds \sin\theta = \frac{dz}{\cos\theta} vp \quad \text{.....3.16}$$

By integrating equation 3.16 over depth, z

$$X = 2\int_0^z \frac{vp}{\sqrt{1-v^2p^2}}\, dz \quad \text{.....3.17}$$

The Travel time, which is the time it takes the wave to reach and be recorded at a surface seismic station is calculated as

$$T = 2\int_0^z \frac{dz}{v^2\sqrt{u^2-p^2}} \quad \text{.....3.18}$$

This can be rewritten as

$$T = pX + \int_0^z \sqrt{u^2(z) - p^2}\, dz \quad \text{.....3.19}$$

Equations 3.17 and 3.19 allows a prediction of the distance a ray will reach a given point p and velocity structure for a flat earth. The equations are valid for models in which v(z) is a continuous function of depth. For a spherical earth, equations 3.17 and 3.19 can be generalized and thus written as:

$$\Delta = 2\int_{r_1}^{r_0} \frac{vp}{r\sqrt{r^2 - v^2p^2}}\, dr \qquad \ldots\ldots\ldots\ldots\ldots\ldots\ldots\ldots\ldots\ldots\ldots\ldots\ldots\ldots\ldots\ldots 3.20$$

where Δ is the epicentral distance and T the travel time

$$T = p\Delta + 2\int_{r_0}^{r_1} \frac{\sqrt{r^2/v^2(z) - p^2}}{r^2}\, dr \qquad \ldots\ldots\ldots\ldots\ldots\ldots\ldots\ldots\ldots\ldots\ldots\ldots\ldots\ldots\ldots 3.21$$

The first term in equation 3.21 depends only on the horizontal distance, while the second term depends on r(z), that is, the vertical dimension.

3.2.4 Travel time curves and delay times

Generally in the earth, X(p) will increase as p decreases; that is, as the takeoff angle decreases, the horizontal distance increases (Fig.3.8). In this case the derivative dX/dp becomes negative.

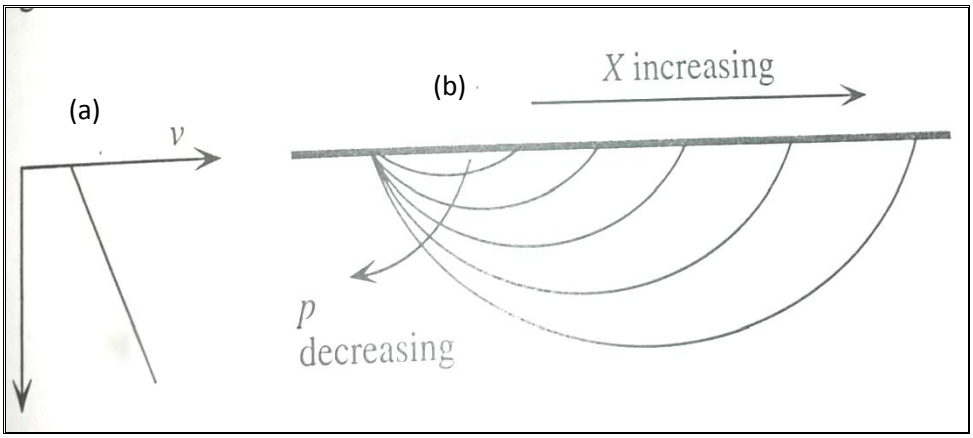

Fig.3.8: (a) Velocity depth profile for continuous velocity gradient (b) as the take-off angle decreases the range also increases (dX/dp <0).

When $^{dX}/_{dp}$ < 0, the branch of the travel time curve can be said to be prograde. Occasionally, because of rapid velocity transition, especially at boundaries in the earth, $^{dX}/_{dp}$ > 0, and the ray turns back (Fig.3.9). Therefore, when $^{dX}/_{dp} > 0$ the travel time curve is termed retrograde. The transition from prograde to retrograde and back to prograde generates a triplication in the travel time curve (Fig.3.10). The endpoints on the triplication are termed caustics. These are points where $^{dX}/_{dp} = 0$, called stationary points (Shearer, 1999).

At large values of p the rays turn at shallow depths and travel only short distances. As the ray parameter p decreases, the turning point depth increases and the range, X, increases. When the turning points enter the steep velocity gradient, X begins to decrease with increasing p as shown in Fig.3.9. Once the rays break through the steep velocity gradient and turn in the shallower depth below, X once again increases with increasing p.

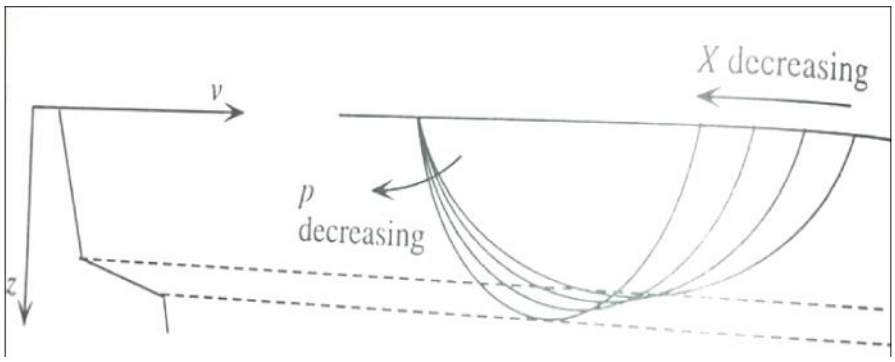

Fig.3.9: Rapid velocity transition at discontinuity boundary as take-off angle increases the range decreases (dX/dp >0)

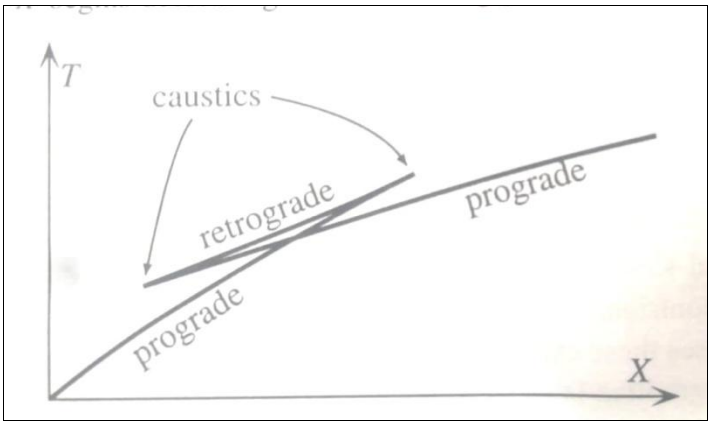

Fig. 3.10: A triplication in a travel time curve resulting from a steep velocity increase

3.2.5 Travel time Inversion

In the preceding section, I have derived expressions for a one-dimensional (1-D) velocity model in which the velocity varies only with depth. In this section, I examine the case where travel times and travel distances have been obtained from observations made at different stations and wish to invert for a velocity structure that can explain the data. Typical method of solving this problem includes, finding an average 1-D velocity-depth function or if enough data are available, we can get a 3-D model from travel time residuals relative to a 1-D reference model. The 3-D model is referred to as seismic tomography. This inversion method is possible only if the number of stations and data are large enough. In this research, based on the number of stations and hence the data available I will restrict myself to 1-D inversion.

Assuming a simple travel time curve (Fig. 3.11) without any triplications or low-velocity zones. Each point on the T(X) curve has a slope, which gives the velocity at the turning

point of the ray. Thus, we know that a particular velocity must be present at the turning point; the problem is to determine where the turning point occurs along the ray path. This is equivalent to assigning a depth to each point along the travel time curve.

The surface-to-surface travel time and distance for a 1-D velocity model (Shearer, 1999) are given as:

$$T(p) = 2\int_0^{z_p} \frac{u^2(z)}{(u^2(z)-p^2)^{1/2}}\,dz \qquad \text{.....3.22}$$

And

$$X(p) = 2p\int_0^{z_p} \frac{dz}{(u^2(z)-p^2)^{1/2}} \qquad \text{.....3.23}$$

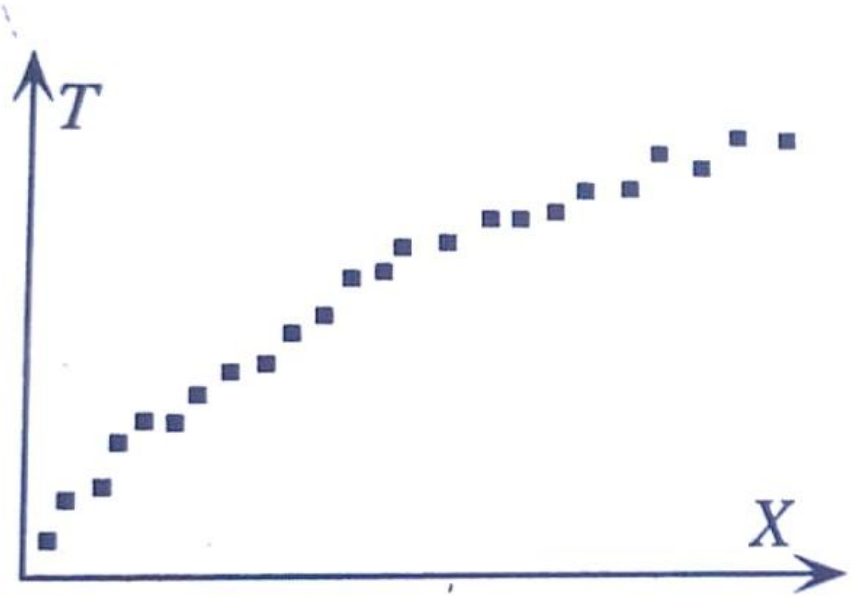

Fig.3.11: Typical example of travel time observations

Assuming we have a complete T(X) curve. P can be obtained by measuring its slope of, thus

$$P = dT/dX$$

and hence X(p) and T(p) as a function of p are also obtained. Our goal is to invert these for u(z). To do this, the equation (3.23) can be put into an analogous form by using u^2 as the integration variable:

$$\frac{X(p)}{2p} = \int_{u_0^2}^{p^2} \frac{dz/d(u^2)}{(u^2-p^2)^{1/2}} d(u^2) \quad \ldots\ldots\ldots\ldots\ldots\ldots\ldots\ldots\ldots\ldots\ldots\ldots\ldots\ldots\ldots\ldots 3.24$$

where u_0 is the slowness at z = 0. Integrating equation (3.24) by parts, we obtain

$$z(u) = \frac{1}{\pi} \int_0^{X(u)} \cosh^{-1}(p/u) dX \quad \ldots\ldots\ldots\ldots\ldots\ldots\ldots\ldots\ldots\ldots\ldots\ldots\ldots\ldots\ldots\ldots 3.25$$

the equation (3.25) is referred to as Herglotz-Wiechert equation (Aki and Richards, 1980). In order to use this equation to obtain a velocity depth function, I selected a value for the slowness u. The upper limit of the integration X(u), represents the range for a ray with ray parameter p = u was obtained from the X(p) curve. The integral was then computed for values of X ranging from 0 to X(u) which gives z(u), that is, the depth to the slowness u. By repeating this calculation for different values of u I can obtain u(z) and thus the desired velocity profile. However the equation (3.25) is seldom used in modern seismology because it assumes a continuous T(X) curve which in practice the travel time data are finite and are somewhat noisy. A typical example is shown in Fig.(3.11), where a small timing shifts results in jitter in the T(X) points and connecting these points with the smooth physically realizable T(X) curve that is expected for a 1-D velocity model is impossible

(Shearer, 1999). The simplest approach to velocity inversion is to fit the travel time data with a series of straight lines (Garmany *et al.*, 1979). The slope of each line determines a seismic velocity, it therefore becomes straight forward to invert the data for a simple model consisting of a small number of homogeneous layers (Fig. 3.12). The model can be obtained most easily by converting each line segment to a point in $\tau(p)$. For a series of homogeneous layers, $\tau(p)$ which is the reduced travel time is given as:

$$\tau(p) = 2\sum_i (u_i^2 - p^2)^{1/2} \Delta z_i \; u_i > p \qquad \ldots\ldots\ldots\ldots\ldots\ldots\ldots\ldots\ldots\ldots\ldots\ldots\ldots\ldots\ldots\ldots 3.26$$

Note that $\tau_1 = 0$ and that the slowness of the top layer is determined by the slope of the first line segment ($u_1 = p_1$) and the slowness of the second layer is set by the slope of the second line segment ($u_2 = p_2$).

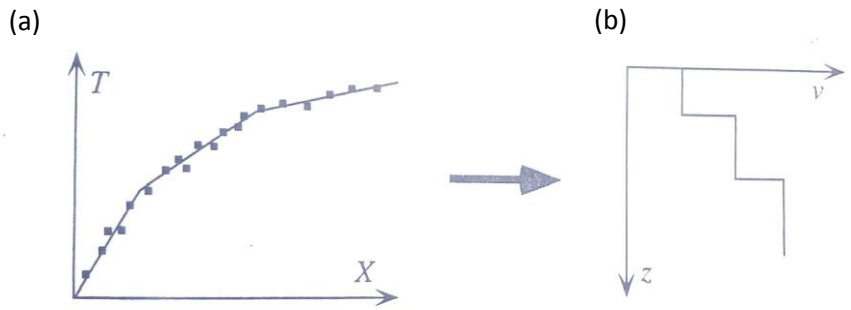

Fig.3.12: (a) Straight lines fit to T(X) data (b) Velocity model (After, Shearer, 1999)

3.2.6 Travel time residuals

Observed travel times typically exhibit some scatter compare to the travel times predicted even by the best reference 1-D earth model. For a particular event, j, recorded at a station i, the absolute travel time residual, R_{ij}, is defined as the difference between the observed travel time and the calculated travel time. It can be formulated as follows:

$$R_{ij}=(t_{ij}-t_{oj})-c_{ij} \quad \text{.....3.29}$$

where,

t_{ij} is the observed arrival time of event j at station i,

t_{oj} is the origin time of event j

c_{ij} is the calculated travel time.

The absolute travel time residuals contain information about the difference of a particular ray path from a standard earth model. Beside this, they are not independent of source characteristics and are affected by the errors because of the mislocated hypocenters. To minimize this kind of effects, relative travel time residuals, r_{ij}, are usually calculated. These are calculated by subtracting the average event absolute travel time from each of the travel time residuals for a particular station in a group of stations (Dorbarth *et al.*, 1986; Oniku, *et al*., 2005).

$$r_{ij} = R_{ij} - R_j \quad \text{.....(3.30)}$$

where, R_j is the mean residual for the events.

In the calculation of the absolute travel time residual, a negative value of residual results from early arrival and is an indicative of faster-than-average velocity structure, while positive residuals are late arrivals, suggestive of slow velocity structure.

3.3 Seismic Instrumentation

Quantitative analysis of seismic disturbances requires that the earth vibrations be instrumentally recorded at observatories spread across the globe. The instrumentation must (1) be able to detect the transient vibrations within a moving reference frame (the instrument moves with the Earth as it shakes); (2) operate continuously with a very sensitive detection capability with precise timing so that the ground motion can be recorded as a function of time, producing a seismogram; and (3) have a fully known linear response to ground motion, or instrument calibration, which allows the seismic recording to be accurately related to the amplitude and frequency content of the causal ground motion. Such a recording system is called a seismograph, and the actual ground-motion sensor that converts ground motions into some form of signal is called a seismometer in earthquake seismology, or a geophone in exploration seismology. The observatories are usually grouped together and this grouping is referred to as network. This is to enhance the data collection. The design and development of seismic recording systems is called seismometry.

3.3.1 Seismograph

These are devices that make a record of seismic waves caused by an earthquake, explosion, or other earth-shaking phenomenon. Seismographs are equipped with elnectromagnetic sensors that translate ground motions into electrical charges which are processed and recorded by analog or digital instruments. A seismograph consists of seismometer (sensor) and recorder (digitizer and data logger). The record of the ground motion as a function of time is referred to as the seismograms. The seismograms provide the basic data with which the seismologists study the elastic waves as they spread through the earth. An example of a modern seismic recording is shown in Figure 3.13. Three orthogonal components of ground motions (up-down, north-south, and east-west) are shown, as are needed to record the total (vector) ground displacement history, at station

Ife (Ile-Ife, Obafemi Awolowo University). The house, which is usually built to specification housing the seismograph, is referred to as seismograph station.

The Nigerian National Network of Seismic Stations (NNNSS), seismographic stations are equipped with state of art seismic instruments, high efficient electrochemical seismometers,

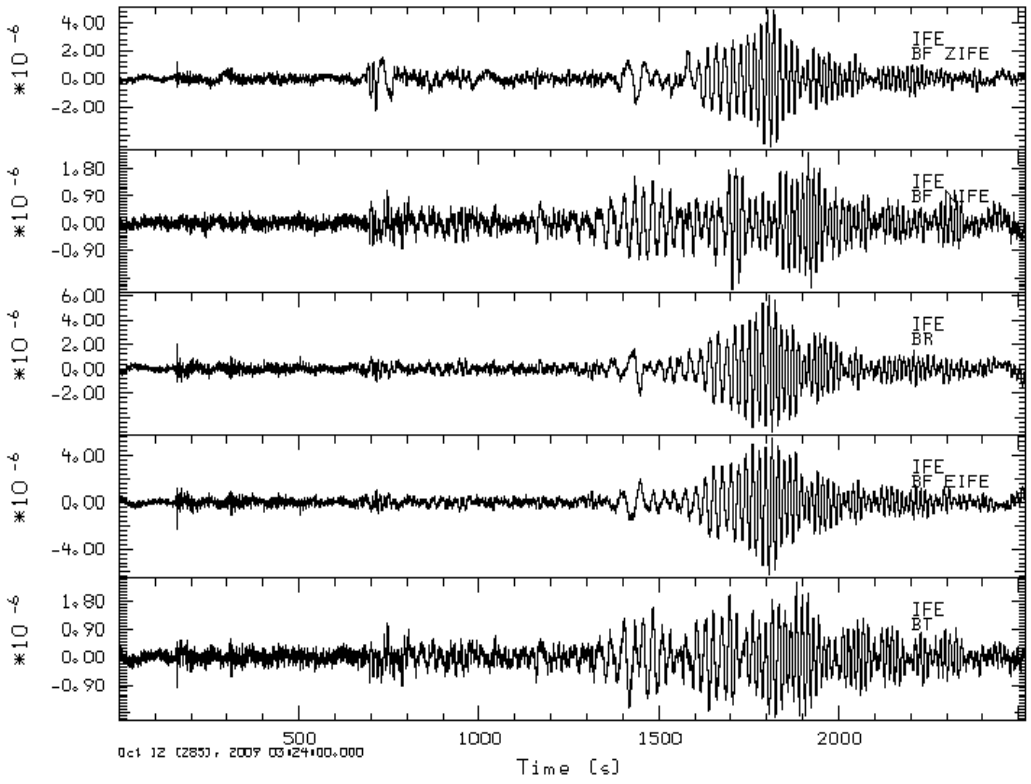

Fig.3.13 Modern seismic recording (Seismogram) taken for IFE station

extremely low power consumption and one unit data acquisition system consisting of digitizer, data logger, communication accessories to ensure real time data transfer, connectors (input/output) and trigger and event detection units. The seismograph stations are remotely located, away from sources of noise such as traffic, ocean waves, human activities, *etc* to minimize noise.

3.3.2 Seismometer

Seismometers, commonly called seismic sensors are instruments that measure motions of the ground, including those of seismic waves generated by earthquakes, nuclear explosions, and other seismic sources. This motion is dynamic and the seismic sensor or seismometer also has to give a dynamic physical variable related to this motion. Since the measurements are done in a moving reference frame (the earth's surface), almost all seismic sensors are based on the inertia of a suspended mass, which will tend to remain stationary in response to external motion. The relative motion between the suspended mass and the ground will then be a function of the ground's motion (Fig.3.14).

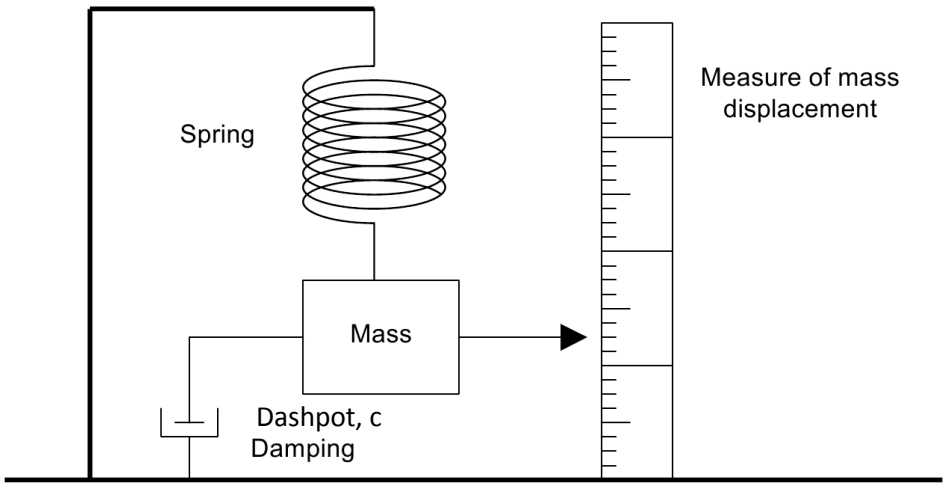

Fig.3.14: The principle behind the inertial seismometer

There are five basic types of seismometers, these are: short period (SP), long period (LP), broadband (BB), very broadband (VBB) and strong motion (accelerometer). The short period seismometers operate on frequency between 1 - 100 Hz and are constructed to have

a very short natural frequency and a correspondingly high resonant frequency which is higher than most frequencies in a seismic wave. Examples are Mark Products L4-3D and Geotech S13.

The long period seismometer sometimes called displacement meter operates on frequency that is less than 1Hz with a very low resonating frequency. The lag between the seismometer and the ground motion becomes zero and the amplitude of the seismometer displacement becomes equal to the amplified ground displacement. Examples of LP are Streckeisen STS-1 and Geotech KS5400.

The broadband seismometer operates in a large band of frequency containing both SP and LP from 100 mHz to 50 Hz. They can be utilized for registering a very wide range of signals and the dynamic range extends from ground noise up to string acceleration such as would come from a very major earthquake, and the periods that can be recorded range from high frequency body waves to the very long period oscillations associated with Earth Tides. Examples are Guralp 3T, Guralp 40T, Geotech KS2000, Nanometrics Trillium Compact, EENTEC's EP105 AND SP400. Very Broadband (VBB) operates in a large band of frequency containing both Short Period and Long Period but a wider band than BB from 10 mHz to 50 Hz**.** Example is EP105, while the Strong motion (Accelerometer) operates in acceleration DC to 200 Hz. Examples are Guralp 5T and Kinemetrics.

The Nigerian National Network of Seismic Stations (NNNSS), uses EENTEC's broadband seismometers (Fig.3.15) at all its stations. These are:

i. EP105 0.0166 – 50 Hz (60sec) – Very broadband

ii. EP105 0.033 – 50 Hz (30sec) – Broadband

iii. SP400 0.06 – 50 Hz (16sec) – Broadband

(a)  (b) 

Fig.3.15: (a) EENTEC SP400 Broadband seismometer, (b) EENTEC EP105 Broadband seismometer (EENTEC, 2003)

The electrochemical nature of EENTEC's seismometers have made them to be characterized by

i. Ruggedness

ii. No need of any maintenance (mass locking and centering)

iii. Extremely low power consumption

iv. Ability to operate normally at large installation tilts (*i.e.* when the ground is not level).

3.3.3 The theory of how a seismometer works

In order to understand the basic principle upon which a seismometer works, consider a simple seismometer design that detects vertical ground motion. A mass *m*, suspended by a spring of elastic constant k and a dashpot with viscous damping c (Fig.3.14). When the frame of the pendulum is displaced by x(t), the mass moves y(t), and the relative displacement of the mass with respect to the frame is

$$z(t) = y(t) - x(t) \quad \text{.....(3.31)}$$

with respect to a frame of reference system at rest, since the spring and the dashpot are affected only by the relative motion of the frame and the mass z(t) and the equation of motion for the mass is given by

$$m\ddot{y} = -kz - c\dot{z} \quad \text{.....(3.32)}$$

Re-arranging equation 3.32 and dividing through by m, gives

$$\ddot{y} + \frac{c}{m}\dot{z} + \frac{k}{m}z = 0 \quad \text{.....(3.33)}$$

For a system without damping, (c = 0), the solution of equation 3.33 is given by harmonic motion:

$$z(t) = A\sin(\omega_o t) \quad \text{.....(3.34)}$$

the natural frequency of the undamped system is given by

$$\omega_o = \left(k/m\right)^{\frac{1}{2}} \quad \text{.....(3.35)}$$

Substituting ω_o in equ 3.33, we have

$$\ddot{z} + 2\beta\omega_o\dot{z} + \omega_o^2 z = 0 \quad \text{.....(3.36)}$$

Where β is the damping factor (Udias, 1999), given by

$$\beta = \frac{c}{2(km)^{1/2}} \qquad \text{.....(3.37)}$$

if β = 1, the system is critically damped and $c = 2(km)^{1/2}$

for damped system, the solution of equ. 3.36 is

$$z = Ae^{-\beta\omega_o t}\sin\left[\omega_o(1-\beta^2)^{\frac{1}{2}}t + \varepsilon\right] \qquad \text{.....(3.38)}$$

where A (amplitude) and ε (the phase) are constants. Equ (3.38) represent damped harmonic motion of frequency $\omega_o(1-\beta^2)^{\frac{1}{2}}$

if the frame is displaced by x(t), then, on making the substitution y(t) = z(t) + x(t) in equ.(3.32) we obtain

$$\ddot{z} + 2\beta\omega_o\dot{z} + \omega_o^2 z = -\ddot{x} \qquad \text{.....(3.39)}$$

where $\ddot{x}(t)$ is the ground acceleration. Equ(3.39) is called the equation of motion of the seismometer.

3.3.4 Seismic recorder

The seismic recorder consists of the digitizer and the data logger. The digitizer consists of analogue-to-digital Converters (ADC) which is in-built in the seismic recorders and converts the analogue seismic signals to a sequence of digital samples for further processing and storage. There are two important aspects of the digitizer; these are the sample interval (step in time direction) and the resolution (step in amplitude direction), which corresponds to one step in the numerical output from the digitizer. A schematic diagram of a digitizing process is shown in Fig.(3.16), while Fig.(3.17) is a typical analogue to digital conversion process diagram (Havskov, 2002). Digitizers are usually

classified as 12 bit, 16 bit or 24 bit signifying the number of discrete values of the digitizer uses.

For example, a digitizer of 24 bit is equated to 144.5 dB and can be computed thus:

$= \quad 20\log (2^{24})$

$= \quad 20\text{Log}(16777216)$

$= \quad 144.4943979187109662 \text{ dB}$

$= \quad 144.5 \text{ dB}$

The data logger, also referred to as the recorder is the storage medium in form of a hard disk where all the event signals from seismic events monitored are stored. All recorders also have an additional facility for recording the time of event. The digitizer and the recorder are often one unit referred to as EENTEC DR4000 (Fig.4.6).

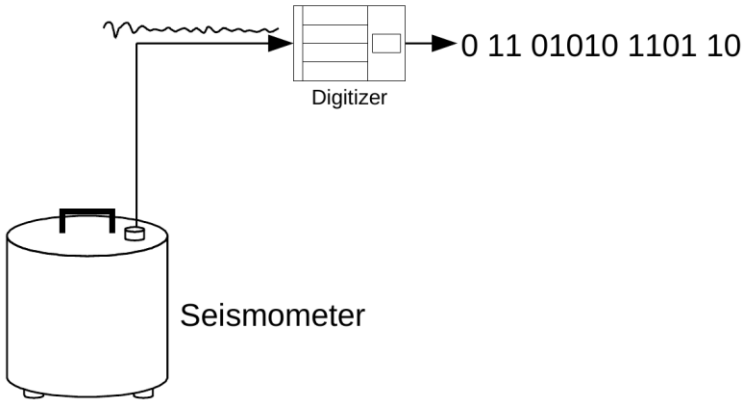

Fig.3.16: Schematic diagram of a digitizing process (Adapted from Havskov *et al.*, 2002)

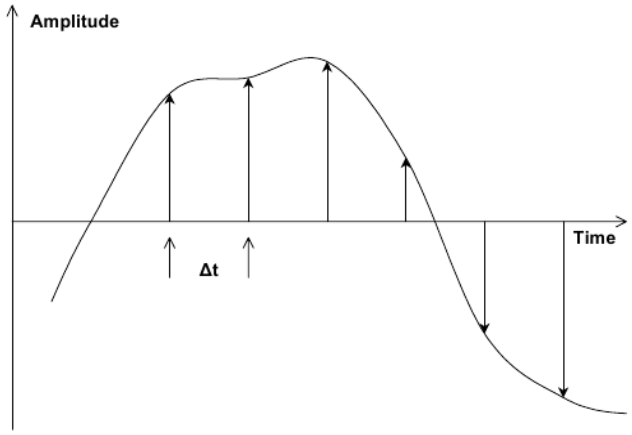

Fig.3.17: Schematic diagram of a typical analogue to digital conversion process. (Havskov**,** *et al*., 2002)

Fig.3.18: EENTEC DR-4000 Seismic data Acquisition System (EENTEC, 2003)

3.3.5 Seismic signal processing

In the preceding sections, seismic recording and seismic data storage technique were discussed. Seismic signals which are product of earthquake data are mostly in digital form and this has afforded seismic data analyst many options for viewing the data in different ways and performing advance signal processing tasks. Signal processing is necessary because of the noise associated with most earthquake data and the contributions from the component elements of the seismograph. The following processes are the major techniques applied in the processing of earthquake data to obtain a noise free signal:

1. Filtering
2. Removal of instrument response
3. Rotation of seismogram component
4. Re-sampling
5. Correlation

3.4 Seismic station location

Seismic equipments are not just located anywhere outside on the field, but requires a carefully selected site based on the aim and objectives or the subsequent uses of observed data. But the main goal in station location is to achieve a sensor installation which is as insensitive to ambient noise sources (human and environment) as possible. This is to ensure that the sensitivity for earthquake generated signal is high. In other words, the station should be as far away from the oceans and humans activities as possible.

When setting up a new station, they can be either part of a local or regional network, or each one can be a single station which can be part of a global network. Stations that are part of a local network cannot be located anywhere, since the network must have some optimal configuration in order to best locate events in the given region. Within the NNNSS networks, the stations are located in triangulations so as to be able to calculate earthquake epicentres once they occur. Since stations are remotely located, adequate power is required for the equipment. Solar power option has been considered for NNNSS.

It is important to install all sensors on basement rock, if possible. The depth of the installation is then only important to the extent of eliminating low frequency noise caused mainly by temperature changes. Short period sensors are even sometimes installed in concrete over-ground bunkers, which at the same time serve as housing for equipment and a secure installation. If there is no hard rock within the area, it is always an advantage to put the sensor (any kind) few meters underground. Vaults are usually constructed for the sensor. Fig.3.19 shows examples of vaults for BB from the GEOFON network while structures built to specification were provided to house the seismic recorder and the power batteries.

3.5 Seismic network

The three main purposes of seismic networks are for seismic alarm, or general or specific seismic monitoring, and research on the interior of the Earth. However, the very first and most basic goal is the determination of accurate earthquake locations. For that purpose, generally at least three stations are needed to form a triangulation. The seismic alarm function, which requires an immediate response after strong earthquakes, serves civil

defense purposes with the goal of mitigating the social and economic consequences of an earthquake with a probability to cause some damages or destruction.

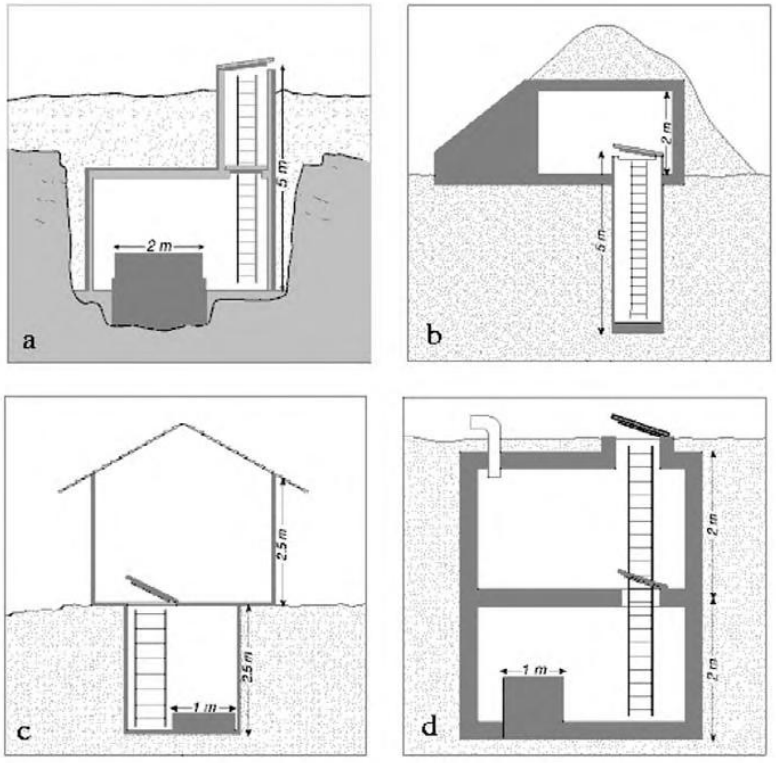

Fig. 3.19: Example of BB vaults from the GEOFON network

Seismic monitoring aides in the long-term mitigation of seismic risk in a region or country as well as resolving the seismotectonics. Seismic hazard maps of the region can be produced to aid the development and implementation of proper building codes. Some cases of seismic monitoring related to seismic risk caused by human activity are of special political concern. This includes monitoring for seismicity induced by large dams or around large mines. Monitoring of seismicity in a volcanic region is also dedicated to volcanic risk mitigation through the prediction of eruptions. Another important function of seismic

networks is for explosion monitoring, particularly underground nuclear explosions. Seismic networks are one of the most important tools used in monitoring the international nuclear test ban treaty. Local, regional and global research into the Earth's interior is the oldest goal of seismology. Seismic networks are and will probably forever be the only tool that enables study of the detailed structure and physical properties of the deeper Earth's interior as the seismic wave travels deeper into the earth's interior.

CHAPTER FOUR

Data Collection, Data Correction and Results

4.1 Data Collection

The data set used in this study, consisted of all captured seismic events from July, 2009 to July 2012, at three seismological stations at Ile-Ife, Osun state, Nsukka, Enugu state and Kaduna, Kaduna state all in Nigeria. These stations are maintained among other stations by the Centre for Geodesy and Geodynamics, Toro, Bauchi state and are referred to as the Nigerian National Network of seismic stations. The stations and their elevations are shown in Table 4.1. Four of the stations in Ibadan, Abakiliki, Abuja and Minna are proposed, while Oyo station has been closed down due to faulty equipment. The stations at Toro and Awka did not start working until 2011, therefore, only data from these three stations (Ile-ife, Nsukka and Kaduna) were considered from among other stations because of the consistency of recordings within the period considered. The stations are equipped with 24-bit multi-channel broadband recorders, and 30 seconds period seismometer. The data acquired by the equipment at the stations are recorded in the Miniseed format developed by Incorporated Research Institutions for Seismology (IRIS) at a sampling rate of 40 samples per second (sps).

Other information such as the origin time of event, the theoretical/calculated travel time, epicentral distances, and azimuth were calculated using the travel time calculator (neic.usgs.gov/cgi-bin/tt/compute_tt.cg) (specimen1). The calculator is based on IASP91 velocity model.

The travel time data for all the events was obtained by subtracting the origin time (time of occurrence) T_o, of event from the observed arrival time T_a, of the event at the station, given by:

$$t_o = T_a - T_o \qquad \ldots\ldots\ldots\ldots\ldots\ldots\ldots\ldots\ldots\ldots\ldots\ldots\ldots\ldots\ldots\ldots\ldots\ldots\ldots\ldots\ldots\ldots 4.1$$

Table 4.1: Seismographic stations in Nigeria

S/no	Station name	Latitude	Longitude	Elevation (m)
1	Oyo	07^o 53.131'N	03^o 57.078'E	295
2	Ibadan	07^o 27.251'N	03^o 53.520'E	193
3	Ile-Ife	07^o 32.800'N	04^o 32.815'E	289
4	Awka	06^o 14.561'N	07^o 06.693'E	50
5	Nsukka	06^o 52.011'N	07^o 25.045'E	430
6	Abakiliki	06^o 23.453'N	08^o 01.474'E	82
7	Abuja	08^o 89.126'N	07^o 23.380'E	432
8	Toro (Central)	10^o 03.303'N	09^o 07.089'E	882
9	Kaduna	10^o 26.101'N	07^o 38.484'E	668
10	Minna	09^o 30.702'N	06^o 26.411'E	203

Specimen 1: Earthquake Travel Times Calculator

Generate a listing of the times that phases arrived at your seismic station from a specified earthquake.

Seismic station coordinates:

Latitude [ ]
-90,+90 decimal degrees north positive, south negative

Longitude [ ]
-180,+180 decimal degrees east positive, west negative

Location and origin time of the earthquake:

Latitude [-22.00]

Longitude [-176.90]

Depth (km) [166.0]

Hour, minute, and second of event (eg: 221257)
[000000]

Magnitude of event (eg 5.5) [5.5]

Phases:

- (•) P, Pdiff, PKP, and PKiKP
- ( ) P, Pdiff, PKP, PKiKP, S, Sdiff, and SKS
- ( ) All branches

[COMPUTE] [Reset to Default Values]

Earthquake Travel Time Information and Calculator

Travel times are based on the IASP91 earth model (Kennett, and Engdahl, 1991), Traveltimes for global earthquake location and phase identification.

The absolute travel time residual was obtained from the difference between the observed travel time t_o, and the calculated (theoretical) travel time, calculated based on the travel time calculator (specimen I). However, the absolute travel time residual is affected by the contributions from the earth structures near the earthquake source region, the lateral in-homogeneity along the travel path within the upper or lower mantle and the station region variation in crustal materials. Therefore, in this work we tried to remove the contributions due to the earthquake region and the effect due to lateral in-homogeneity along the travel path by calculating the relative travel time for each event reporting at each of the station as presented in the section below.

4.2 Data Correction

To use the data so obtained and carryout the analysis as required in this work, some corrections must be applied on the relative station residuals. This is because the differences of elevations of the stations and the latitudes of the events might have contributed to the errors in the residuals (Yazici, 1989).

Firstly, a travel time correction for elevation, dt, must be applied by subtracting, dt from the absolute residuals for each station. The correction is computed using the following formula.

$$dt = \frac{h \cos\theta}{v_0} \qquad \text{.....(4.2)}$$

and

$$\sin\theta = \frac{v_0}{v_1} \qquad \text{..... (4.3)}$$

where,

h is the elevation of the station in km

θ is the incidence angle,

v_o is the velocity of the sedimentary cover and,

v_1 is the velocity of the layer beneath the sedimentary layer

In this work we have assumed the compressional wave velocity values of v_o and v_1 as 0.625 km/s and 1.7 km/s, respectively. The assumed values are based on average value for surface soil and the weathered basement compressional wave velocities obtained by Osemeikhian and Asokhia, (1990). This was applied to all the data collected.

Secondly, ellipticity correction for travel time was applied by adding the effect to the relative station residuals for each event. A simple formula for calculating the ellipticity correction (in seconds) given by Dziewonski and Gilbert (1976), which take into consideration the various normalization of Legendre functions. The formula is given as:

$$dt = \frac{1}{4}(1 + 3\cos 2\theta)\tau_o(\Delta) + \frac{\sqrt{3}}{2}\sin 2\theta \cos\varepsilon\, \tau_1(\Delta) + \frac{\sqrt{3}}{2}\sin^2\theta \cos 2\varepsilon\, \tau_2(\Delta) \quad \ldots\ldots\ldots(4.4)$$

where, θ is the epicentral co-latitude,

Δ is the epicentral distance and,

ε is the azimuth from the epicenter to station.

The ellipticity correction coefficients, $\tau_m(\Delta)$, computed at 5^o intervals in epicentral distance as recommended by the author is given in Table 4.2 below.

Table 4.2: Ellipticity coefficients for the P phases (After Dziewonski and Gilbert, 1976)

Epi dist (Δ)	τ_o	τ_1	τ_2
20	-0.63	-0.16	-0.06
25	-0.63	-0.23	-0.10
30	-0.65	-0.28	-0.15
35	-0.66	-0.33	-0.20
40	-0.66	-0.37	-0.26
45	-0.64	-0.39	-0.32
50	-0.61	-0.40	-0.40
55	-0.58	-0.39	-0.47
60	-0.54	-0.35	-0.54
65	-0.51	-0.29	-0.60
70	-0.47	-0.22	-0.67
75	-0.45	-0.12	-0.72
80	-0.44	-0.01	-0.76
85	-0.45	-0.12	-0.80
90	-0.47	-0.25	-0.81
95	-0.51	-0.39	-0.82

4.3 Results

All the events used in this research work were those carefully selected from the seismograms recorded at the three stations under considerations for the period July 2009 to July 2011. These events and their locations are plotted on the world map (Fig. 4.1). The red triangles represent the stations while red squares are the event epicenters. The table showing the detail of the earthquake location and regions is shown in Appendix I.

The plot of the arrival times versus the epicentral distance in degree for events reporting at each of the stations are shown in Fig. 4.2 to fig. 4.4. A comparison of the plot with a standard reference plot IASP91 (Kenneth and Enghal, 1991) given in Fig. 4.5 shows that the P-phases reporting at the stations are P, P-diffracted and PKP. The P-phases are in the epicentral range of approximately 30^o to 90^o, as there are no events in the epicentral

distance 0^{o} to 30^{o} indicative of events at teleseismic distances. Based on the aim and objectives of this work and the unambiguous nature of P-phases associated with its clear onset only P-phases will be employed for this work.

Teleseismic P-wave travel time residuals find useful applications in the study of crustal and upper mantle structure especially with regards to the geodynamics processes taking place in these regions.

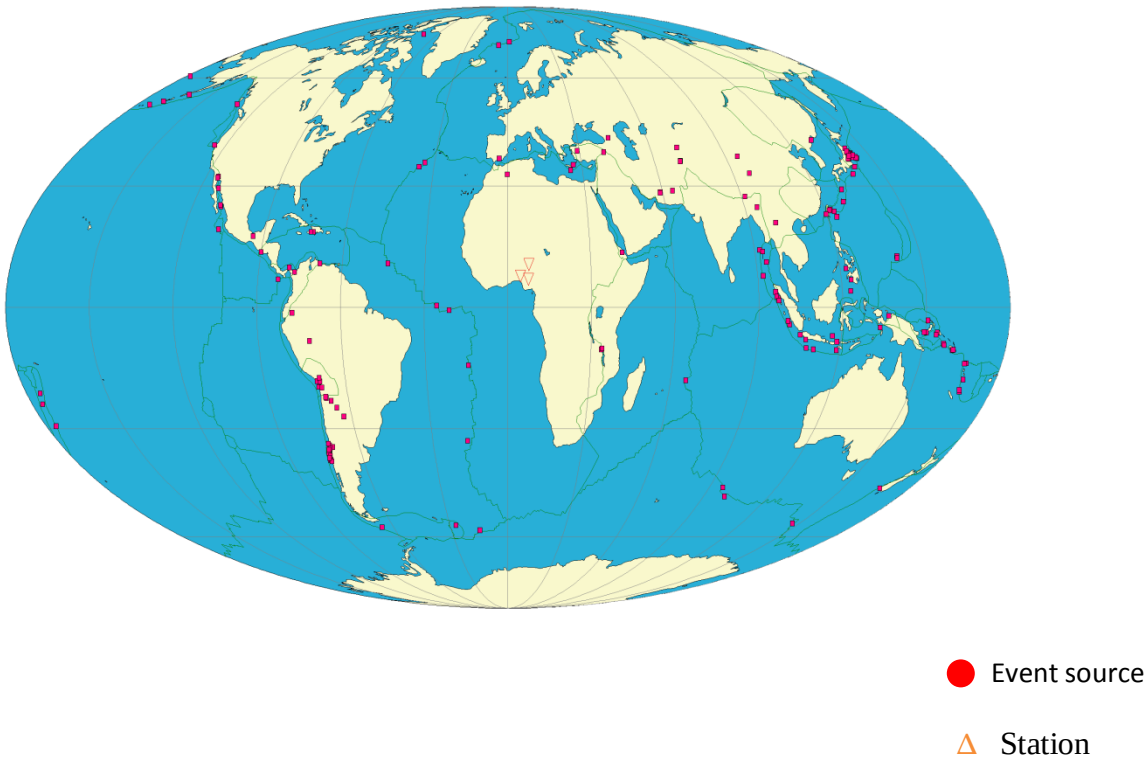

Fig.4.1: Earthquake locations from July 2009 to July 2011 obtained from the seismograms for the three stations

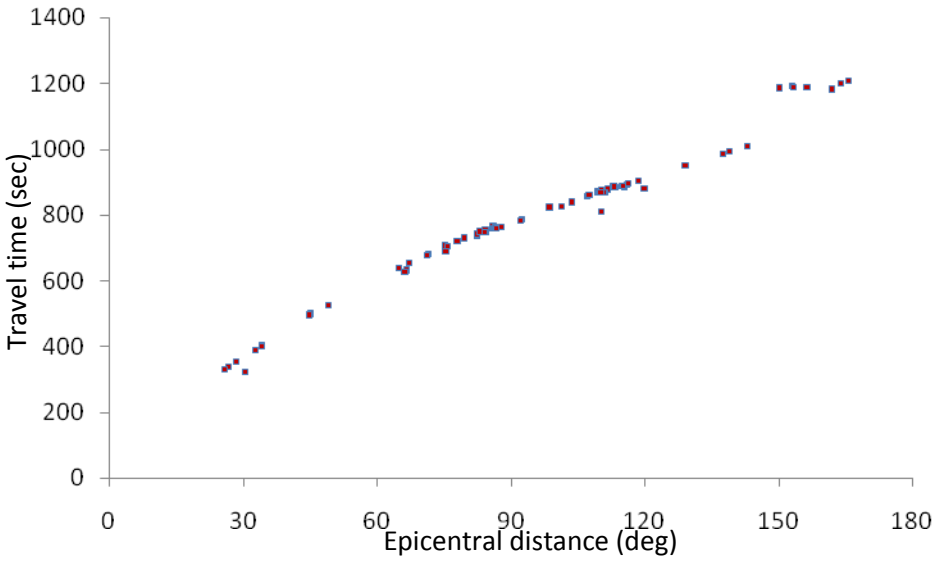

Fig.4.2: Travel time versus epicentral distance plot for IFE station

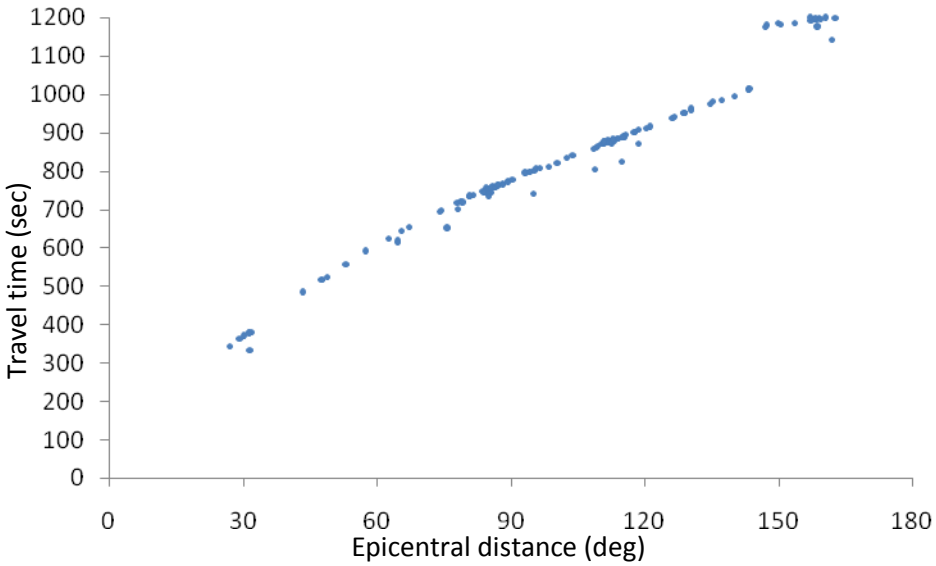

Fig.4.3: Travel time versus epicentral distance plot for NSUKKA station

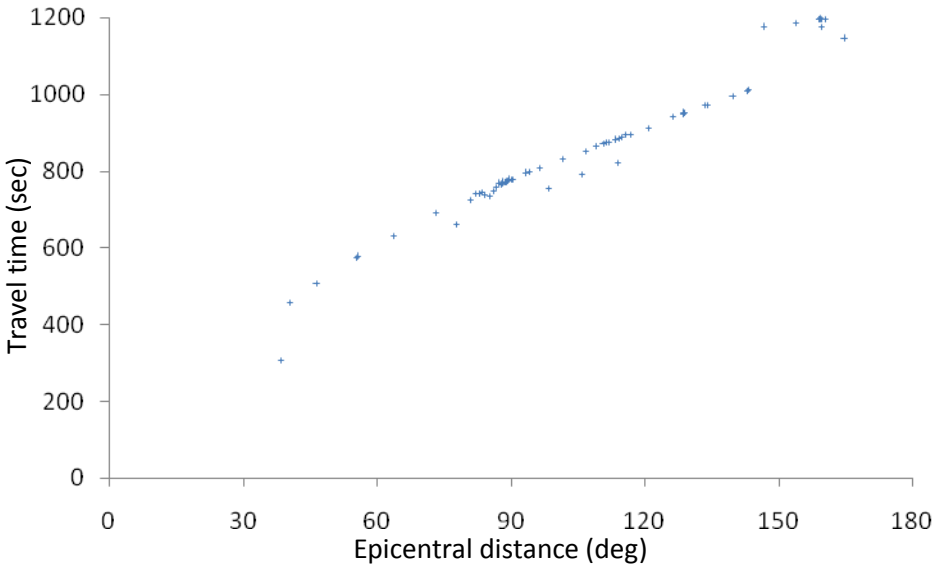

Fig.4.4: Travel time versus epicentral distance plot for KADUNA station

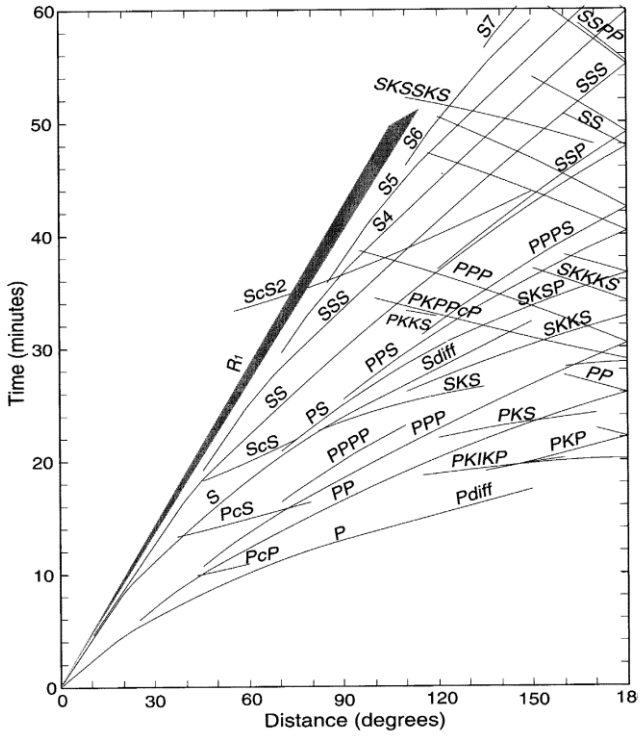

Fig.4.5: Travel time versus epicentral distance curves calculated using IASP91 velocity model (Kenneth and Engdahl, 1991).

The travel time residuals is an indication of the regional deviation of travel times from the standard reference earth model, therefore, the absolute travel time residual was calculated for each of the event. The results of residuals for each of the stations are shown, Table 4.3 for Ile-Ife, Table 4.4 for Nsukka and Table 4.5 for Kaduna. From the tables, absolute travel time residual for Ile-Ife varies between -0.52 s and 4.93 s with an average value of 1.93 ± 0.9 s, while that of Nsukka varies between -1.15 s and 4.45 s with an average value of 2.27 ± 1.4 s and Kaduna varies between -0.35 s and 4.86 s with an average value of 2.45 ±1.3 s.

The results obtained are fully interpreted and discussed in chapters six and seven respectively.

Table 4.3: Absolute travel time residuals for IFE station

Date	Lat (deg)	Long(deg)	T(obs) sec	T(calcu) sec	Tt residual	Epi dist(deg)	bazi(deg)	depth(km)
20090701	34.1	25.4	391.59	390.07	1.52	32.75	33.2	30
20090704	9.7	-79.0	740.06	737.51	2.55	82.39	278.8	43
20090707	75.3	-72.2	727.21	726.43	0.78	79.42	345.4	10
20090810	14.0	92.0	763.81	760.32	3.49	86.67	76.4	33
20090820	72.3	1.0	640.03	639.97	0.06	64.77	358.8	2
20090828	37.7	95.0	762.63	759.93	2.70	85.87	52.7	10
20090907	42.7	43.5	528.19	526.89	1.30	49.03	37.9	10
20090912	10.7	-68.0	682.32	681.06	1.26	71.52	278.8	10
20090921	27.3	91.4	751.21	750.38	0.83	83.87	63.3	7
20091022	36.5	70.9	630.91	629.38	1.53	66.63	53.5	196
20091022	6.8	-82.6	763.00	761.92	1.08	86.27	276.7	10
20091029	36.5	70.9	628.63	627.73	0.90	66.47	53.5	202
20091104	36.1	-33.9	497.28	496.50	0.78	45.14	314.8	10
20091113	-19.4	-70.2	721.73	719.84	1.89	78.22	248.4	10
20091114	-22.9	-66.6	690.88	689.70	1.18	75.67	244.1	141
20091126	13.5	-89.9	786.98	787.20	-0.22	92.52	283.9	37
20091206	-10.2	33.8	406.55	404.35	2.20	34.06	120.7	10
20091209	-0.7	-21.1	341.28	340.22	1.06	26.80	253.4	10
20091214	33.0	-0.2	331.93	331.89	0.04	25.74	350.9	2
20091219	-9.9	34.0	399.35	399.87	-0.52	34.09	120.0	47
20100105	-58.0	-14.9	656.44	654.59	1.85	67.25	191.0	10
20100112	18.4	-72.0	705.17	703.24	1.93	75.28	287.0	10
20100117	-57.0	-65.9	761.97	760.75	1.22	86.03	210.5	10
20100120	18.4	-72.9	710.52	706.13	4.39	75.76	287.1	9
20100127	-14.1	-14.4	357.03	355.44	1.59	28.50	221.2	10
20100205	-48.0	99.6	823.13	820.35	2.78	98.93	137.4	10
20100227	-35.9	-72.6	751.63	746.84	4.79	84.03	232.7	35
20100228	-34.7	-70.9	743.64	738.40	5.24	82.39	233.6	35
20100305	-36.5	-73.1	752.56	749.66	2.90	84.58	232.1	35
20100308	38.8	40.1	493.4	492.94	0.46	44.69	40.3	10
20100311	-34.3	-71.9	748.18	745.74	2.44	83.09	234.1	11
20100316	-36.2	-73.2	753.36	749.59	3.77	84.57	232.5	35
20100328	-35.0	-72.0	748.99	749.31	-0.32	84.05	233.4	35
20100330	13.6	92.9	761.52	759.09	2.53	86.72	76.8	45
20100406	2.2	97.0	789.29	784.42	4.87	92.19	87.5	48
20100411	37.1	-3.5	324.93	323.31	1.62	30.35	347.3	623
20100413	33.3	96.7	768.94	764.01	4.93	87.77	56.9	46

20110514	36.4	70.7	753.36	749.59	3.77	84.57	232.5	207
20110515	0.5	-25.6	341.28	340.22	1.06	26.8	253.4	9
20110519	39.1	29.1	391.59	390.07	1.52	32.75	33.2	7
20110601	-37.5	-73.7	753.36	749.59	3.77	84.57	232.5	15
20110608	-17.1	-69.5	721.73	719.84	1.89	78.22	248.4	101
20110612	13.4	41.7	324.93	323.31	1.62	30.35	347.3	2
20110620	-21.9	-68.3	690.88	689.70	1.18	75.67	244.1	111
20110716	-33.8	-72.1	748.18	745.74	2.44	83.09	234.1	22
20110719	40.1	71.4	628.63	627.73	0.90	66.47	53.5	1
20110727	10.7	-43.4	528.19	526.89	1.30	49.03	37.9	6

Table 4.4: Absolute travel time residuals for NSUKKA station

Date	Lat (deg)	Long(deg)	T(obs)	T(calcu)	Tt residual	Epi dist(deg)	bazi(deg)	depth(km)
20090701	34.1	25.4	383.17	381.72	1.45	31.8	29.1	30
20090704	9.7	-79.0	754.57	752.59	1.98	85.35	279.2	43
20090707	75.3	-72.2	734.63	733.71	0.92	80.77	345.3	10
20090810	14.0	92.0	752.67	747.01	5.66	84.0	76.7	33
20090820	72.3	1.0	644.68	644.65	0.03	65.49	357.8	2
20090828	37.7	95.0	751.94	753.09	-1.15	84.5	52.8	10
20090907	42.7	43.5	518.16	517.38	0.78	47.8	35.9	10
20090912	10.7	-68.0	702.32	698.61	3.71	74.48	279.2	10
20090921	27.3	91.4	739.43	738.4	1.03	81.56	63.5	7
20091022	36.5	70.9	776.48	776.03	0.45	89.22	52.9	196
20091022	6.8	-82.6	617.82	616.96	0.86	64.69	276.7	10
20091029	36.5	70.9	616.88	615.30	1.58	64.53	52.9	202
20091104	36.1	-33.9	516.78	516.31	0.47	47.66	313.7	10
20091113	-19.4	-70.2	736.58	733.29	3.29	80.69	249.1	10
20091114	-22.9	-66.6	704.9	702.82	2.08	78.01	244.9	141
20091126	13.5	-89.9	802.39	800.76	1.63	95.48	284.2	37
20091206	-10.2	33.8	381.22	379.89	1.33	31.26	122.6	10
20091209	-0.7	-21.1	363.97	363.71	0.26	29.43	256.3	10
20091214	33.0	-0.2	342.95	342.83	0.12	26.96	345.8	2
20091219	-9.9	34.0	375.39	375.34	0.05	31.28	121.9	47
20100105	-58.0	-14.9	655.34	654.41	0.93	67.22	192.6	10
20100112	18.4	-72.0	720.69	719.94	0.75	78.28	287.3	10
20100117	-57.0	-65.9	766.42	765.33	1.09	86.97	211.0	10
20100120	18.4	-72.9	726.57	722.72	3.85	78.71	287.4	9
20100127	-14.1	-14.4	369.81	369.11	0.7	30.04	226.1	10
20100205	-48.0	99.6	804.61	809.51	-4.9	96.5	137.5	10
20100227	-35.9	-72.6	758.73	756.52	2.21	85.96	233.3	35
20100228	-34.7	-70.9	753.76	748.49	5.27	84.35	234.2	35
20100305	-36.5	-73.1	763.03	759.14	3.89	86.49	232.7	35
20100308	38.8	40.1	483.94	482.23	1.71	43.36	37.9	10
20100311	-34.3	-71.9	758.2	755.84	2.36	85.08	234.7	11
20100316	-36.2	-73.2	763.57	759.15	4.42	86.5	233.1	35
20100328	-35.0	-72.0	762.35	759.11	3.24	86.0	233.9	35
20100330	13.6	92.9	748.92	745.76	3.16	84.04	77.0	45
20100406	2.2	97.0	775.79	771.11	4.68	89.32	87.9	48
20100411	37.1	-3.5	337.55	334.79	2.76	31.7	343.2	623

20100413	33.3	96.7	758.72	755.66	3.06	85.68	57.1	46
20100503	-38.1	-73.7	768.37	765.02	3.35	87.25	231.3	20
20100505	-4.1	101.1	801.24	797.39	3.85	94.14	93.6	18
20100509	3.7	96.1	774.53	764.57	9.96	88.26	86.5	61
20100525	35.3	-35.9	526.67	524.86	1.81	48.76	311.7	10
20100531	11.1	93.7	744.81	741.46	3.35	85.07	79.5	127
20100612	7.7	92.0	750.67	745.46	5.21	83.76	83.0	35
20100712	-22.2	-68.2	720.44	716.09	4.35	79.4	246.0	91
20100714	-38.0	-73.3	766.70	762.25	4.45	86.92	231.3	28
20100812	-1.3	-77.4	736.61	734.12	2.49	85.01	268.1	189
20100816	-17.8	65.7	624.87	623.82	1.05	62.53	114.0	10
20101025	-3.3	100.5	797.55	793.76	3.79	93.44	92.9	21
20101220	28.4	59.1	560.38	558.19	2.19	53.23	59.6	12
20110101	-26.8	-63.1	655.34	654.41	0.93	67.22	192.6	562
20110102	-38.4	-73.3	768.37	765.02	3.35	87.25	231.3	16
20110118	28.8	64.0	617.82	616.96	0.86	64.69	276.7	10
20110129	71.0	-6.7	560.38	558.19	2.19	53.23	59.6	2
20110204	24.6	94.7	655.34	654.41	0.93	67.22	192.6	88
20110211	-36.4	-73.0	744.81	741.46	3.35	85.07	79.5	18
20110214	-35.4	-72.7	763.57	759.15	4.42	86.5	233.1	25
20110306	-18.1	-69.4	758.72	755.66	3.06	85.68	57.1	87
20110306	-56.4	-27.0	655.34	654.41	0.93	67.22	192.6	86
20110322	-33.1	-16.0	526.67	524.86	1.81	48.76	311.7	14
20110324	20.7	100.0	776.48	776.03	0.45	89.22	52.9	10
20110401	35.5	26.6	375.39	375.34	0.05	31.28	121.9	60
20110402	-19.6	-69.1	720.44	716.09	4.35	79.4	246.0	83
20110406	1.7	97.2	776.48	776.03	0.45	89.22	52.9	18
20110407	17.4	-94.0	801.24	797.39	3.85	94.14	93.6	167
20110514	36.4	70.7	617.82	616.96	0.86	64.69	276.7	207
20110515	0.5	-25.6	337.55	334.79	2.76	31.7	343.2	9
20110519	39.1	29.1	483.94	482.23	1.71	43.36	37.9	7
20110601	-37.5	-73.7	763.57	759.15	4.42	86.5	233.1	15
20110608	-17.1	-69.5	720.44	716.09	4.35	79.4	246.0	101
20110612	13.4	41.7	483.94	482.23	1.71	43.36	37.9	2
20110620	-21.9	-68.3	768.37	765.02	3.35	87.25	231.3	111
20110716	-33.8	-72.1	763.57	759.15	4.42	86.5	233.1	22
20110719	40.1	71.4	748.92	745.76	3.16	84.04	77.0	1
20110727	10.7	-43.4	526.67	524.86	1.81	48.76	311.7	6

Table 4.5: Absolute travel time residuals for KADUNA station

Date	Lat (deg)	Long(deg)	T(obs)	T(calcu)	Tt residual	Epi dist(deg)	bazi(deg)	depth(km)
20090701	34.1	25.4	354.73	353.86	0.87	28.64	31.9	30
20090912	10.7	-68.0	699.26	696.69	2.57	74.15	278.2	10
20090921	27.3	91.4	729.93	729.03	0.90	79.81	64.0	7
20091022	36.5	70.9	603.99	602.10	1.89	62.42	54.3	196
20091022	6.8	-82.6	775.35	775.06	0.29	89.01	276.7	10
20091029	36.5	70.9	601.46	600.42	1.04	62.26	54.3	202
20091104	36.1	-33.9	500.19	498.80	1.39	45.43	311.1	10
20091113	-19.4	-70.2	742.41	741.06	1.35	82.16	248.7	10
20091114	-22.9	-66.6	713.99	712.11	1.88	79.72	244.4	141
20091126	13.5	-89.9	801.57	797.67	3.90	94.80	284.6	37
20091206	-10.2	33.8	398.18	396.17	2.01	33.12	127.4	10
20091209	-0.7	-21.1	377.88	374.40	3.48	30.64	250.6	10
20091214	33.0	-0.2	312.43	312.35	0.08	23.60	343.4	2
20091219	-9.9	34.0	390.95	391.30	-0.35	33.10	126.7	47
20100105	-58.0	-14.9	678.34	676.18	2.16	70.72	192.4	10
20100112	18.4	-72.0	716.15	715.29	0.86	77.40	286.6	10
20100117	-57.0	-65.9	781.30	780.16	1.14	90.10	211.0	10
20100120	18.4	-72.9	721.45	718.09	3.36	77.87	286.7	9
20100127	-14.1	-14.4	394.43	392.69	1.74	32.72	222.3	10
20100205	-48.0	99.6	824.30	820.49	3.81	98.97	137.2	10
20100227	-35.9	-72.6	772.67	767.55	5.12	88.24	233.2	35
20100228	-34.7	-70.9	763.19	759.65	3.54	86.60	234.0	35
20100305	-36.5	-73.1	771.90	770.19	1.71	88.80	232.6	35
20100308	38.8	40.1	460.19	458.71	1.48	40.48	40.3	10
20100311	-34.3	-71.9	769.2	766.75	2.45	87.29	234.6	11
20100316	-36.2	-73.2	771.93	770.11	1.82	88.79	233.0	35
20100328	-35.0	-72.0	770.66	770.00	0.66	88.26	233.8	35
20100330	13.6	92.9	742.99	740.73	2.26	83.06	77.5	45
20100406	2.2	97.0	774.39	769.53	4.86	88.99	88.0	48
20100411	37.1	-3.5	308.41	306.58	1.83	28.40	341.1	623
20100413	33.3	96.7	748.66	743.37	5.29	83.60	57.4	46
20100503	-38.1	-73.7	780.15	776.24	3.91	89.62	231.3	20
20100505	-4.1	101.1	801.45	797.43	4.02	94.14	93.4	18
20100509	3.7	96.1	766.09	762.6	3.49	87.84	86.7	61
20100525	35.3	-35.9	508.64	508.25	0.39	46.63	309.2	10
20100531	11.1	93.7	741.28	737.25	4.03	84.23	79.8	127

20100612	7.7	92.0	745.62	742.26	3.36	83.13	83.4	35
20100712	-22.2	-68.2	728.46	724.91	3.55	81.04	245.5	91
20100714	-38.0	-73.3	781.15	773.61	7.54	89.29	231.3	28
20100816	-17.8	65.7	633.66	632.46	1.2	63.83	115.7	10
20101025	-3.3	100.5	797.05	793.65	3.4	93.41	92.7	21
20101220	28.4	59.1	572.84	570.20	2.64	55.43	60.7	12
20110101	-26.8	-63.1	655.34	654.41	0.93	67.22	192.6	562
20110102	-38.4	-73.3	768.37	765.02	3.35	87.25	231.3	16
20110118	28.8	64.0	617.82	616.96	0.86	64.69	276.7	10
20110129	71.0	-6.7	560.38	558.19	2.19	53.23	59.6	2
20110204	24.6	94.7	655.34	654.41	0.93	67.22	192.6	88
20110211	-36.4	-73.0	744.81	741.46	3.35	85.07	79.5	18
20110214	-35.4	-72.7	763.57	759.15	4.42	86.5	233.1	25
20110306	-18.1	-69.4	758.72	755.66	3.06	85.68	57.1	87
20110306	-56.4	-27.0	655.34	654.41	0.93	67.22	192.6	86
20110322	-33.1	-16.0	526.67	524.86	1.81	48.76	311.7	14
20110324	20.7	100.0	776.48	776.03	0.45	89.22	52.9	10
20110401	35.5	26.6	375.39	375.34	0.05	31.28	121.9	60
20110402	-19.6	-69.1	720.44	716.09	4.35	79.4	246.0	83
20110406	1.7	97.2	776.48	776.03	0.45	89.22	52.9	18
20110407	17.4	-94.0	801.24	797.39	3.85	94.14	93.6	167
20110514	36.4	70.7	617.82	616.96	0.86	64.69	276.7	207
20110515	0.5	-25.6	337.55	334.79	2.76	31.7	343.2	9
20110519	39.1	29.1	483.94	482.23	1.71	43.36	37.9	7
20110601	-37.5	-73.7	763.57	759.15	4.42	86.5	233.1	15
20110608	-17.1	-69.5	720.44	716.09	4.35	79.4	246.0	101
20110612	13.4	41.7	483.94	482.23	1.71	43.36	37.9	2
20110620	-21.9	-68.3	768.37	765.02	3.35	87.25	231.3	111

CHAPTER FIVE

Interpretation of Results

5.1 Introduction

Seismograms are the basic information about earthquakes, chemical and nuclear explosions, mining-induced earthquakes, rock bursts and other earth motion induced events generating seismic waves. Seismograms reflect the combined influence of the seismic source, the propagation path, the frequency response of the recording instrument and the ambient noise at the recording site. Accordingly, our knowledge of seismicity, Earth's structure, and the various types of seismic sources is mainly derived from the analysis and interpretation of seismograms. The more complete we quantify and interpret the seismograms, the more we understand the Earth's structure, seismic sources and the underlying earth's fracture causing processes. In this section, the results obtained from seismograms from the seismic stations as presented in the preceding chapters are interpreted for a better understanding of the crustal and upper mantle structure beneath the stations.

5.2 Earthquake location and distribution

The database for this study consisted of about five hundred and sixty-six (566) events carefully selected from the seismograms recorded at the three stations considered, Nsukka station reported 240 events, and Kaduna station reported 217 events while Ile-Ife station reported 109 events. The events reporting at Ile – Ife station are low because the station did not work for most part of 2010 and some parts of 2011. Nsukka and Kaduna stations have

been very stable since installation. All the reporting events together with their source parameters, regions, origin time and magnitudes are listed in Appendix I. The locations of the events are plotted in Fig. 5.1 – Fig. 5.3 in equidistant azimuthal projection centered on each of the station (Ife, Nsukka and Kaduna). The plots are limited to events in the epicentral range up to 98 degrees. Each concentric ring represents an increment of 20 degree in epicentral distance and the red dots indicate events location. The dots are average location as each dot could indicate more than one event. The plots show that the reporting events at all the stations are mainly from the world earthquake regions around the pacific margin, mid-ocean ridge and other world fracture zones (Shearer, 1999; Thorne and Terry, 1995). All the earthquakes reporting at the stations are large earthquakes with magnitude equal or greater than six (magnitudes ≥ 6).

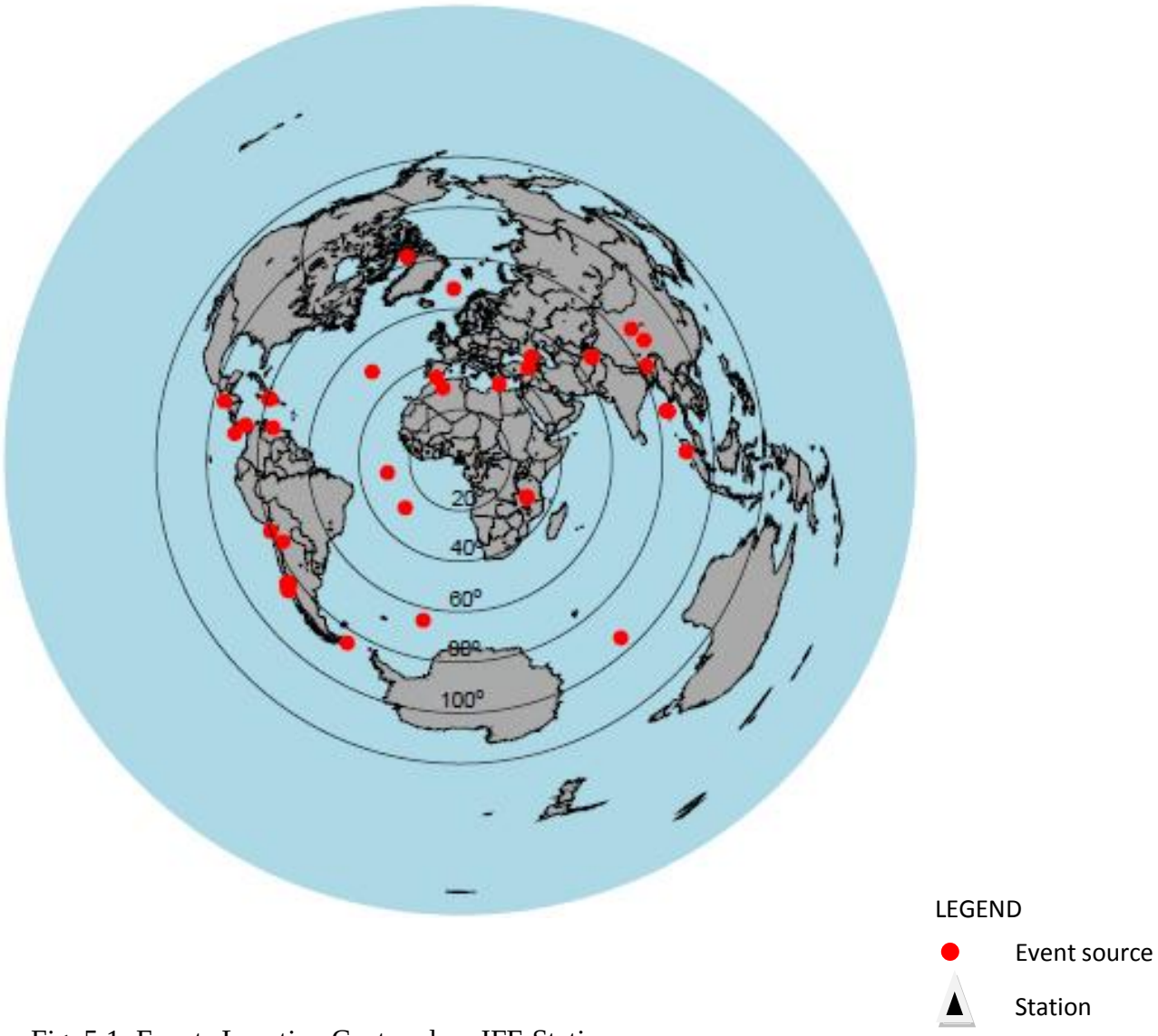

Fig. 5.1: Events Location Centered on IFE Station

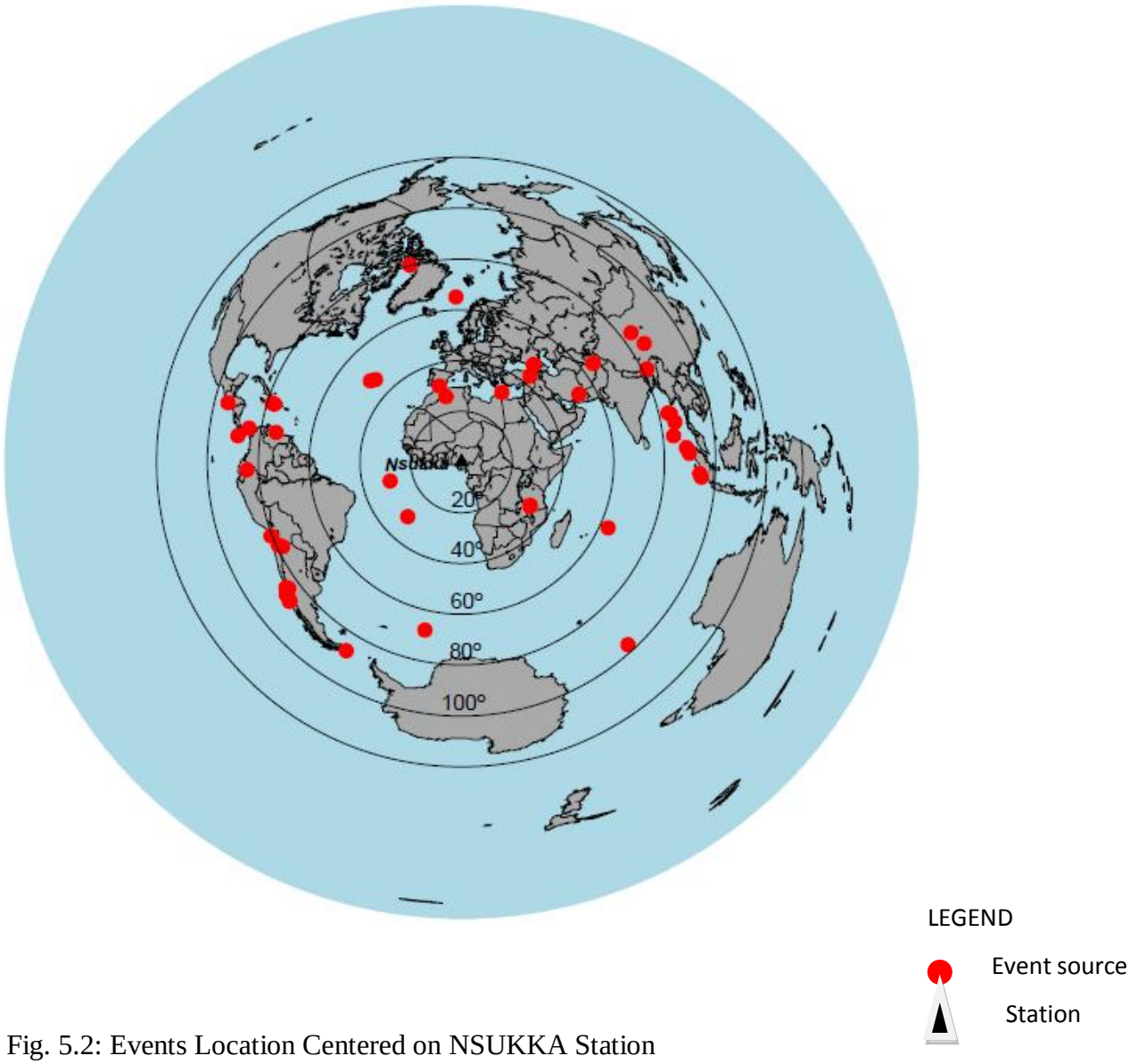

Fig. 5.2: Events Location Centered on NSUKKA Station

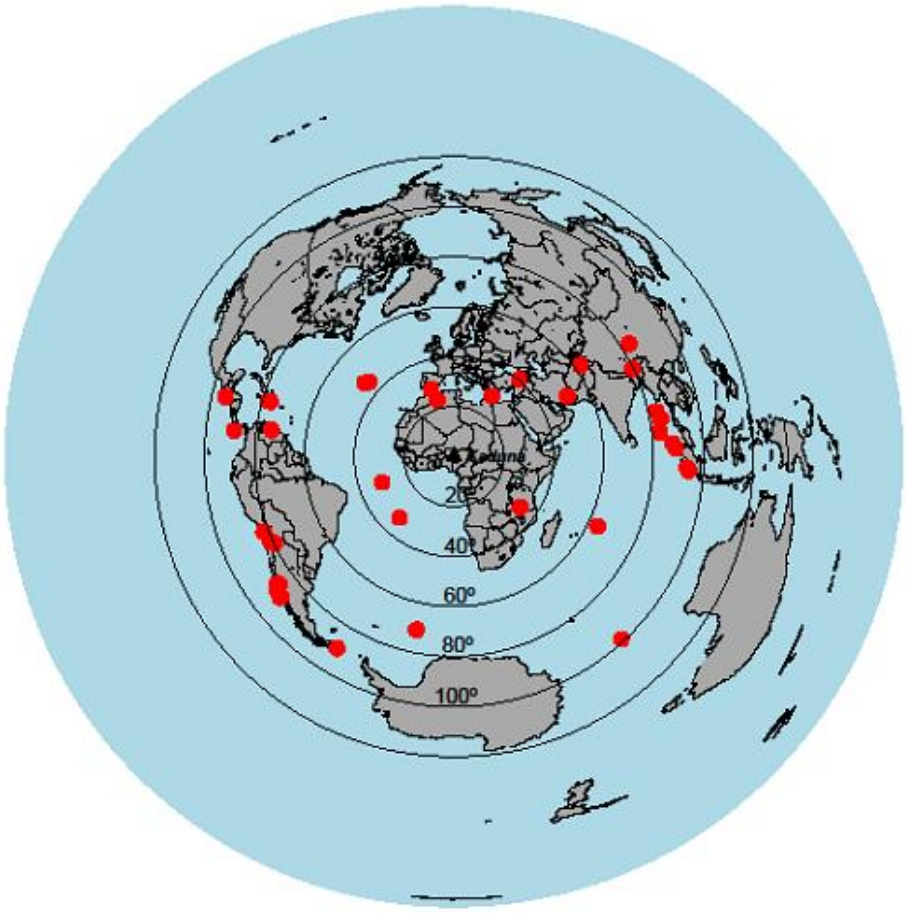

Fig.5.3: Events Location Centered on KADUNA Station

5.3 Travel times

The earthquake travel time is the time taken by an earthquake signal to reach the seismic recording station. It is the difference between the origin time of event and the arrival time of event at the recording station. The travel time for this work was calculated by subtracting the origin time of the event obtained from USGS from the event arrival time at each of our seismic station. The observed travel time is dependent on the distance of the event from the recording station, the dilatants behavior within the stressed medium (*i.e*. the nature of the propagating media) and the external processes such as heat, pressure and other similar effect along the propagation path of the seismic wave (Ojo, 1994). The observed travel times (sec) at each of the stations were then plotted against the epicentral distance (deg) and the results shown in Fig. 4.2 to Fig.4.4. From these plots, it is seen that no P-wave arrival below epicentral distance of 25^{o} which is an indication that there were no local or regional earthquakes. And when compared with Fig.4.5 which is based on theoretical travel time calculation using IASP91 for all seismic phases, it is seen that P-diff (*i.e.* diffracted P-wave) occurs at epicentral distance of about 98^{o}, this is a region of rapid transition which corresponds to a discontinuity boundary (Shearer, 1999). Also at about epicentral distance 148^{o} there is a sudden jump in the travel time and to reappear as PKP-phase (Astiz *et al.*, 1996). This zone of jump corresponds to a shadow zone, indicative of a low velocity zone for which the amplitudes of P-waves are much reduced. Such a shadow zone is an indication of a discontinuity surface.

5.4 Travel time Residuals

The absolute travel time residual for Ile-Ife varies between -0.52 s and 4.93 s with an average value of 1.83 ± 1.3 s, while that of Nsukka and Kaduna between -1.15 s and 4.4 s with an average value of 1.89 ± 1.4 s and -0.35 s and 4.86 s with an average value of 2.17 ± 1.3 s respectively. Both elevation and ellipticity corrections which could affect the residual were applied to the travel time residuals to eliminate the effects due to the elevations of the stations and the ellipticity of the earth at the poles. The travel time residuals calculations were limited to epicentral distance of 98^{o} since we are concerned with P-wave which travels in the crust and the mantle. This now reduces the number of data for the stations, Nsukka (60), Kaduna (52) and Ile – Ife (47), these are then used for our crustal and upper mantle velocity analysis. However, based on (Kennett and Engdahl, 1991; Oniku, 1999) residual values greater than 5.0 s were regarded as gross errors and were also eliminated. The large scatter observed in the values of the absolute residuals is expected and may have been due to changes in propagation paths of the seismic waves and difference in source region, therefore, resulting in large standard deviation of the average residuals. To reduce the scatter, the events originating from the same region were grouped together and the resulting average residuals and the standard deviations calculated and the result shown in Table 5.1. By this method, the errors in residual associated with source effect has been reduced and the changes in the station residuals are associated with the changes in crustal and upper mantle thickness as well as lateral variations in velocity. These, within a fairly homogeneous azimuthal region are the main contributors to the residuals.

Table 5.1: Teleseismic P-wave station absolute travel time residuals

Station	Total event res	Region I(30^o-90^o)	Region II(210^o-270^o)	Region III(270^o-330^o)
Ile – Ife	1.83 ± 1.3 s	1.82 ± 0.6 s	1.81 ± 0.3 s	1.49 ± 0.4 s
Nsukka	1.89 ± 1.4 s	1.83 ± 0.9 s	1.90 ± 0.5 s	1.51 ± 0.7 s
Kaduna	2.17 ± 1.3 s	2.19 ± 0.6 s	2.20 ± 0.5 s	1.68 ± 0.6 s

Region I include earthquakes coming from the azimuthal region between 30^o to 90^o (which include Burma, India, China, Japan and some other parts of Asian regions). The values of the residuals obtained for the region does not show much difference from the result obtained for the whole earthquakes, positive residuals indicating a low velocity structure around this region. Region II includes earthquakes from the azimuthal range between 210^o to 270^o (South America and the Mid-Atlantic regions), the residuals obtained for this region are also similar and values close to the calculated value for the whole earthquakes. This result, indicate the presence of a low velocity structure in the crust around this region. Finally, for region III which also includes events within the azimuthal range 270^o to 330^o (Central America and North America). The residuals in this region even though positive as we have in regions I and II, but are lower in values compared to the whole earthquake, indicating that the low velocity structure in this region are less thick than in other regions.

5.5 Relative travel time Residuals

The absolute travel time residuals discussed in section 5.4 are made up of contributions from the source region, propagation path and station region, except at large epicentral

distances when the source and station effects become small compared to the propagation path effect. This means that the Nigerian National Network of Seismographic Stations data, which are mainly teleseismic, are affected mainly by propagation path effect which could be responsible for the large scatter observed in the values of the absolute travel time residuals. In order to minimize the scatter in the absolute travel time residuals and to determine the station region effect on the absolute residuals, the relative travel time residuals were studied. These were done by comparing relative travel time residuals of some events recorded at the three stations in Ife, Nsukka and Kaduna as presented in Table 5.2. The computation was done by subtracting the average of the absolute residuals of event recorded by the three stations from each absolute residual for the station.

Table 5.2: Relative travel time residual (in sec) for the three stations

Tt residual(Ife)	Tt residual(Nsukka)	Tt residual(Kad)	Mean Tt Res	Rel Tt res(Ife)	Rel Tt res (Nsuk)	Rel Tt res(Kad)
1.52	1.45	0.87	1.28	0.24	0.17	-0.41
2.55	1.98					
0.78	0.92					
3.49	5.66					
0.06	0.03					
2.70	-1.15					
1.30	0.78					
1.26	3.71	2.57	2.51	-1.25	1.20	0.06
0.83	1.03	0.90	0.92	-0.09	0.11	-0.02
1.53	0.45	1.89	1.29	0.24	-0.84	0.60
1.08	0.86	0.29	0.74	0.34	0.12	-0.45
0.90	1.58	1.04	1.17	-0.27	0.41	-0.13
0.78	0.47	1.39	0.88	-0.10	-0.41	0.51
1.89	3.29	1.35	2.18	-0.29	1.11	-0.83
1.18	2.08	1.88	1.71	-0.53	0.37	0.17
-0.22	1.63	3.90	1.77	-1.99	-0.14	2.13
2.20	1.33	2.01	1.85	0.35	-0.52	0.16
1.06	0.26	3.48	1.60	-0.54	-1.34	1.88
0.04	0.12	0.08	0.08	-0.04	0.04	0.00
-0.52	0.05	-0.35	-0.27	-0.25	0.32	-0.08
1.85	0.93	2.16	1.65	0.20	-0.72	0.51
1.93	0.75	0.86	1.18	0.75	-0.43	-0.32
1.22	1.09	1.14	1.15	0.07	-0.06	-0.01
4.39	3.85	3.36	3.87	0.52	-0.02	-0.51
1.59	0.70	1.74	1.34	0.25	-0.64	0.40
2.78	-4.90	3.81	0.56	2.22	-5.46	3.24
4.79	2.21	5.12	4.04	0.75	-1.83	1.08
5.24	5.27	3.54	4.68	0.56	0.59	-1.14
2.90	3.89	1.71	2.83	0.07	1.07	-1.12
0.46	1.71	1.48	1.22	-0.76	0.49	0.26
2.44	2.36	2.45	2.42	0.02	-0.06	0.03
3.77	4.42	1.82	3.34	0.43	1.08	-1.52
-0.32	3.24	0.66	1.19	-1.51	2.05	-0.53
2.53	3.16	2.26	2.65	-0.12	0.51	-0.39
4.87	4.68	4.86	4.80	0.07	-0.12	0.06

1.62	2.76	1.83	2.07	-0.45	0.69	-0.24
4.93	3.06	5.29	4.43	0.50	-1.37	0.86
1.53	0.45	1.89	1.29	0.24	-0.84	0.60
1.08	0.86	0.29	0.74	0.34	0.12	-0.45
1.62	2.76	1.83	2.07	-0.45	0.69	-0.24
2.90	3.89	1.71	2.83	0.07	1.07	-1.12
-0.52	0.05	-0.35	-0.27	-0.25	0.32	-0.08
0.78	0.47	1.39	0.88	-0.10	-0.41	0.51
4.87	4.68	4.86	4.80	0.07	-0.12	0.06
0.04	0.12	0.08	0.08	-0.04	0.04	0.00
2.76	1.62	1.83	2.07	-0.45	0.12	-0.45

The mean relative residual for the stations are; Ife station -0.03 s, Nsukka station -0.13 s and Kaduna station 0.15 s. The relative travel time residual is due mainly to the heterogeneity of the crust and upper mantle structure within the vicinity of the station region. Therefore, the negative relative residual for Ile-Ife and Nsukka stations is an indication of the presence of fast velocity structures in the crust beneath the two stations. However, the low value of the relative residual at Ile-Ife station shows that the crust there may be thinner than that at Nsukka. Kaduna station however has positive relative residuals (+ 0.15 s) indicating the presence of a slow velocity structures within the crust around this station region.

5.6 Velocity Inversion of Travel Time

The observed travel time data form a discrete set of points from which it is required to calculate the velocity as a function of depth (*i.e.* to determine the velocity model which fit the data). Typical method to solving this inverse problem includes, finding an average 1-D velocity-depth function. This was done by fitting a series of straight lines to the travel time

T(X) curves Fig.5.4, Fig.5.5 and Fig.5.6. Each of the travel time data were fitted with three straight line segments leading to models containing three homogeneous layers. The slope and the intercept on the travel time axis were then determined. The slope and the intercept gives the ray parameter, p (or the slowness, u = p = 1/v) and the reduced travel time, τ(p) respectively.

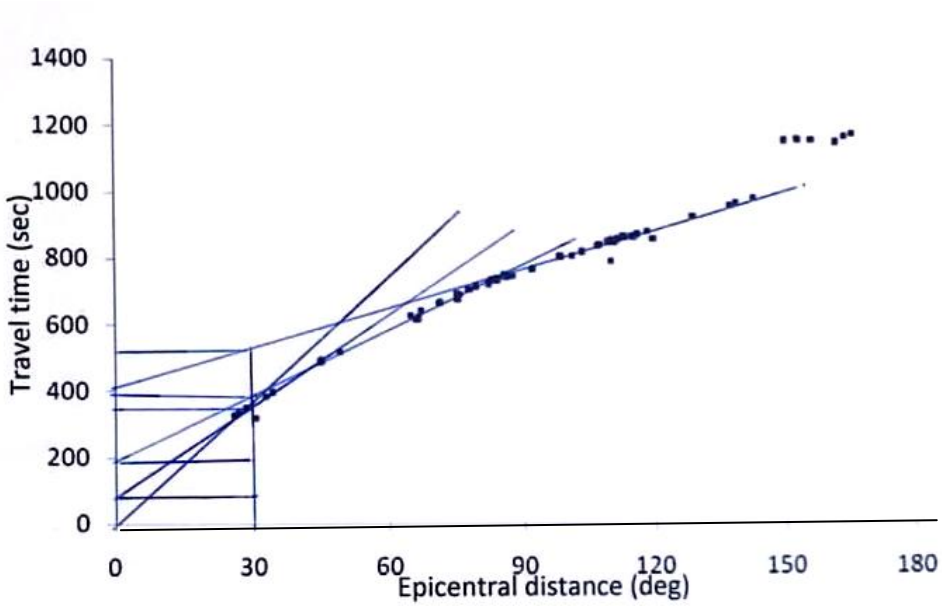

Fig.5.4: Series of straight line fittings on Travel time curve of IFE station

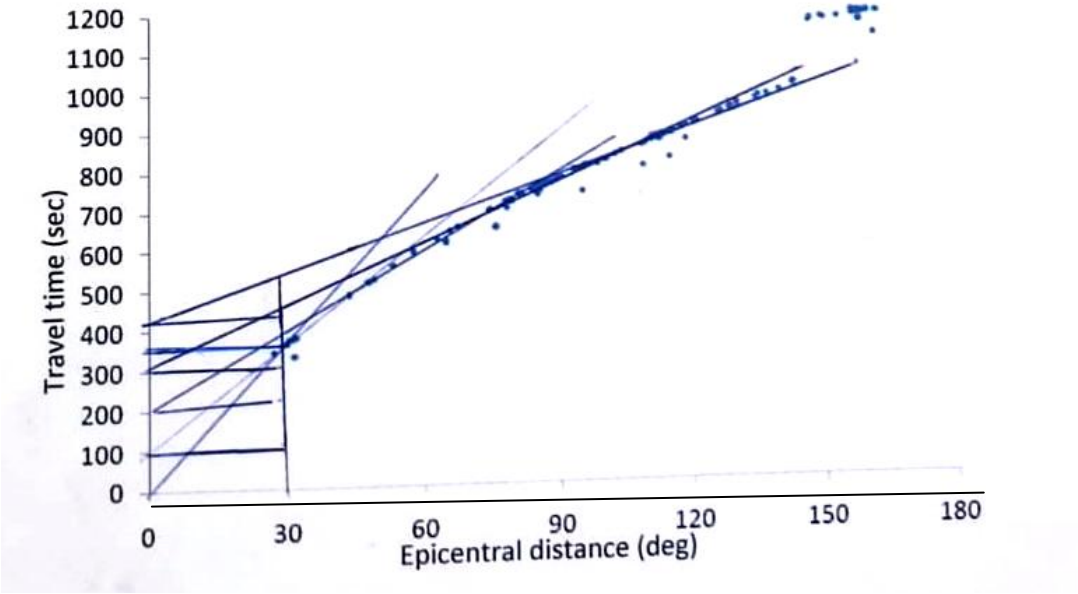

Fig.5.5: Series of straight line fittings on Travel time curve of NSUKKA station

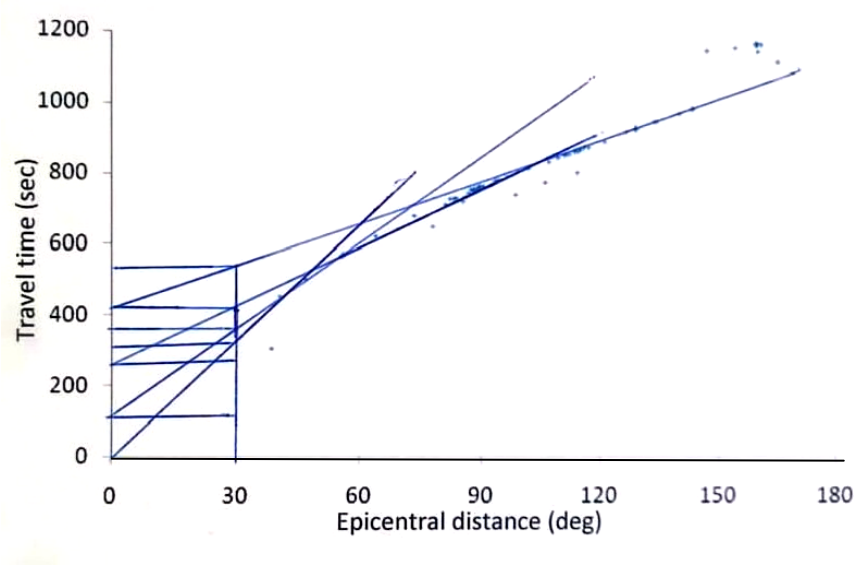

Fig.5.6: Series of straight line fittings on Travel time curve of KADUNA station

To simplify the process, a Fortran 77 program which performs the inversion of the travel time data was developed based on the $\tau(p)$ equation (3.26). The velocity depth models

obtained for each of the stations are shown in Fig.5.7, Fig.5.8 and Fig.5.9. The models could not model the crustal velocity because all the seismic events arriving at our stations had their turning point in the mantle; hence the program only extrapolates to zero at the surface.

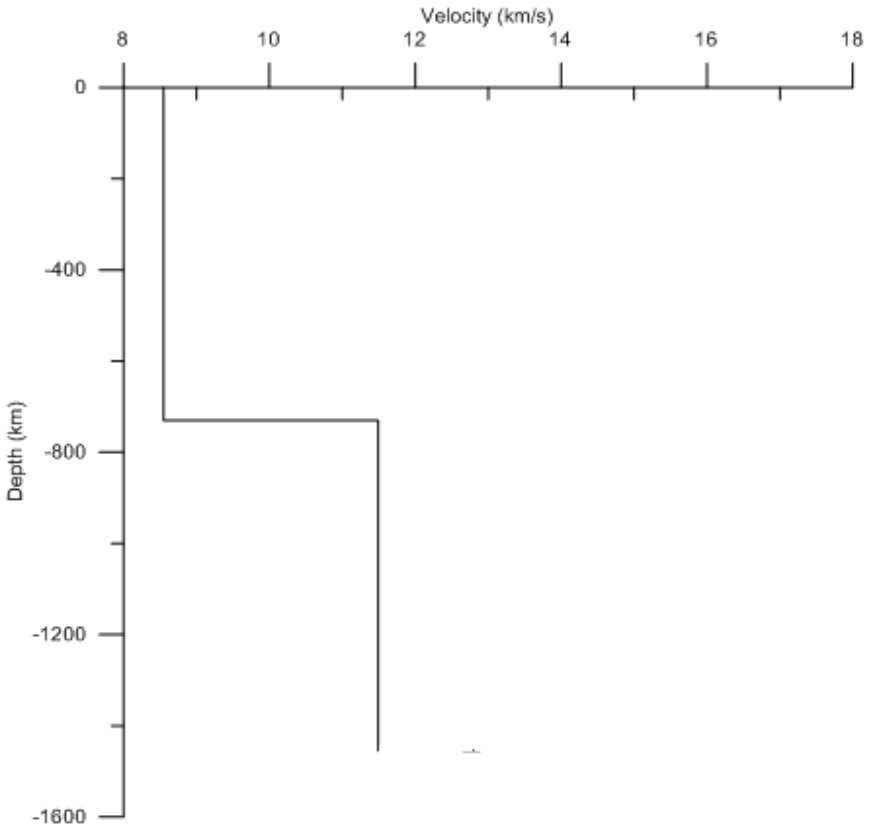

Fig.5.7: Mantle velocity - depth model for IFE station

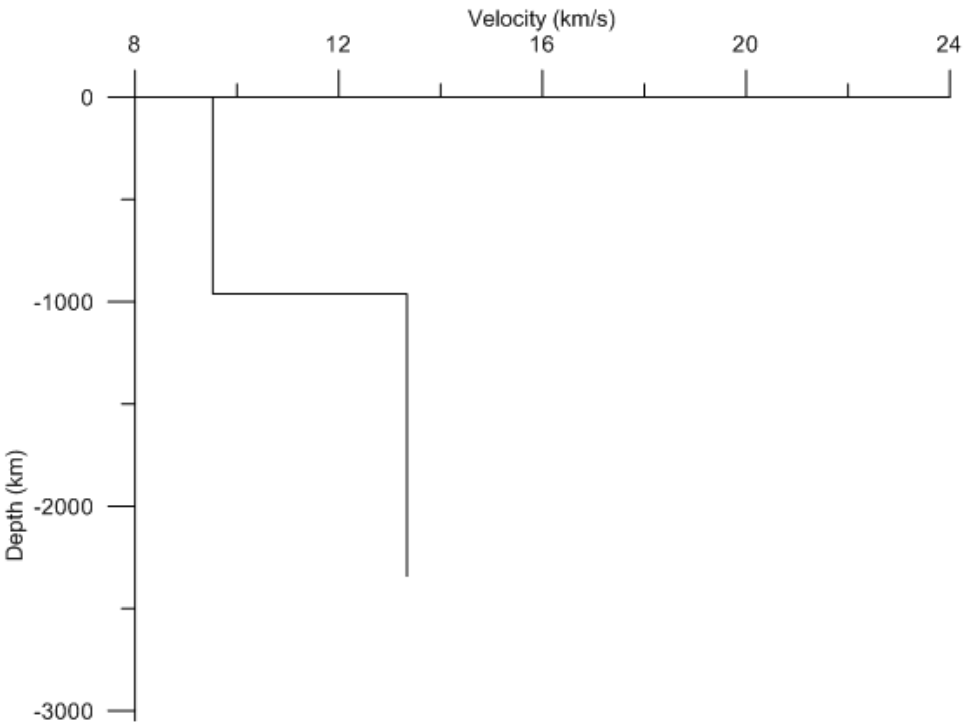

Fig.5.8: Mantle velocity - depth model for NSUKKA station

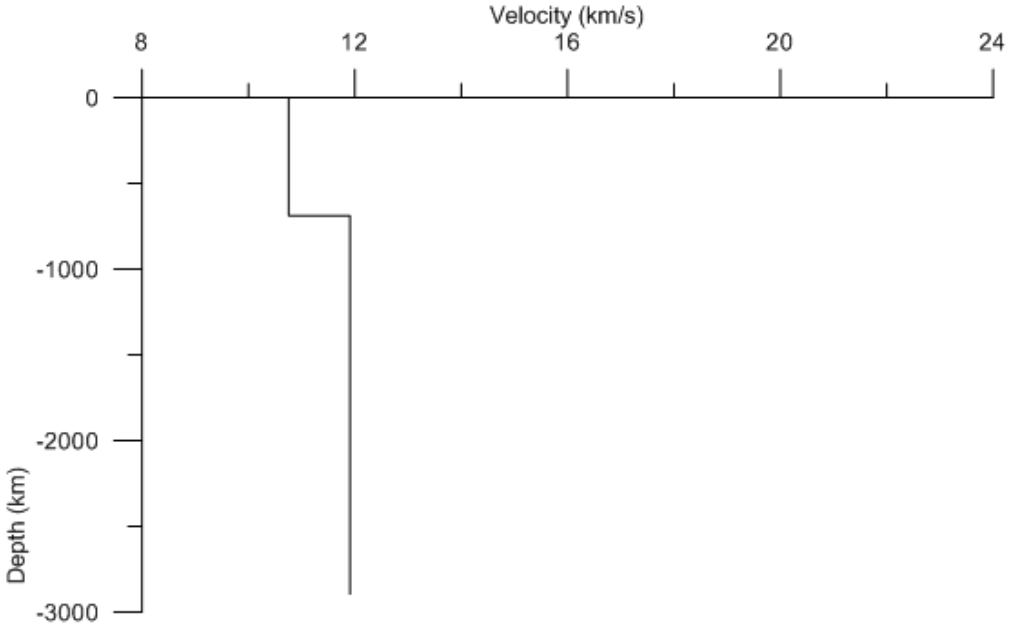

Fig.5.9: Mantle velocity - depth model for KADUNA station

Generally, the velocity varies between 8.5 km/s and 12.8 km/s with a transition occurring at an average depth of about 720 km within the mantle.

CHAPTER SIX

DISCUSSION, CONCLUSION AND RECOMMENDATIONS

6.1 Discussion of Results

The events recorded at the three stations at, Ile-Ife, Nsukka and Kaduna formed the data base for this research. All the events considered in this work lie within the epicentral distance of 25^o and 180^o, implying that all events are at teleseismic distances (Lay and Wallace, 1995). The events are mainly from three regions which has been classified as Regions I, II and III. Region I (azimuthal range 30^o to 90^o), include events from the Burma, India, China, Japan and some other parts of Asian regions. The travel paths of the events passed under the upper mantle region beneath the eastern Mediterranean, Coast of Turkey, Syria, Lebanon and the Red sea. The processes taking place in this region involve a collision of the African plate and the Eurasian plate and also movement between the small Aegean and Turkish plates (Mckenzie, 1970) which involve the consumption of the Mediterranean Sea floor. The Red sea region is also an active spreading centre and new crusts are continuously being created (Burke *et al.*, 1977). All these could have accounted for the resulting low velocity structures (positive residuals) (Table 5.1) in the travel path in this region to the recording seismic stations.

Region II (azimuthal range 210^o to 270^o) comprises of events from South America and the Mid-Atlantic regions. The travel paths passed under the upper mantle region within the south American Plate collision with the Nazca Plate which is a subduction zone, and new oceanic lithosphere are continuously consumed and reabsorbed into the mantle and the Mid-Atlantic Ridge, where it is believed that plates are spreading apart and new oceanic

lithosphere are being formed (Shearer, 1999). This explains the low velocity structure (positive residuals) (Table 5.1) along this path to the recording station. Region III (azimuthal range 270^{o} to 330^{o}), include events from Central America. The travel path passed under the upper mantle region within the Mid-Atlantic ridge which is an active spreading zone with a spreading rate estimated at an average of 2.0 cm/yr (Minister, *et al*., 1974) and beneath the African Plate through the Hoggar shield in the North Africa, a region in the eastern flank of the stable west African Craton affected by the Pan-African Orogeny. The collision at the cratonic margin resulting in steep thermal gradient in the crust probably caused the low velocity structure (positive residual) (Table 5.1) observed in the travel path in this region.

Absolute travel time residual is made up of three components; the source region, travel path and the station region effects. At large epicentral distances, that is, teleseismic distances, the travel path effect become dominant and overshadow the source and station region effects (Oniku,1999). However, this study mainly considered the station region effect so that the crustal and upper mantle structure within the station region could be understood, hence the relative travel time residuals were calculated for the three stations. The results of the relative travel time residuals calculated for the three stations shows that IFE station has an average of -0.03 s, NSUKKA station -0.13 s and KADUNA station 0.15 s. The relative travel time residual is due to the effect of the crustal and upper mantle materials within the station areas on the travel time.

The station relative travel time residual for IFE station is negative (-0.03 s), indicating the presence of a fast velocity structure within the crust and upper mantle in this region. This

could be due to the structural pattern and tectonic evolution of the basement complex within this region. Rahaman and Ocan, (1978) reported over ten evolutionary events with the emplacement of dolerite dykes as the youngest. Also, the entire Southwest Nigeria had been the most active seismically within the Nigerian Sub-Plate (Adepelumi, 2009).

NSUKKA station also shows a negative (-0.13 s) relative travel time residual. The value being higher than that of IFE is an indication that the fast velocity structure in NSUKKA is thicker than that in IFE. Nsukka station is located within a sedimentary basin and within the Ajali formation in the Southeast Nigeria, the origin and tectonic history of which is associated with the breakup of the continents of Africa and South America (Murat, 1988). The drifting apart of these continents, the opening of the South Atlantic and the growth of the mid-Atlantic Ridge all may have resulted in the observed negative relative travel time residual.

The KADUNA station shows a positive (0.15 s) relative travel time residual indicating the presence of a slow velocity structure within this region. The station is located within the Northern Nigeria basement complex. According to Wright *et al.,* (1987), the basement within this region comprise of polymetamorphic migmatite-gneiss complex, metasediments and metavolcanics and syntetonic to late tectonic granitoids. Metamorphism is generally in the amphibiolite facies grade. Dada (1989) related the amphibolites facies to subduction- related magma generation of volcanic arc settings for the gneisses of the basement based on the high R, Sr, K/Rb, K/Sr, low Ca and chondrite normalized negative anomalies of Nb, P, Ti, coupled with a high Al_2O_3/TiO_2 while the amphobolites are of low Mg tholleites and poorer in LILE but enriched in P. This pattern

tend to support a multistage evolution that involved an early basaltic crust transformed to amphibolites which may have caused the resulting positive relative travel time residual as obtained for this station.

The velocity model for the three stations shows a three layer mantle structure, with a transition at an average depth of about 720 km., and the velocity varying between 8.5 and 12.8 km/s. This is generally in agreement with mantle velocity model of Dziewonski and Anderson, (1981). According to Dziewonski and Anderson (1981) Fig. 6.1, transition occurs in the upper mantle between about 300 and 700 km depth. This is a region where several mineralogical phase changes are believed to occur (shown as dashed lines in Fig.6.1)

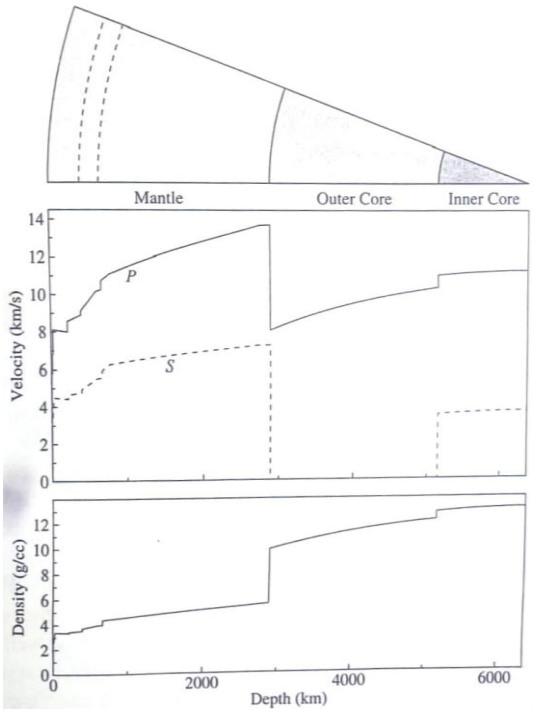

Fig.6.1: Earth's P velocity, S velocity and density as a function of Depth plotted from the Preliminary Reference Earth Model (PREM) of Dziewonski and Anderson (1981)

From the depth of about 700 km to near the core mantle boundary (CMB), the velocity increase fairly gradually with depth; this increase is in general agreement with that expected from the changes in pressure and temperature on rocks of uniform composition and crystal structure.

6.2 Conclusion

This research work has shown that variations in travel time residuals, also called delay times, are good indicators of the upper mantle structure. This variation in travel time residual, which indicates the regional deviation from the standard travel time, is also an indication of lateral variations in velocity structure along the travel path of the seismic wave. The results of the study showed that the residuals derived from recordings at all the three stations were delayed arrivals that is, positive residuals; indicative of materials which slows down the speed of seismic waves. The materials with these tendencies are referred to as low velocity structures. The azimuthal variation of the residuals was effected by categorizing the earthquakes into three regions where the events are more concentrated and the results showed that the values of the absolute travel time residuals for regions I and II are larger than for region III, indicating that the slow velocity slab in the upper mantle structure in regions I and II are thicker than in region III.

Analysis of the relative travel time residuals showed that the crustal and upper mantle structures beneath IFE and NSUKKA station are fast velocity structures with the waves arriving faster compared with the standard, while the KADUNA station revealed a delayed relative travel time residuals, indicative of a slow velocity structures in the crust and upper

mantle. The mantle velocity model shows a three layer mantle structure with an average transition thickness of about 720 km.

6.3 Recommendations

From the results of the study, I noted that there are no local events ($0^o< \Delta<13^o$), all recorded events are teleseismic *i.e.,* between 28^o and 180^o in epicentral distance. This however, made it impossible for me to develop the crustal velocity model as the entire events arriving at our stations had their turning point in the mantle. I therefore recommend that, seismic waves which travel basically within the crust be generated from artificial sources (*e.g.,* quarry explosion) close to the seismic stations.

This work which was aimed at investigating the crustal and upper mantle structures under the seismic stations considered had intended to carry out seismic tomography of the crust and the upper mantle structure to reveal the detailed heterogenic properties of the crust and the upper mantle and the possible geodynamic processes taking place, but because of the scatter nature of our stations and the relatively few data available, this could not be possible. I therefore recommend that the necessary authority be encouraged to increase the station number and coverage within the country for effective crustal monitoring.

Reference

Adepelumi, A. A. (2009). Short- term probabilistic forecasting of earthquakes occurrence in Southwestern Nigeria. A technical report submitted to Center for Geodesy and Geodynamics (CGG), Toro.

Adepelumi, A. A., Ako, B. D., Ajayi, T. R., Olorunfemi, A.O., Awoyemi, M. O. and Falebita, D. E. (2008). Integrated geophysical mapping of the Ifewara transcurrent fault system, Nigeria. Journal of African Earth Sciences 52(4-5), 161-166

Ajakaiye, D.E Hall D.H., Millar, T.W.,Verheijen, P.J., Awad, M.B., and Ojo, S.B. (1986). Aeromagnetic Anomalies and Tectonic Trends in and around the Benue Trough, Nigeria.Nature, 319, 582-584.

Ajakaiye, D. E., Daniyan, M. A., Ojo, S. B. and Onuoha, K. M. (1987). The July 28, 1984 southwestern Nigeria earthquake and its implications for the understanding of the tectonic structure of Nigeria. In: Wassef A M, Boud A, Vyskocil P (eds.), Recent Crustal Movements in Africa. *Jour. Geody.*, 7**:** 205-214.

Ajakaiye, D. E., Olatinwo, M. D. and Scheidegger, A. E. (1988). Another possible earthquake near Gombe in Nigeria on the 18-19 June 1985. Bull. Seism. Soc. Amer., **78** (2): 1006-1010.

Ajakaiye, D. E., Ojo, S. B., Daniyan, M. A., and Abatan, O. A. (1989). (Editors), Proceedings of the National Seminar on earthquakes in Nigeria.

Ajibade, A.C.,Woaks, M., and Rahaman, M.A. (1987): Proterozoic crustal development in Pan-African regime of Nigeria: In A. Kroner (ed) Proterozoic Lithospheric Evolution. America Geophysical Union Special publication, 51, pp 259-271.

Aki, K. and Richards, P. G. (1980). Quantitative seismology: Theory and Methods. W. H. Freeman and company, San Fransisco.

Akpan, O. U. and Yakubu, A. Y. (2010). Earthquake Science, 23, p.289-294.

Akpati, B. N. (1989). The geology of Nigerian continental margin and its bearing on the recent earthquakes in southwestern Nigeria In: Ajakaiye, D. E., Ojo, S. B., Daniyan, M. A., and Abatan, A.O., (1989). (Editors). Proceedings of the National Seminar on Earthquakes in Nigeria.

Ananaba, S. E. (1991). Dam sites and crustal megalineaments in Nigeria. ITC Jour., **1**: 26-29.

Astiz, L. Earle, P., and Shearer, P. (1996). Global stacking of broadband seismograms, Seis. Res. Lett., **67**, 8-18.

Black, R. and Caby, R. (1979). Evidence for late Precambrian Plate ttectonics in West Africa. Nature 278: 223-227.

Burke, K.C. and Dewey, J.F (1972). Orogeny in Africa . In African Geology A.J. Dessauragie, T.F.J. Whiteman (eds), pp 583-608, University of Ibadan Press, Nigeria.

Burke, K.C., Freeth S.J. and Grant, N.K. (1976): The structure and sequence of geological events in the basement complex of Ibadan area Western Nigeria Precamb. Res.3, pp 537-545

Burke, K., Dewey, J., and Kidd, W. S. F. (1977). World distribution of sutures – the sites of former oceans. Tectonophysics, **40**, 66-99.

Dada, S. S. (1989). Geochemistry and petrogenesis of the reworked Archaean gneiss complex of North Central Nigeria: Major and trace element studies on Kaduna amphibolites and migmatitic gneisses. Global J. of Pure and Appl. Sci., 5: 543.

Dada, S.S, Briqueu, K.L., Birck. J.L. (1998): Primodial crustal growth in northern Nigeria Preliminary Rb-Sr and Sm-Nd constraints from Kaduna migmatite gneiss complex. J. of Min. and Geol. 34, pp1-6.

Dorbath, C., Dorbath, L., Fairhead, J.D and Stuart, G.W. (1986). A teleseismic delay time study across the central African Shear zine in the Adamawa region of Cameroon, West Africa, geophys. J. R. astr. Soc., **86**, 751-766.

Dugda, M. T., Nyblade, A. A., and Julia, J., (2009). S-wave velocity structure of the crust and upper mantle beneath Kenya in comparision to Tanzania and Ethiopia: Implications for the formation of the East African and Ethiopian Plateaus. South African Jour. of Geol., **112**; 241-250.

Dziewonski, A. M. and Anderson, D. L. (1981). Preliminary reference Earth model, Phys. Earth Planet. Inter., **25**, 297-356.

Dziewonski, A.M. and Gilbert, F. (1976). The effects of small, Aspherical perturbation on travel times and re-examination of the corrections for ellipticity. Geophys. Jour. Royal astr. Sco., **44**, 7-17.

EENTEC (2003). DR-4000 Instruction Manual

Elueze, A. A. (2003). Evaluation of the 7 March 2000 earth tremor in Ibadan area, southwestern Nigeria. Jour. of Min. and Geol., **39** (2): 79-83.

Eze, C. L., Sunday, V. N., Ugwu, S. A., Uko, E. D., and Ngah, S. A. (2011). Mechanical

model for Nigerian intraplate Earth tremors. Published in Articles, Disaster management and Earth observations www.earthzine.com posted 17th May 2011.

Fabre, I. (2005). General geology of west African Craton. Geologie du sahara et central. Serie/Reek: Tervuren African geosciences collection (www.largeigne.com).

Garba, I. (2003). Geochemical characteristics of mesothermal gold mineralisation in the Pan-African (600 ± 150 Ma) basement of Nigeria. Applied Earth Science : IMM Transactions section B, 112(.3), 319-325

Garmany, J., Orcutt, J. A., and Parker, R. L. (1979). Travel time inversion: a geometrical approach, Jour. of geophys. Res., 3615-3622.

Gubbins, D. (1990). Seismology and Plate Tectonics. Cambridge University Press. ISBN 0-521-37141.

Hansen, S. E., Nyblade, A. A., and Julia, J., (2009). Estimates of crustal and lithospheric thickness in sub-saharan Africa from S-wave receive functions. South African Jour. of Geol. Vol., 112; 229-240.

Hasting, D. A. and Bacon, M. (1979).Geologic structure and evolution of the Keta basin, West Africa. Geological Society of America Bulletin September, 90, 889-891

Havskov, J., Kvamme, L.B., Hansen, R.A., Bungum, H., and Lindholm, C. D. (2002). The Northern Norway seismic Network: Design, Operation and Results. Bull. Seism. Soc.Am. 82, 481-496.

Havskov, J. And Ottemoller, L. (2008). Routine Data Processing. 304 pp.

Havskov, J. and Alguacil G. (2010). Instrumentation in earthquake seismology. Springer, revised reprint, 358 pp.

Hubbard, F. A. (1975). Precambrian crustal development in Western Nigeria: indications from the Iwo region. Bulletin of Geological Society of America. 86, 548-554

Ige, E.A., Ike, E.C and Woakes, M. (1985). Some Geological Aspects of Nigerian Seismicity: Paper presented at the National Seminar on Earthquakes in Nigeria, Ahmadu Bello University, Zaria Nigeria, Abstract Volume,10.

Kennett, B. N. L. (2005). Seismological Tables: ak135. Produced by Research School of Earth Sciences, The Australian National University. Canberra ACT 0200, pg 240.

Kennett, B.N.L., and Engdahl, E.R. (1991). Travel times for global earthquake location and Phase identification. Geophys. J. Int., **106**, 429-465.

Kennett, B. L. N., Engdahl E. R. and Buland R. (1995). Constraints on seismic velocities in the Earth from traveltimes, Geophys J. Int., **122**, 108-124.

Kennedy, W. (1964). The structural differentiation of Africa in the Pan-African (+500 my). tectonic episode. 8th Ann. Res. Inst. Africa, Leeds Univ. U.K.

Kogbe, C. A. (1989). Paleogeographic history of Nigeria from Albian times. In Geology of Nigeria (Ed.) Kogbe C. A. Rock View Nigeria Limited, Jos. 257-275.

Kumar, P., Yuan, X., Ravi Kumar, M. Kind, R., Li, X. and Chadha, R. (2007). The rapid drift of the Indian tectonic plate. Nature, **449**, 894-897.

Lawrence, B. (2007). Upseis educational site. Michigan Technological University www.geo.mtu.edu/Upseis/index.html

Le blanc, (1976). Proterozoic oceanic crust at Bou Azzer. Nature 261: 34-35

Lowrie, W., (1999). Fundamentals of Geophysics. Cambridge University Press, United Kingdom. 279p

Lay, T., and Wallace, T. C. (1995). Modern Global Seismology, Academic Press, New York.

Mckenzie, D.P. (1970). Plate tectonics of the Mediterranean region. Nature, 226; 239-243.

Merki, P.J. (1970). Structural Geology of the Cenozoic Niger Delta. African Geology. Procceedings of Ibadan Conference on African Geology; Ibadan, Nigeria.

Minster, J.B., Jordan, T.H., Monlar, P. and Haines, E. (1974). Numerical modeling of instantaneous plate tectonics. Geophys. Jour., 36, 541-576.

Murat, R. C. (1988). Airphoto Interpretation as an aid to Litho – Structural Mapping In tropical Terrain – The New Federal Capital City Site, Abuja, Nigeria. Mineral Resources Exploration. Bulletin, 108, 65-75.

Murat, R.C. (1972). "Stratigraphy and Palaeogeography of the Cretaceous and Lower Tertiary in South Nigeria". In: Dessauvagie, T.F.J. and Whiteman, A. (eds.). African Geology: UI Press: Ibadan, Nigeria. 635 – 641.

Neev, D., Hall, J. K., and Saul, J. M. (1982). The Pelusium Megashear System Across African and Associated Lineament Swarms. Journal of Geophysical Research 87, 015-1030

Nwachukwu, S.O. (1972). The tectonic evolution of the southern portion of the Benue trough, Nigeria, Geological Magazine, 109, 411-419.

Odeyemi, I. B. (2006). The Ifewara fault in Southwestern Nigeria: Its relationship with fracture zones along the Nigerian Coast. Lecture delivered at the Centre for Geodesy and Geodynamics, Toro, Bauchi State. 13p.

Ojo, O. M. (1995). Survey of occurrences in Nigeria of natural and man-made hazards related to geological processes. In: Onuoha K M and Offodile M E (eds.), Proceedings of the International workshop on natural and man-made hazards in Africa, Awka, Nigeria, 10- 14.

Ojo, S.B. (1994). Teleseismic P-wave travel time residuals at the Ahmadu Bello University, Seismic station, Zaria. Journal of Mining and geology, vol.,30, no.1, 75-80.

Oldham, R. D. (1906). The Constitution of the Interior of the Earth, as Revealed by Earthquakes. Quarterly Journal of the Geological Society **62** (1-4): 456–475.

Oluyide, P.O., and Udoh, A.N. (1989). Preliminary comments on the fracture systems in Nigeria In: Ajakaiye D E, Ojo S B, Daniyan M A, Abatan A O (eds.), Proceedings of the National Seminar on Earthquakes in Nigeria, Lagos, Nigeria, 97-109.

Oniku, S.A. (1999). A detailed study of Teleseismic P-wave travel time residuals at Ahmadu Bello University seismic station, Zaria. Unpublished M.Sc Thesis.

Oniku, S.A. (2005). Station History of the Seismic Station in Ahmadu Bello University Zaria. Global Journal of Pure and Applied Sciences Vol. 11. No.2 309-315

Oniku, S.A**.**, Ojo, S. B. and Osazuwa, I.B. (2006). Study of Relative Travel Time Residuals of P- wave at Teleseismic Distances at the Ahmadu Bello University, Zaria Seismic Station. Global Journal of Pure and Applied Sciences. Vol. 12. No.3. 397-402

Onuoha, K. M. (1989). Historical perspectives of earthquakes in West Africa. In: Ajakaiye D E, Ojo S B, Daniyan M A, Abatan A O (eds.), Proceedings of the National Seminar on Earthquakes in Nigeria, Lagos, Nigeria, 129-141.

Osagie, E. O. (2008). Seismic activity in Nigeria. The Pacific Jour Sci and Tech **9** (2): 1-6.

Osemeikhan, J.E.A. and Asokhia, M.B. (1990). Applied geophysics (for Engineers and Geologists). University Press Ltd.

Oyinloye, A.O. (2011): Beyond Petroleum Resources: Solid Minerals to the rescue: 31st Inaugural Lecture of the University of Ado-Ekiti, Nigeria Press, 1-36

Oyinloye, A.O. (2006): Metallogenesis of the lode gold deposits in Ilesha Area of Southwestern Nigeria: Inferences from lead isotope systematic, Pak. J. Sci. Ind. Res. 49 (11) pp 1-11.

Oyinloye,A.O. (2004): Petrochemistry, pb isotope systematic and geotectonic setting of granite gneisses in Ilesha schist belt southwestern Nigeria Global Jour. Geol. Sci.2(1) 1-13.

Oyinloye,A.O. (2002a): Geochemical Studies of granite gneisses: the implication on source determination. Jour. Chem. Soc. Nigeria (26) (1) 131-134.

Oyinloye, A.O. (2002b): Geochemical characteristics of some granite gneisses in Ilesha area southwestern Nigeria: Implication on evolution of Ilesha schist belt, southwest Nigeria. Trends in Geochemistry India vol 2, 59-71.

Rahaman, M.A (1988):Recent advances in the study of the basement complex of Nigeria. Symposium on the Geology of Nigeria, Obafemi Awolowo University, Nigeria.

Rahaman, M.A and Ocan O.O.(1978): On relationship in the Precambrian migmatitic gneisses of Nigeria J. Min. and Geol. Vol. 15, No.1 (abs).

Scheidegger, A.E. and Ajakaiye, D.E. (1985). Geodynamics of Nigerian shield areas. African Journal of Earth Sciences 3, 461-70

Scherbaum, F. (2001). Of poles and zeroes: fundamentals of digital seismometry. Kluwer Academic Publisher, Dordrecht, 256 pp.

Schwitzer, J. (2011). User manual for LAUFZE and LAUFPS, versions Laufze 6.2 and Laufps 3.2

Shearer, P.M. (1999). Introduction to seismology. Cambridge University, page Press 259

Thorne, L. and Terry W. C. (1995). Modern global seismology. Academic press. Page 535.

Udias, A. (1999). Principles of Seismology. Cambridge University press. Pp 714

Ugodulunwa, F. X. O., Ajakaiye, D. E., Guiraud, M. and Hossan, M. T. (1986). The Pindiga and Obi fractures-possible earthquake sites in Nigeria. In: Proceedings of the 3rd International Conference on current research in geophysics and geophysical research in Africa, Jos, Nigeria, 6p.

Wen, L. and Helmberger, D. V. (1998). Ultra-Low Velocity Zones Near the Core-Mantle Boundary from Broadband PKP Precursors. *Science* **279** (5357): 1701–1703.

Woakes, M. Ajibade C.A., Rahaman, M.A., (1987): Some metallogenic features of the Nigerian Basement, Jour. of Africa Science Vol. 5 pp. 655-664.

Wright, J.B., 1976, Fracture systems in Nigeria and initiation of fracture zones in South Atlantic: Tectonophysics 34, 43-47.

Wright, J. L., Ajibade, A. C., and Mc-Curry, P. (1987). The Geology of the Precambrian to Lower Paleozoic Rocks of Northern Nigeria. A Review, in Geology of dited by Nigeria, C.A. Kogbe. Published by Elizabethan Co. Lagos, pp. 15-39.

Yazici, O. (1989). Crustal structure of western Turkey from the study of Teleseismic P-Wave delay times. Bogazici University, unpublished M.Sc thesis.

www.neic.usgs.gov/cgi-bin/tt/compute_tt.cg
www.geosphere.gsapubs.org

APPENDICES APPENDIX I: List of Events observed at IFE station

S/N	DATE/ORIGIN TIME OF EVENT	LATITUDE	LONGITUDE	MAGNITUDE	DEPTH	REGION
1	2009-07-01 09:30:11	34.1	25.4	6.4	30.0	Crete, Greece
2	2009-07-04 06:49:36	9.7	-79.0	6.0	43	Panama
3	2009-07-07 19:11:45	75.3	-72.2	5.9	10.0	Baffin Bay
4	2009-07-13 10:52:22	-9.2	119.2	6.1	86	Indonesia
5	2009-07-13 18:05:02	24.0	122.2	6.3	24	Taiwan
6	2009-08-03 17:59:59	29.4	-112.8	6.9	10.0	Gulf of California
7	2009-08-09 10:55:56	33.1	138.0	7.1	303	Japan
8	2009-08-10 19:55:39	14.0	92.9	7.6	33.0	India
9	2009-08-17 00:05:47	23.5	123.5	6.7	10.0	Japan
10	2009-08-20 06:35:03	72.3	1.0	6.1	2.0	Norway
11	2009-08-28 01:52:06	37.7	95.7	6.2	10.0	China
12	2009-09-02 07:55:01	-7.8	107.3	7.0	49.0	Indonesia
13	2009-09-07 16:12:21	-10.2	110.6	6.1	15.0	Indonesia
14	2009-09-07 22:41:36	42.7	43.5	6.1	10.0	Caucasus
*15	2009-09-12 20:06:24	10.7	-68.0	6.3	10.0	Near coast of Ver
15	2009-09-18 06:23:58	12.6	120.5	6.0	10.0	Philippine Island
16	2009-09-21 08:53:05	27.3	91.4	6.3	7.0	Bhutan
17	2009-09-24 07:16:21	19.1	-107.3	6.4	4.0	Mexico
18	2009-10-11 04:47:46	-17.2	66.6	6.0	10	Mauritius
19	2009-10-16 09:52:52	-6.6	105.2	6.1	50	Indonesia
20	2009-10-22 00:51:39	6.8	-82.6	6.1	10	Panama
21	2009-10-22 19:51:28	36.5	70.9	6.2	196	Afghanistan
22	2009-10-23 11:15:28	-0.9	134.1	6.0	35	Indonesia

23	2009-10-24 14:40:44	-6.2	130.3	7.0	138	Banda sea
24	2009-10-29 17:44:31	36.5	70.7	6.0	202.0	Afghanistan
25	2009-10-30 07:03:39	29.1	129.9	6.9	35.0	Japan
26	2009-11-04 18:41:44	36.1	-33.9	6.0	10	Azores
27	2009-11-08 19:41:44	-8.3	118.7	6.7	18.0	Indonesia
28	2009-11-09 10:44:54	-17.2	178.4	7.2	585.0	Fiji Island
29	2009-11-13 03:05:55	-19.4	-70.2	6.5	10	Chile
30	2009-11-14 19:44:22	-22.9	-66.5	6.1	141.0	Argentina
31	2009-11-17 15:30:46	52.1	-131.5	6.6	10	Canada
32	2009-11-26 19:08:10	13.5	-89.9	5.9	37	El Salvador
33	2009-11-28 06:04:25	-10.4	118.9	6.2	35.0	Indonesia
34	2009-12-06 17:36:35	-10.2	33.8	10	5.8	Malawi
35	2009-12-09 16:00:42	-0.7	-21.1	6.4	10.0	Mid-Atlantic ridg
36	2009-12-18 07:33:00	-18.0	65.6	5.9	2.0	Mauritius
37	2009-12-19 13:02:16	23.8	121.7	6.4	44	Taiwan
38	2009-12-19 23:19:23	-9.9	34.0	6.2	47	Tanzania
39	2009-12-24 00:23:27	42.2	134.8	6.3	348.0	Russia
40	2009-12-26 08:57:24	-5.6	131.1	6.0	57	Banda sea
41	2010-01-03 21:48:06	-8.8	157.2	6.5	10.0	Bougainville
42	2010-01-05 04:55:39	-58.1	-14.9	6.7	10.0	Sandwich Islands
43	2010-01-09 05:51:34	-9.2	157.6	6.3	35.0	Bougainville
44	2010-01-10 00:27:39	40.7	-124.7	6.5	16.0	N.Califonia
45	2010-01-12 21:53:09	18.4	-72.4	7.0	10.0	Haiti
46	2010-01-15 10:14:02	-32.0	-177.1	5.9	10.0	Kermadec Islands
47	2010-01-17 12:00:02	-57.7	-65.9	6.3	10.0	Drake Passage
48	2010-01-18 15:40:32	23.8	-90.2	6.0	103.0	Guatemala
49	2010-01-20 11:03:44	18.4	-72.9	6.1	9.0	Haiti
50	2010-01-27 17:42:45	-14.1	-14.4	5.8	10.0	Southern Mid-Atl
51	2010-02-04 20:20:21	40.4	-124.9	6.0	11.0	N. California
52	2010-02-05 06:59:06	-48.0	99.6	6.1	10.0	Indian Ridge
53	2010-02-06 04:44:59	47.0	152.0	6.1	35.0	Russia
54	2010-02-07 06:10:00	23.5	123.7	6.4	16.0	Japan
55	2010-02-13 02:34:29	-21.9	-174.8	6.3	10.0	Tonga Islands
56	2010-02-18 01:18:17	42.61	130.8	6.7	562.0	China border
57	2010-02-22 07:00:54	-23.7	-176.0	6.0	35.0	Fiji Islands
58	2010-02-26 20:31:26	26.0	128.4	7.0	22.0	Japan
59	2010-02-27 06:34:14	-35.9	-72.6	8.8	35.0	Chile
60	2010-02-27 08:01:24	-37.2	-75.2	6.9	39.0	Chile
61	2010-02-28 11:25:35	-34.7	-70.9	6.2	35.0	Chile-Argentina b
62	2010-03-04 00:18:53	22.9	120.9	6.4	35.0	Chile
63	2010-03-04 14:02:30	-13.6	167.1	6.4	200.0	Chile

64	2010-03-05 11:47:10	-36.5	-73.1	6.6	35.0	Chile
65	2010-03-08 02:32:34	38.8	40.1	6.1	10.0	Turkey
66	2010-03-11 14:39:44	-34.3	-71.9	6.9	11.0	Chile
67	2010-03-16 02:22:00	-36.2	-73.2	6.0	35.0	Chile
68	2010-03-28 21:43:13	-35.3	-72.8	6.1	19.0	Chile
69	2010-03-30 16:54:48	13.6	92.9	6.4	45.0	India
70	2010-04-02 05:38:55	19.1	-68.0	8.0	13.0	North Atlantic Oc
71	2010-04-04 22:40:39	32.1	-115.2	6.9	32.0	California
72	2010-04-06 22:15:02	2.2	97.0	7.8	48.0	N/ Sumatra
73	2010-04-07 14:33:05	-3.8	141.9	6.0	37.0	New Guinea
74	2010-04-11 09:40:30	-10.9	161.1	6.8	60.0	Islands region
75	2010-04-11 22:08:11	37.1	-3.5	6.2	623.0	Spain
76	2010-04-13 23:49:42	33.3	96.7	6.9	46.0	China
77	2010-12-07 04:27:22	-58.0	-7.6	5.8	13.0	East of South San
78	2010-12-08 06:47:18	7.4	126.6	6.1	69.0	Mindabo, Philipp
79	2010-12-12 20:48:16	71.5	-4.6	4.5	10.0	Jan Mayen Island
80	2010-12-13 01:14:43	-6.6	155.7	6.1	144.0	Bougainville, Solo
81	2010-12-13 09:44:52	39.4	-29.4	5.0	4.8	Azores Island, Po
82	2010-12-20 18:41:59	28.4	59.1	6.3	12.0	Southern Iran
83	2010-12-23 14:00:33	53.2	171.2	6.2	22.0	United State
84	2010-12-28 08:34:17	-23.4	-179.8	6.3	551.0	South of Fiji Islan
85	2010-12-29 06:54:21	-19.7	168.2	6.6	31.0	Vanuatu Islands
86	2011-04-23 04:16:55	-10.3	161.2	6.9	81.0	Bougainville-Solo
87	2011-05-10 08:55:11	-20.2	168.2	7.1	26.0	Loyalty Island
88	2011-05-14 21:07:22	36.4	70.7	5.9	207.0	Afghanistan
89	2011-05-15 13:08:13	0.5	-25.6	6.0	9.0	Central Mid-Atlan
90	2011-05-19 20:15:23	39.1	29.1	5.9	7.0	Turkey
91	2011-06-01 12:55:21	-37.5	-73.7	6.4	15.0	Central Chile
92	2011-06-03 00:05:00	37.3	143.9	6.5	10.0	Eastern Honshu J
93	2011-06-05 11:51:12	-55.9	146.6	6.3	10.0	West of Macquar
94	2011-06-08 03:06:18	-17.1	-69.5	6.0	101.0	Peru-Bolivia Bord
95	2011-06-12 20:32:39	13.4	41.7	5.6	2.0	Ethiopia
96	2011-06-20 16:35:57	-21.9	-68.3	6.3	111.0	Chile-Bolivia Bord
97	2011-06-22 21:50:47	39.9	142.3	6.7	3.0	Eastern Honshu J
98	2011-06-24 03:09:39	52.0	-173.7	7.4	43.0	Fox Islands Unite
99	2011-07-06 19:03:16	-29.3	-176.2	7.7	10.0	Kermadec Islands
100	2011-07-10 00:57:12	38.0	143.3	7.0	34.0	Eastern Honshu J
101	2011-07-11 20:47:14	9.5	122.2	6.2	19.0	Negros, Philippin
102	2011-07-16 00:26:13	-33.8	-72.1	6.0	22.0	Central Chile
103	2011-07-16 19:59:14	54.9	-161.3	6.1	48.0	Alaska Peninsula,
104	2011-07-19 19:35:40	40.1	71.4	6.2	1.0	Tajikistan

105	2011-07-23 04:34:24	39.0	142.0	6.4	35.0	Eastern Honshu J
106	2011-07-24 18:51:25	37.8	141.5	6.2	35.0	Eastern Honshu J
107	2011-07-25 00:50:50	-3.2	150.7	6.2	34.0	New Ireland, Pap
108	2011-07-26 17:44:21	25.2	-109.5	5.9	10.0	Gulf of California
109	2011-07-27 23:00:29	10.7	-43.4	5.9	6.0	Northern Mid-At

APPENDIX II: List of Events observed at NSUKKA station

S/N	DATE/ORIGIN TIME OF EVENT	LATITUDE	LONGITUDE	MAGNITUDE	DEPTH	REGION

1	2009-07-01 09:30:11	34.1	25.4	6.4	30.0	Crete, Greece
2	2009-07-04 06:49:36	9.7	-79.0	6.0	43	Panama
3	2009-07-07 19:11:45	75.3	-72.2	5.9	10.0	Baffin Bay
4	2009-07-13 10:52:22	-9.2	119.2	6.1	86	Indonesia
5	2009-07-13 18:05:02	24.0	122.2	6.3	24	Taiwan
6	2009-08-03 17:59:59	29.4	-112.8	6.9	10.0	Gulf of California
7	2009-08-09 10:55:56	33.1	138.0	7.1	303	Japan
8	2009-08-10 19:55:39	14.0	92.9	7.6	33.0	India
9	2009-08-17 00:05:47	23.5	123.5	6.7	10.0	Japan
10	2009-08-20 06:35:03	72.3	1.0	6.1	2.0	Norway
11	2009-08-28 01:52:06	37.7	95.7	6.2	10.0	China
12	2009-09-02 07:55:01	-7.8	107.3	7.0	49.0	Indonesia
13	2009-09-07 16:12:21	-10.2	110.6	6.1	15.0	Indonesia
14	2009-09-07 22:41:36	42.7	43.5	6.1	10.0	Caucasus
*15	2009-09-12 20:06:24	10.7	-68.0	6.3	10.0	Near coast of Ver
15	2009-09-18 06:23:58	12.6	120.5	6.0	10.0	Philippine Island
16	2009-09-21 08:53:05	27.3	91.4	6.3	7.0	Bhutan
17	2009-09-24 07:16:21	19.1	-107.3	6.4	4.0	Mexico
18	2009-10-11 04:47:46	-17.2	66.6	6.0	10	Mauritius
19	2009-10-16 09:52:52	-6.6	105.2	6.1	50	Indonesia
20	2009-10-22 00:51:39	6.8	-82.6	6.1	10	Panama
21	2009-10-22 19:51:28	36.5	70.9	6.2	196	Afghanistan
22	2009-10-23 11:15:28	-0.9	134.1	6.0	35	Indonesia
23	2009-10-24 14:40:44	-6.2	130.3	7.0	138	Banda sea
24	2009-10-29 17:44:31	36.5	70.7	6.0	202.0	Afghanistan
25	2009-10-30 07:03:39	29.1	129.9	6.9	35.0	Japan
26	2009-11-04 18:41:44	36.1	-33.9	6.0	10	Azores
27	2009-11-08 19:41:44	-8.3	118.7	6.7	18.0	Indonesia
28	2009-11-09 10:44:54	-17.2	178.4	7.2	585.0	Fiji Island
29	2009-11-13 03:05:55	-19.4	-70.2	6.5	10	Chile
30	2009-11-14 19:44:22	-22.9	-66.5	6.1	141.0	Argentina
31	2009-11-17 15:30:46	52.1	-131.5	6.6	10	Canada
32	2009-11-26 19:08:10	13.5	-89.9	5.9	37	El Salvador
33	2009-11-28 06:04:25	-10.4	118.9	6.2	35.0	Indonesia
34	2009-12-06 17:36:35	-10.2	33.8	10	5.8	Malawi
35	2009-12-09 16:00:42	-0.7	-21.1	6.4	10.0	Mid-Atlantic ridg
36	2009-12-18 07:33:00	-18.0	65.6	5.9	2.0	Mauritius
37	2009-12-19 13:02:16	23.8	121.7	6.4	44	Taiwan
38	2009-12-19 23:19:23	-9.9	34.0	6.2	47	Tanzania
39	2009-12-24 00:23:27	42.2	134.8	6.3	348.0	Russia
40	2009-12-26 08:57:24	-5.6	131.1	6.0	57	Banda sea

41	2010-01-03 21:48:06	-8.8	157.2	6.5	10.0	Bougainville
42	2010-01-05 04:55:39	-58.1	-14.9	6.7	10.0	Sandwich Islands
43	2010-01-09 05:51:34	-9.2	157.6	6.3	35.0	Bougainville
44	2010-01-10 00:27:39	40.7	-124.7	6.5	16.0	N.Califonia
45	2010-01-12 21:53:09	18.4	-72.4	7.0	10.0	Haiti
46	2010-01-15 10:14:02	-32.0	-177.1	5.9	10.0	Kermadec Islands
47	2010-01-17 12:00:02	-57.7	-65.9	6.3	10.0	Drake Passage
48	2010-01-18 15:40:32	23.8	-90.2	6.0	103.0	Guatemala
49	2010-01-20 11:03:44	18.4	-72.9	6.1	9.0	Haiti
50	2010-01-27 17:42:45	-14.1	-14.4	5.8	10.0	Southern Mid-Atl
51	2010-02-04 20:20:21	40.4	-124.9	6.0	11.0	N. California
52	2010-02-05 06:59:06	-48.0	99.6	6.1	10.0	Indian Ridge
53	2010-02-06 04:44:59	47.0	152.0	6.1	35.0	Russia
54	2010-02-07 06:10:00	23.5	123.7	6.4	16.0	Japan
55	2010-02-13 02:34:29	-21.9	-174.8	6.3	10.0	Tonga Islands
56	2010-02-18 01:18:17	42.61	130.8	6.7	562.0	China border
57	2010-02-22 07:00:54	-23.7	-176.0	6.0	35.0	Fiji Islands
58	2010-02-26 20:31:26	26.0	128.4	7.0	22.0	Japan
59	2010-02-27 06:34:14	-35.9	-72.6	8.8	35.0	Chile
60	2010-02-27 08:01:24	-37.2	-75.2	6.9	39.0	Chile
61	2010-02-28 11:25:35	-34.7	-70.9	6.2	35.0	Chile-Argentina b
62	2010-03-04 00:18:53	22.9	120.9	6.4	35.0	Chile
63	2010-03-04 14:02:30	-13.6	167.1	6.4	200.0	Chile
64	2010-03-05 11:47:10	-36.5	-73.1	6.6	35.0	Chile
65	2010-03-08 02:32:34	38.8	40.1	6.1	10.0	Turkey
66	2010-03-11 14:39:44	-34.3	-71.9	6.9	11.0	Chile
67	2010-03-16 02:22:00	-36.2	-73.2	6.0	35.0	Chile
68	2010-03-28 21:43:13	-35.3	-72.8	6.1	19.0	Chile
69	2010-03-30 16:54:48	13.6	92.9	6.4	45.0	India
70	2010-04-02 05:38:55	19.1	-68.0	8.0	13.0	North Atlantic Oc
71	2010-04-04 22:40:39	32.1	-115.2	6.9	32.0	California*
72	2010-04-06 22:15:02	2.2	97.0	7.8	48.0	N/ Sumatra
73	2010-04-07 14:33:05	-3.8	141.9	6.0	37.0	New Guinea
74	2010-04-11 09:40:30	-10.9	161.1	6.8	60.0	Islands region
75	2010-04-11 22:08:11	37.1	-3.5	6.2	623.0	Spain
76	2010-04-13 23:49:42	33.3	96.7	6.9	46.0	China
77	2010-04-17 23:15:24	-6.7	147.3	6.3	66.0	New Guinea
78	2010-04-23 10:03:07	-37.4	-72.9	6.1	35.0	Central Chile
79	2010-04-24 07:41:03	-1.9	128.2	6.1	53.0	Indonesia
80	2010-04-26 02:59:51	22.2	123.7	6.5	22.0	Taiwan
81	2010-04-30 23:11:44	60.6	-177.9	6.3	15.0	Bering Sea

82	2010-04-30 23:16:29	60.5	-177.7	6.0	15.0	Bering Sea
83	2010-05-03 23:09:45	-38.1	-73.7	6.4	20.0	Central Chile
84	2010-05-05 16:29:02	-4.1	101.1	6.3	18.0	Indonesia
85	2010-05-06 02:42:44	-18.0	-70.5	6.4	11.0	Northern Chile
86	2010-05-08 03:22:11	-8.1	118.2	6.1	20.0	Sumbawa Indone
87	2010-05-09 05:59:44	3.7	96.1	7.4	61.0	Indonesia
88	2010-05-15 15:18:07	-23.5	176.6	5.9	30.0	Fiji Islands
89	2010-05-19 04:15:42	-5.1	-77.6	6.0	125.0	Northern Peru
90	2010-05-24 16:18:29	-8.1	-71.6	6.3	578.0	Western Brazil
91	2010-05-25 10:09:06	35.3	-35.9	6.3	10.0	N Mid-Atlantic Ri
92	2010-05-26 08:53:06	25.8	130.0	6.4	4.0	Japan
93	2010-05-27 17:14:48	-13.7	166.5	7.4	36.0	Vanuatu Islands
94	2010-05-27 20:48:00	-13.6	166.7	6.4	32.0	,, ,,
95	2010-05-31 10:16:02	6.9	124.0	6.0	33.0	Philippina Island
96	2010-05-31 19:51:48	11.1	93.7	6.4	127.0	India
97	2010-06-01 03:26:16	9.3	-84.3	6.1	29.0	Costa Rica
98	2010-06-09 23:23;19	-18.6	169.5	6.0	17.0	Vanuatu Island
99	2010-06-12 19:26;50	7.7	92.0	7.7	35.0	India
100	2010-06-13 03:32:54	37.4	141.6	6.1	7.0	Coast of Eastern
101	2010-06-16 03:06:05	-2.5	136.5	6.4	25.0	Indonesia
102	2010-06-16 03:16:29	-2.1	136.5	7.0	28.0	Indonesia
103	2010-06 16 03:58:10	-2.4	136.5	6.6	19.0	Indonesia
104	2010-06-30 04:30:59	-23.2	179.2	6.3	536.0	Fiji Island
105	2010-06-30 07:22:28	16.5	-97.8	6.2	20.0	Mexico
106	2010-07-02 06:04:04	-13.7	166.4	6.4	35.0	Vanuatu Island
107	2010-07-04 21:55:51	39.7	142.5	6.4	23.0	Coast of Eastern
108	2010-07-10 11:43:32	11.1	146.1	6.2	10.0	Mariana Island
109	2010-07-12 00:11:18	-22.2	-68.2	6.2	91.0	Northern Chile
110	2010-07-14 08:32:22	-38.0	-73.3	6.5	28.0	Coast of Central
111	2010-07-18 05:56:49	53.0	-169.5	6.7	35.0	Aleutian
112	2010-07-18 13;04:13	-6.1	150.5	6.9	57.0	New Britain
113	2010-07-18 13:35:02	-6.0	150.5	7.3	57.0	Papua New Guine
114	2010-07-18 13:42:35	49.1	1379.7	6.0	33.0	Russia
115	2010-07-20 19:18:23	-5.9	150.7	6.3	35.0	Papua New
116	2010-07-22 05:04:01	-15.2	168.2	6.2	35.0	Vanuatu Island
117	2010-07-23 22:08:11	6.7	123.5	7.3	604.0	Philippine
118	2010-07-23 22:51:11	6.5	123.5	7.4	575.0	Philippine
119	2010-07-23 23:15:08	6.8	123.3	7.4	616.0	Philippine
120	2010-07-24 05:35:01	6.2	123.5	6.5	555.0	Philippine
121	2010-08-04 07:15:33	-5.5	146.8	6.4	213	Papua new Guine
122	2010-08-10 05:23:46	-17.6	168.0	7.5	36.0	Vanuatu Island

123	2010-08-12 11:54:14	-1.3	-77.4	6.9	189	Ecuador
124	2010-08-13 21:19:33	12.5	141.5	6.9	10.0	Mariana island
125	2010-08-14 23:01:05	12.2	141.4	6.6	22.0	Mariana Island
126	2010-08-16 03:30:55	-17.8	65.7	6.3	10.0	Mauritius
127	2010-08-20 17:56:19	-6.6	154.1	6.4	50.0	Solomon Island
128	2010-09-11 19:21:13	36.5	70.8	6.3	199.0	Afghanistan
129	2010-09-26 12:12:38	-5.3	133.9	6.0	8.0	Indonesia
130	2010-09-29 17:10:51	-4.9	133.7	6.2	10.0	Indonesia
131	2010-10-04 13:28:39	24.3	125.3	6.3	35.0	Japan
132	2010-10-08 03:26:13	51.4	-175.4	6.4	20.0	United state
133	2010-10-08 03:49:11	51.5	-175.5	6.1	35.0	United state
134	2010-10-08 05:43:10	2.8	128	6.3	144.0	Indonesia
135	2010-10-12 12:02:55	-21	-173	6.1	9.0	Tonga Island
136	2010-10-16 15:44:32	-7.3	125	6.1	20.0	Banda sea
137	2010-10-21 17:53:14	24.8	-109.2	6.7	9.0	California, Mexic
138	2010-10-25 22:59:53	-3.3	100.5	6.2	21.0	Indonesia
139	2010-10-30 15:18:38	-56.8	-142.6	6.4	20.0	Pacific-Antarctic
140	2010-11-03 11:18:17	-4.7	134.1	6.1	29.0	Indonesia
141	2010-11-03 23:34:44	-20.4	-174.3	6.0	33.0	Tonga Island
142	2010-11-10 04:05:24	-45.5	96.4	6.3	10.0	Indian Ridge
143	2010-11-16 01:39:43	-2.0	139.0	5.9	18.0	Indonisia
144	2010-11-17 15:53:30	-7.9	129.4	5.9	13.0	Banda Sea
145	2010-11-22 16:18:41	-33.6	-178.8	5.9	1.0	Kermadac Island
146	2010-11-23 09:01:08	-6.0	149.0	6.0	73.0	New Britain,Papu
147	2010-11-30 03:24:41	28.4	139.1	6.6	478.0	Japan
148	2010-12-07 04:27:22	-58.0	-7.6	5.8	13.0	East of South San
149	2010-12-08 06:47:18	7.4	126.6	6.1	69.0	Mindabo, Philipp
150	2010-12-12 20:48:16	71.5	-4.6	4.5	10.0	Jan Mayen Island
151	2010-12-13 01:14:43	-6.6	155.7	6.1	144.0	Bougainville, Sol
152	2010-12-13 09:44:52	39.4	-29.4	5.0	4.8	Azores Island, Po
153	2010-12-20 18:41:59	28.4	59.1	6.3	12.0	Southern Iran
154	2010-12-23 14:00:33	53.2	171.2	6.2	22.0	United State
155	2010-12-28 08:34:17	-23.4	-179.8	6.3	551.0	South of Fiji Islan
156	2010-12-29 06:54:21	-19.7	168.2	6.6	31.0	Vanuatu Islands
157	2011-01-01 09:56:57	-26.8	-63.1	6.9	562.0	Argentina
158	2011-01-02 20:20:16	-38.4	-73.3	7.1	16.0	Central Chille
159	2011-01-05 06:46:17	-22.3	171.6	6.3	135.0	Loyalty Islands
160	2011-01-09 10:03:43	-19.0	168.3	6.6	17.0	Vanuatu Islands
161	2011-01-09 17:21:55	-19.3	168.1	6.4	32.0	Vanuatu Islands
162	2011-01-12 21:32:55	26.9	140.0	6.5	520.0	Japan
163	2011-01-13 16:16:41	-20.6	168.5	7.0	5.0	Loyalty Islands

164	2011-01-18 20:23:17	28.8	64.0	7.4	10.0	Pakistan
165	2011-01-42 02:45:29	38.4	72.8	6.1	89.0	Tajikistan
166	2011-01-26 15:42:29	2.1	96.7	6.1	26.0	Indonesia
167	2011-01-29 06:55:24	71.0	-6.7	6.0	2.0	Islands region
168	2011-02-03 20:25:22	-15.6	-173.0	6.0	60.0	Tonga Islands
169	2011-02-04 13:53:47	24.6	166.5	6.4	88.0	Border region
170	2011-02-07 19:53:42	-7.2	155.3	6.2	413.0	Islands region
171	2011-02 10 14:39:28	4.1	123.0	6.5	528.0	Celebes sea
172	2011-02-10 14:41:57	4.0	123.1	6.7	512.0	Celebes sea
173	2011-02-11 20:05:30	-36.4	-73.0	7.0	18.0	Central Chile
174	2011-02-12 01:17:02	-37.0	-73.1	6.1	8.0	Central Chile
175	2011-02-12 17:57:56	-20.8	-175.6	6.1	81.0	Tonga Islands
176	2011-02-13 10:35:06	-36.6	-73.2	6.0	13.0	Central Chile
177	2011-02-14 03:40:10	-35.4	-72.7	6.6	25.0	Central Chile
178	2011-02-15 13:33:53	-2.5	121.5	6.1	20.0	Indonesia
179	2011-02-20 21:43:20	55.9	162.1	6.2	9.0	Russia
180	2011-02-21 10:57:51	-26.1	178.4	6.4	540.0	Fiji Islands
181	2011-02-21 23:51:42	-43.5	172.6	6.3	4.0	New Zealand
182	2011-02-28 01:29:26	-37.2	-73.1	6.0	16.0	central
183	2011-03-01 00:53:46	-29.3	-112.1	5.8	9.0	Easter Island regi
184	2011-03-03 12:52:09	5.0	126.6	5.5	80	Philippine Islands
185	2011-03-04 04:07:49	-8.9	157.3	5.7	12.0	Bougainville, Solo
186	2011-03-06 12:31:56	-18.1	-69.4	6.2	87.0	Northern Chile
187	2011-03-06 14:32:36	-56.4	-27.0	6.6	86.0	South Sandwich I
188	2011-03-07 00:09:38	-10.6	160.8	6.6	30	Bougainville, Solo
189	2011-03-09 02:45:18	38.5	142.8	7.2	14.0	Eastern Honshu J
190	2011-03-09 02:57:16	38.4	142.8	5.6	17.0	Eastern Honshu J
191	2011-03-09 18:16:15	38.3	142.7	6.0	12.0	Eastern Honshu J
192	2011-03-10 17:08:36	-6.9	116.8	6.2	510.0	Bali Sea
193	2011-03-11 05:46:23	38.3	142.4	8.8	24.0	Eastern Honshu J
194	2011-03-11 06:06:11	39.0	142.3	6.4	25.0	Eastern Honshu J
195	2011-03-11 06:07:21	36.4	141.9	6.4	35.0	Eastern Honshu J
196	2011-03-11 06:25:51	38.1	144.6	7.1	26.0	Eastern Honshu J
197	2011-03-11 06:57:14	35.8	141.0	6.3	30.0	Eastern Honshu J
198	2011-03-11 08:19:24	36.2	142.0	6.5	19.0	Eastern Honshu J
199	2011-03-12 01:47:16	37.6	143.7	6.8	25.0	Eastern Honshu J
200	2011-03-14 06:12:36	37.8	142.5	6.1	14.0	Eastern Honshu J
201	2011-03-22 07:18:47	37.2	144.0	6.6	26.0	Eastern Honshu J
202	2011-03-22 13:31:29	-31.1	-16.0	6.0	14.0	Southern Mid-Atl
203	2011-03-24 13:55:12	20.7	100.0	7.0	10.0	Laos
204	2011-03-25 11:36:24	38.8	141.9	6.4	39.0	Eastern Honshu J

205	2011-03-27 22:23:58	38.4	142.1	6.1	17.0	Eastern Honshu J
206	2011-03-29 10:54:33	37.4	142.2	6.3	18.0	“
207	2011-03-31 07:15:30	39.0	142.0	6.2	39.0	“
208	2011-04-01 13:29:11	35.5	26.6	6.2	60.0	Crete, Greece
209	2011-04-02 10:59:37	-19.6	-69.1	5.9	83.0	Northern Chile
210	2011-04-03 20:06:42	-9.8	107.8	6.7	24.0	Jawa Indonesia
211	2011-04-06 14:01:43	1.7	97.2	5.8	18.0	Sumatera Indone
212	2011-04-07 13:11:24	17.4	-94.0	6.5	167.0	Chiapas Mexico
213	2011-04-07 14:32:41	38.2	141.6	7.1	49.0	Eastern Honshu J
214	2011-04-11 08:16:13	37.0	140.0	6.6	10.0	Eastern Honshu J
215	2011-04-11 23:08:15	35.0	140.0	6.4	5.0	Eastern Honshu J
216	2011-04-12 05:07:41	37.1	140.4	6.0	10.0	Eastern Honshu J
217	2011-04-23 04:16:55	-10.3	161.2	6.9	81.0	Bougainville-Solo
218	2011-05-10 08:55:11	-20.2	168.2	7.1	26.0	Loyalty Island
219	2011-05-14 21:07:22	36.4	70.7	5.9	207.0	Afghanistan
220	2011-05-15 13:08:13	0.5	-25.6	6.0	9.0	Central Mid-Atlan
221	2011-05-19 20:15:23	39.1	29.1	5.9	7.0	Turkey
222	2011-06-01 12:55:21	-37.5	-73.7	6.4	15.0	Central Chile
223	2011-06-03 00:05:00	37.3	143.9	6.5	10.0	Eastern Honshu J
224	2011-06-05 11:51:12	-55.9	146.6	6.3	10.0	West of Macquar
225	2011-06-08 03:06:18	-17.1	-69.5	6.0	101.0	Peru-Bolivia Bord
226	2011-06-12 20:32:39	13.4	41.7	5.6	2.0	Ethiopia
227	2011-06-20 16:35:57	-21.9	-68.3	6.3	111.0	Chile-Bolivia Bord
228	2011-06-22 21:50:47	39.9	142.3	6.7	3.0	Eastern Honshu J
229	2011-06-24 03:09:39	52.0	-173.7	7.4	43.0	Fox Islands Unite
230	2011-07-06 19:03:16	-29.3	-176.2	7.7	10.0	Kermadec Islands
231	2011-07-10 00:57:12	38.0	143.3	7.0	34.0	Eastern Honshu J
232	2011-07-11 20:47:14	9.5	122.2	6.2	19.0	Negros, Philippin
233	2011-07-16 00:26:13	-33.8	-72.1	6.0	22.0	Central Chile
234	2011-07-16 19:59:14	54.9	-161.3	6.1	48.0	Alaska Peninsula,
235	2011-07-19 19:35:40	40.1	71.4	6.2	1.0	Tajikistan
236	2011-07-23 04:34:24	39.0	142.0	6.4	35.0	Eastern Honshu J
237	2011-07-24 18:51:25	37.8	141.5	6.2	35.0	Eastern Honshu J
238	2011-07-25 00:50:50	-3.2	150.7	6.2	34.0	New Ireland, Pap
239	2011-07-26 17:44:21	25.2	-109.5	5.9	10.0	Gulf of California
240	2011-07-27 23:00:29	10.7	-43.4	5.9	6.0	Northern Mid-Atl

APPENDIX III: List of Events observed at KADUNA station

S/N	DATE/ORIGIN TIME OF EVENT	LATITUDE	LONGITUDE	MAGNITUDE	DEPTH	REGION
1	2009-09-12 20:06:24	10.7	-68.0	6.3	10.0	Near coast of Ver
2	2009-09-18 06:23:58	12.6	120.5	6.0	10.0	Philippine Island
3	2009-09-21 08:53:05	27.3	91.4	6.3	7.0	Bhutan
4	2009-09-24 07:16:21	19.1	-107.3	6.4	4.0	Mexico
5	2009-10-11 04:47:46	-17.2	66.6	6.0	10	Mauritius
6	2009-10-16 09:52:52	-6.6	105.2	6.1	50	Indonesia
7	2009-10-22 00:51:39	6.8	-82.6	6.1	10	Panama
8	2009-10-22 19:51:28	36.5	70.9	6.2	196	Afghanistan
9	2009-10-23 11:15:28	-0.9	134.1	6.0	35	Indonesia
10	2009-10-24 14:40:44	-6.2	130.3	7.0	138	Banda sea
11	2009-10-29 17:44:31	36.5	70.7	6.0	202.0	Afghanistan
12	2009-10-30 07:03:39	29.1	129.9	6.9	35.0	Japan
13	2009-11-04 18:41:44	36.1	-33.9	6.0	10	Azores
14	2009-11-08 19:41:44	-8.3	118.7	6.7	18.0	Indonesia

15	2009-11-09 10:44:54	-17.2	178.4	7.2	585.0	Fiji Island
16	2009-11-13 03:05:55	-19.4	-70.2	6.5	10	Chile
17	2009-11-14 19:44:22	-22.9	-66.5	6.1	141.0	Argentina
18	2009-11-17 15:30:46	52.1	-131.5	6.6	10	Canada
19	2009-11-26 19:08:10	13.5	-89.9	5.9	37	El Salvador
20	2009-11-28 06:04:25	-10.4	118.9	6.2	35.0	Indonesia
21	2009-12-06 17:36:35	-10.2	33.8	10	5.8	Malawi
22	2009-12-09 16:00:42	-0.7	-21.1	6.4	10.0	Mid-Atlantic ridg
23	2009-12-18 07:33:00	-18.0	65.6	5.9	2.0	Mauritius
24	2009-12-19 13:02:16	23.8	121.7	6.4	44	Taiwan
25	2009-12-19 23:19:23	-9.9	34.0	6.2	47	Tanzania
26	2009-12-24 00:23:27	42.2	134.8	6.3	348.0	Russia
27	2009-12-26 08:57:24	-5.6	131.1	6.0	57	Banda sea
28	2010-01-03 21:48:06	-8.8	157.2	6.5	10.0	Bougainville
29	2010-01-05 04:55:39	-58.1	-14.9	6.7	10.0	Sandwich Islands
30	2010-01-09 05:51:34	-9.2	157.6	6.3	35.0	Bougainville
31	2010-01-10 00:27:39	40.7	-124.7	6.5	16.0	N.Califonia
32	2010-01-12 21:53:09	18.4	-72.4	7.0	10.0	Haiti
33	2010-01-15 10:14:02	-32.0	-177.1	5.9	10.0	Kermadec Islands
34	2010-01-17 12:00:02	-57.7	-65.9	6.3	10.0	Drake Passage
35	2010-01-18 15:40:32	23.8	-90.2	6.0	103.0	Guatemala
36	2010-01-20 11:03:44	18.4	-72.9	6.1	9.0	Haiti
37	2010-01-27 17:42:45	-14.1	-14.4	5.8	10.0	Southern Mid-Atl
38	2010-10-29 09:20:04	-19.0	169.5	6.0	85.0	Vanuatu Islands
39	2010-02-01 22:28:17	-6.1	154.4	6.2	33.0	Bougainville-Solo
40	2010-02-04 20:20:21	40.4	-124.9	6.0	11.0	N. California
41	2010-02-05 06:59:06	-48.0	99.6	6.1	10.0	Indian Ridge
42	2010-02-06 04:44:59	47.0	152.0	6.1	35.0	Russia
43	2010-02-07 06:10:00	23.5	123.7	6.4	16.0	Japan
44	2010-02-13 02:34:29	-21.9	-174.8	6.3	10.0	Tonga Islands
45	2010-02-18 01:18:17	42.61	130.8	6.7	562.0	China border
46	2010-02-22 07:00:54	-23.7	-176.0	6.0	35.0	Fiji Islands
47	2010-02-26 20:31:26	26.0	128.4	7.0	22.0	Japan
48	2010-02-27 06:34:14	-35.9	-72.6	8.8	35.0	Chile
49	2010-02-27 08:01:24	-37.2	-75.2	6.9	39.0	Chile
50	2010-02-28 11:25:35	-34.7	-70.9	6.2	35.0	Chile-Argentina b
51	2010-03-04 00:18:53	22.9	120.9	6.4	35.0	Chile
52	2010-03-04 14:02:30	-13.6	167.1	6.4	200.0	Chile
53	2010-03-05 11:47:10	-36.5	-73.1	6.6	35.0	Chile
54	2010-03-08 02:32:34	38.8	40.1	6.1	10.0	Turkey
55	2010-03-11 14:39:44	-34.3	-71.9	6.9	11.0	Chile

56	2010-03-16 02:22:00	-36.2	-73.2	6.0	35.0	Chile
57	2010-03-28 21:43:13	-35.3	-72.8	6.1	19.0	Chile
58	2010-03-30 16:54:48	13.6	92.9	6.4	45.0	India
59	2010-04-02 05:38:55	19.1	-68.0	8.0	13.0	North Atlantic Oc
60	2010-04-04 22:40:39	32.1	-115.2	6.9	32.0	California
61	2010-04-06 22:15:02	2.2	97.0	7.8	48.0	N/ Sumatra
62	2010-04-07 14:33:05	-3.8	141.9	6.0	37.0	New Guinea
63	2010-04-11 09:40:30	-10.9	161.1	6.8	60.0	Islands region
64	2010-04-11 22:08:11	37.1	-3.5	6.2	623.0	Spain
65	2010-04-13 23:49:42	33.3	96.7	6.9	46.0	China
66	2010-04-17 23:15:24	-6.7	147.3	6.3	66.0	New Guinea
67	2010-04-23 10:03:07	-37.4	-72.9	6.1	35.0	Central Chile
68	2010-04-24 07:41:03	-1.9	128.2	6.1	53.0	Indonesia
69	2010-04-26 02:59:51	22.2	123.7	6.5	22.0	Taiwan
70	2010-04-30 23:11:44	60.6	-177.9	6.3	15.0	Bering Sea
71	2010-04-30 23:16:29	60.5	-177.7	6.0	15.0	Bering Sea
72	2010-05-03 23:09:45	-38.1	-73.7	6.4	20.0	Central Chile
73	2010-05-05 16:29:02	-4.1	101.1	6.3	18.0	Indonesia
74	2010-05-06 02:42:44	-18.0	-70.5	6.4	11.0	Northern Chile
75	2010-05-08 03:22:11	-8.1	118.2	6.1	20.0	Sumbawa Indone
76	2010-05-09 05:59:44	3.7	96.1	7.4	61.0	Indonesia
77	2010-05-15 15:18:07	-23.5	176.6	5.9	30.0	Fiji Islands
78	2010-05-19 04:15:42	-5.1	-77.6	6.0	125.0	Northern Peru
79	2010-05-24 16:18:29	-8.1	-71.6	6.3	578.0	Western Brazil
80	2010-05-25 10:09:06	35.3	-35.9	6.3	10.0	N Mid-Atlantic Ri
81	2010-05-26 08:53:06	25.8	130.0	6.4	4.0	Japan
82	2010-05-27 17:14:48	-13.7	166.5	7.4	36.0	Vanuatu Islands
83	2010-05-27 20:48:00	-13.6	166.7	6.4	32.0	,, ,,
84	2010-05-31 10:16:02	6.9	124.0	6.0	33.0	Philippina Island
85	2010-05-31 19:51:48	11.1	93.7	6.4	127.0	India
86	2010-06-01 03:26:16	9.3	-84.3	6.1	29.0	Costa Rica
87	2010-06-09 23:23;19	-18.6	169.5	6.0	17.0	Vanuatu Island
88	2010-06-12 19:26;50	7.7	92.0	7.7	35.0	India
89	2010-06-13 03:32:54	37.4	141.6	6.1	7.0	Coast of Eastern
90	2010-06-16 03:06:05	-2.5	136.5	6.4	25.0	Indonesia
91	2010-06-16 03:16:29	-2.1	136.5	7.0	28.0	Indonesia
92	2010-06 16 03:58:10	-2.4	136.5	6.6	19.0	Indonesia
93	2010-06-30 04:30:59	-23.2	179.2	6.3	536.0	Fiji Island
94	2010-06-30 07:22:28	16.5	-97.8	6.2	20.0	Mexico
95	2010-07-02 06:04:04	-13.7	166.4	6.4	35.0	Vanuatu Island
96	2010-07-04 21:55:51	39.7	142.5	6.4	23.0	Coast of Eastern

97	2010-07-10 11:43:32	11.1	146.1	6.2	10.0	Mariana Island
98	2010-07-12 00:11:18	-22.2	-68.2	6.2	91.0	Northern Chile
99	2010-07-14 08:32:22	-38.0	-73.3	6.5	28.0	Coast of Central
100	2010-07-18 05:56:49	53.0	-169.5	6.7	35.0	Aleutian
101	2010-07-18 13;04:13	-6.1	150.5	6.9	57.0	New Britain
102	2010-07-18 13:35:02	-6.0	150.5	7.3	57.0	Papua New Guine
103	2010-07-18 13:42:35	49.1	1379.7	6.0	33.0	Russia
104	2010-07-20 19:18:23	-5.9	150.7	6.3	35.0	Papua New
105	2010-07-22 05:04:01	-15.2	168.2	6.2	35.0	Vanuatu Island
106	2010-07-23 22:08:11	6.7	123.5	7.3	604.0	Philippine
107	2010-07-23 22:51:11	6.5	123.5	7.4	575.0	Philippine
108	2010-07-23 23:15:08	6.8	123.3	7.4	616.0	Philippine
109	2010-07-24 05:35:01	6.2	123.5	6.5	555.0	Philippine
110	2010-08-04 07:15:33	-5.5	146.8	6.4	213	Papua new Guine
111	2010-08-10 05:23:46	-17.6	168.0	7.5	36.0	Vanuatu Island
112	2010-08-12 11:54:14	-1.3	-77.4	6.9	189	Ecuador
113	2010-08-13 21:19:33	12.5	141.5	6.9	10.0	Mariana island
114	2010-08-14 23:01:05	12.2	141.4	6.6	22.0	Mariana Island
115	2010-08-16 03:30:55	-17.8	65.7	6.3	10.0	Mauritius
116	2010-08-20 17:56:19	-6.6	154.1	6.4	50.0	Solomon Island
117	2010-09-11 19:21:13	36.5	70.8	6.3	199.0	Afghanistan
118	2010-09-26 12:12:38	-5.3	133.9	6.0	8.0	Indonesia
119	2010-09-29 17:10:51	-4.9	133.7	6.2	10.0	Indonesia
120	2010-10-04 13:28:39	24.3	125.3	6.3	35.0	Japan
121	2010-10-08 03:26:13	51.4	-175.4	6.4	20.0	United state
122	2010-10-08 03:49:11	51.5	-175.5	6.1	35.0	United state
123	2010-10-08 05:43:10	2.8	128	6.3	144.0	Indonesia
124	2010-10-12 12:02:55	-21	-173	6.1	9.0	Tonga Island
125	2010-10-16 15:44:32	-7.3	125	6.1	20.0	Banda sea
126	2010-10-21 17:53:14	24.8	-109.2	6.7	9.0	California, Mexic
127	2010-10-25 22:59:53	-3.3	100.5	6.2	21.0	Indonesia
128	2010-10-30 15:18:38	-56.8	-142.6	6.4	20.0	Pacific-Antarctic
129	2010-11-03 11:18:17	-4.7	134.1	6.1	29.0	Indonesia
130	2010-11-03 23:34:44	-20.4	-174.3	6.0	33.0	Tonga Island
131	2010-11-10 04:05:24	-45.5	96.4	6.3	10.0	Indian Ridge
132	2010-11-16 01:39:43	-2.0	139.0	5.9	18.0	Indonisia
133	2010-11-17 15:53:30	-7.9	129.4	5.9	13.0	Banda Sea
134	2010-11-22 16:18:41	-33.6	-178.8	5.9	1.0	Kermadac Island
135	2010-11-23 09:01:08	-6.0	149.0	6.0	73.0	New Britain,Papu
136	2010-11-30 03:24:41	28.4	139.1	6.6	478.0	Japan
137	2010-12-07 04:27:22	-58.0	-7.6	5.8	13.0	East of South San

138	2010-12-08 06:47:18	7.4	126.6	6.1	69.0	Mindabo, Philipp
139	2010-12-12 20:48:16	71.5	-4.6	4.5	10.0	Jan Mayen Island
140	2010-12-13 01:14:43	-6.6	155.7	6.1	144.0	Bougainville, Solo
141	2010-12-13 09:44:52	39.4	-29.4	5.0	4.8	Azores Island, Po
142	2010-12-20 18:41:59	28.4	59.1	6.3	12.0	Southern Iran
143	2010-12-23 14:00:33	53.2	171.2	6.2	22.0	United State
144	2010-12-28 08:34:17	-23.4	-179.8	6.3	551.0	South of Fiji Islan
145	2010-12-29 06:54:21	-19.7	168.2	6.6	31.0	Vanuatu Islands
146	2011-01-01 09:56:57	-26.8	-63.1	6.9	562.0	Argentina
147	2011-01-02 20:20:16	-38.4	-73.3	7.1	16.0	Central Chille
148	2011-01-05 06:46:17	-22.3	171.6	6.3	135.0	Loyalty Islands
149	2011-01-09 10:03:43	-19.0	168.3	6.6	17.0	Vanuatu Islands
150	2011-01-09 17:21:55	-19.3	168.1	6.4	32.0	Vanuatu Islands
151	2011-01-12 21:32:55	26.9	140.0	6.5	520.0	Japan
152	2011-01-13 16:16:41	-20.6	168.5	7.0	5.0	Loyalty Islands
153	2011-01-18 20:23:17	28.8	64.0	7.4	10.0	Pakistan
154	2011-01-42 02:45:29	38.4	72.8	6.1	89.0	Tajikistan
155	2011-01-26 15:42:29	2.1	96.7	6.1	26.0	Indonesia
156	2011-01-29 06:55:24	71.0	-6.7	6.0	2.0	Islands region
157	2011-02-03 20:25:22	-15.6	-173.0	6.0	60.0	Tonga Islands
158	2011-02-04 13:53:47	24.6	166.5	6.4	88.0	Border region
159	2011-02-07 19:53:42	-7.2	155.3	6.2	413.0	Islands region
160	2011-02 10 14:39:28	4.1	123.0	6.5	528.0	Celebes sea
161	2011-02-10 14:41:57	4.0	123.1	6.7	512.0	Celebes sea
162	2011-02-11 20:05:30	-36.4	-73.0	7.0	18.0	Central Chile
163	2011-02-12 01:17:02	-37.0	-73.1	6.1	8.0	Central Chile
164	2011-02-12 17:57:56	-20.8	-175.6	6.1	81.0	Tonga Islands
165	2011-02-13 10:35:06	-36.6	-73.2	6.0	13.0	Central Chile
166	2011-02-14 03:40:10	-35.4	-72.7	6.6	25.0	Central Chile
167	2011-02-15 13:33:53	-2.5	121.5	6.1	20.0	Indonesia
168	2011-02-20 21:43:20	55.9	162.1	6.2	9.0	Russia
169	2011-02-21 10:57:51	-26.1	178.4	6.4	540.0	Fiji Islands
170	2011-02-21 23:51:42	-43.5	172.6	6.3	4.0	New Zealand
171	2011-02-28 01:29:26	-37.2	-73.1	6.0	16.0	central
172	2011-03-01 00:53:46	-29.3	-112.1	5.8	9.0	Easter Island regi
173	2011-03-03 12:52:09	5.0	126.6	5.5	80	Philippine Islands
174	2011-03-04 04:07:49	-8.9	157.3	5.7	12.0	Bougainville, Solo
175	2011-03-06 12:31:56	-18.1	-69.4	6.2	87.0	Northern Chile
176	2011-03-06 14:32:36	-56.4	-27.0	6.6	86.0	South Sandwich I
177	2011-03-07 00:09:38	-10.6	160.8	6.6	30	Bougainville, Solo
178	2011-03-09 02:45:18	38.5	142.8	7.2	14.0	Eastern Honshu J

179	2011-03-09 02:57:16	38.4	142.8	5.6	17.0	Eastern Honshu J
180	2011-03-09 18:16:15	38.3	142.7	6.0	12.0	Eastern Honshu J
181	2011-03-10 17:08:36	-6.9	116.8	6.2	510.0	Bali Sea
182	2011-03-11 05:46:23	38.3	142.4	8.8	24.0	Eastern Honshu J
183	2011-03-11 06:06:11	39.0	142.3	6.4	25.0	Eastern Honshu J
184	2011-03-11 06:07:21	36.4	141.9	6.4	35.0	Eastern Honshu J
185	2011-03-11 06:25:51	38.1	144.6	7.1	26.0	Eastern Honshu J
186	2011-03-11 06:57:14	35.8	141.0	6.3	30.0	Eastern Honshu J
187	2011-03-11 08:19:24	36.2	142.0	6.5	19.0	Eastern Honshu J
188	2011-03-12 01:47:16	37.6	143.7	6.8	25.0	Eastern Honshu J
189	2011-03-14 06:12:36	37.8	142.5	6.1	14.0	Eastern Honshu J
190	2011-03-22 07:18:47	37.2	144.0	6.6	26.0	Eastern Honshu J
191	2011-03-22 13:31:29	-31.1	-16.0	6.0	14.0	Southern Mid-Atl
192	2011-03-24 13:55:12	20.7	100.0	7.0	10.0	Laos
193	2011-03-25 11:36:24	38.8	141.9	6.4	39.0	Eastern Honshu J
194	2011-03-27 22:23:58	38.4	142.1	6.1	17.0	Eastern Honshu J
195	2011-03-31 07:15:30	39.0	142.0	6.2	39.0	“
196	2011-04-01 13:29:11	35.5	26.6	6.2	60.0	Crete, Greece
197	2011-04-02 10:59:37	-19.6	-69.1	5.9	83.0	Northern Chile
198	2011-04-03 20:06:42	-9.8	107.8	6.7	24.0	Jawa Indonesia
199	2011-04-06 14:01:43	1.7	97.2	5.8	18.0	Sumatera Indone
200	2011-04-07 13:11:24	17.4	-94.0	6.5	167.0	Chiapas Mexico
201	2011-04-07 14:32:41	38.2	141.6	7.1	49.0	Eastern Honshu J
202	2011-04-11 08:16:13	37.0	140.0	6.6	10.0	Eastern Honshu J
203	2011-04-11 23:08:15	35.0	140.0	6.4	5.0	Eastern Honshu J
204	2011-04-12 05:07:41	37.1	140.4	6.0	10.0	Eastern Honshu J
205	2011-04-23 04:16:55	-10.3	161.2	6.9	81.0	Bougainville-Solo
206	2011-05-10 08:55:11	-20.2	168.2	7.1	26.0	Loyalty Island
207	2011-05-14 21:07:22	36.4	70.7	5.9	207.0	Afghanistan
208	2011-05-15 13:08:13	0.5	-25.6	6.0	9.0	Central Mid-Atlan
209	2011-05-19 20:15:23	39.1	29.1	5.9	7.0	Turkey
210	2011-06-01 12:55:21	-37.5	-73.7	6.4	15.0	Central Chile
211	2011-06-03 00:05:00	37.3	143.9	6.5	10.0	Eastern Honshu J
212	2011-06-05 11:51:12	-55.9	146.6	6.3	10.0	West of Macquar
213	2011-06-08 03:06:18	-17.1	-69.5	6.0	101.0	Peru-Bolivia Bord
214	2011-06-12 20:32:39	13.4	41.7	5.6	2.0	Ethiopia
215	2011-06-20 16:35:57	-21.9	-68.3	6.3	111.0	Chile-Bolivia Bord
216	2011-06-22 21:50:47	39.9	142.3	6.7	3.0	Eastern Honshu J
217	2011-06-24 03:09:39	52.0	-173.7	7.4	43.0	Fox Islands Unite